uOttawa

L'Université canadienne
Canada's university

FACULTÉ DES ÉTUDES SUPÉRIEURES ET POSTDOCTORALES

uOttawa

L'Université canadienne
Canada's university

FACULTY OF GRADUATE AND POSTDOCTORAL STUDIES

Liang Li

AUTEUR DE LA THÈSE / AUTHOR OF THESIS

M.A.Sc. (Electrical Engineering)

GRADE / DEGREE

School of Information and Technology Engineering

FACULTÉ, ÉCOLE, DÉPARTEMENT / FACULTY, SCHOOL, DEPARTMENT

In-Line Monitoring of Styrene/1,3 Butadiene Emulsion Polymerization by ATR-FTRI Spectroscopy

TITRE DE LA THÈSE / TITLE OF THESIS

M. Dube

DIRECTEUR (DIRECTRICE) DE LA THÈSE / THESIS SUPERVISOR

CO-DIRECTEUR (CO-DIRECTRICE) DE LA THÈSE / THESIS CO-SUPERVISOR

EXAMINATEURS (EXAMINATRICES) DE LA THÈSE / THESIS EXAMINERS

A. Macchi

P. Mehrani

Gary W. Slater

Le Doyen de la Faculté des études supérieures et postdoctorales / Dean of the Faculty of Graduate and Postdoctoral Studies

UNIVERSITY OF OTTAWA

Department of Chemical and Biological Engineering

IN-LINE MONITORING OF STYRENE/1,3 BUTADIENE EMULSION POLYMERIZATION BY ATR-FTIR SPECTROSCOPY

by

Liang Li

A thesis submitted to the Faculty of Graduate and Postdoctoral Studies in partial fulfillment of the requirements for the degree of

Master of Applied Science

in Chemical Engineering

Your file Votre référence
ISBN: 978-0-494-61323-8
Our file Notre référence
ISBN: 978-0-494-61323-8

Abstract

Synthetic rubber is a highly valuable commodity polymer. One important synthetic rubber product is styrene-butadiene rubber (SBR). It is principally made via the emulsion copolymerization of styrene and butadiene monomers and the product is referred to as emulsion polymerized SBR or E-SBR. It is one of the most widely used polymers in the world today. Typical E-SBR applications include pneumatic tires and tubes; heels and soles for footwear; and gaskets.

This study focused on demonstrating and validating the use of Attenuated Total Reflectance Fourier Transform Infrared (ATR-FTIR) spectroscopy to the in-line monitoring of E-SBR copolymerization. Based on this objective, a series of styrene/1,3 butadiene emulsion copolymerizations of different monomer feed ratios were carried out in a 1.2L stainless steel reactor using a typical industrial recipe. A special sample-taking valve was developed to account for the presence of the 1,3 butadiene (a gaseous monomer at atmospheric conditions). Monomer conversion was monitored off-line using gravimetry combined with proton nuclear magnetic resonance (^{1}H-NMR) spectroscopy and in-line using ATR-FTIR spectroscopy.

The in-line ATR-FTIR monitoring was accomplished with a ReactIR™ 1000 probe. It was found that a multivariate statistical analysis (Partial Least Squares) was necessary to achieve good results. A comparison of the off-line and in-line results was made and it was demonstrated that no significant differences existed between the two methods. This confirmed the reliability of ATR-FTIR as a tool for monitoring monomer conversion and polymer composition for the E-SBR process.

Statement of Contribution of Collaborators

I hereby declare that I am the sole author of this thesis. I performed the polymerization experiments, polymer characterizations and data analysis except for the acquisition of ^{1}H-NMR spectroscopy data, which were contracted out to the Department of Chemistry at the University of Ottawa.

My thesis supervisor, Dr. Dubé, provided the scientific guidance throughout the project and significant editorial comments for the written work.

Liang Li Date:

Acknowledgements

I would like to express my gratitude to my supervisor, Dr. Dubé, for all the support and guidance he provided me throughout this thesis. I am grateful to all the members of the Polymer Reaction Engineering group, especially Stephane Roberge, Gabriela Fonseca, Lili Qie, Renata Jovanovic, Hong Hua and Nick Brooks, with whom I had the pleasure to work with. I would like to thank the technicians of the Department of Chemical Engineering at the University of Ottawa, Franco Ziroldo, Louis Tremblay and Gérard Nina for their help in repairing and maintaining all the lab equipment.

For the financial support during this project, I am grateful to Omnova Solutions, U.S.A. and the Natural Sciences and Engineering Research Council of Canada.

Table of Contents

List of Figures

List of Tables

Nomenclature

Symbols

f	Initiator efficiency (dimensionless)
f_i	Instantaneous fraction of monomer i (dimensionless)
F_i	Instantaneous mole fraction of monomer i (dimensionless)
k_d	Decomposition of initiator rate constant (L/mol min)
k_{fp}	Chain transfer to polymer rate constant (L/mol min)
$k_{i,j}$	Initiation of monomer j rate constant (L/mol min)
k_p	Polymerization rate constant (L/mol min)
$k_{p,ij}$	Propagation rate constant of monomer j to terminal monomer i, (L/mol min)
$k_{tc,ij}$	Termination by combination rate constant, terminal monomers for the radical chains are i and j, respectively (L/mol min)
$k_{td,ij}$	Termination by disproportionation rate constant, terminal monomers for the radical chains are i and j, respectively (L/mol min)
$k_{tr,ij}$	Chain transfer to monomer rate constant, terminal monomer i and receiving monomer j (L/mol min)
$k_{tr,fCTA}$	Chain transfer to CTA rate constant (L/mol min)
M_1	Styrene (dimensionless)
M_2	1, 3-Butadiene (dimensionless)
$M\cdot_{1,i}$	Radical chain with 1 monomer, ending in monomer i (dimensionless)
$M\cdot_{m,i}$	Radical chain of length m, ending in monomer i (dimensionless)
$M\cdot_{n,i}$	Radical chain of length n, ending in monomer i (dimensionless)
$M\cdot_{r,i}$	Radical chain of length r, ending in monomer i (dimensionless)
P_{n+m}	Dead polymer of length n+m (dimensionless)
r_i	Reactivity ratio of monomer i (dimensionless)
$R\cdot$	Free radical (dimensionless)
R_d	Rate of decomposition of initiator (mol/L min)
R_i	Rate of initiation (mol/L min)

R_p	Rate of polymerization (mol/L min)
$R_{r+1,i}$	Radical chain of length r+1, ending in monomer i and j, respectively (dimensionless)
R_t	Rate of termination (mol/L min)
x_i	Conversion of monomer I (wt. % or mol fraction)
X	Overall conversion (wt. % or mol fraction)

Abbreviations

ATR-FTIR	Attenuated Total Reflectance Fourier Transform Infrared
Bd	1, 3-Butadiene
CHP	Cumene Hydroperoxide
CMC	Critical Micelle Concentration
CTA	Chain Transfer Agent
DDM	n-Dodecyl Mercaptan
EDTA	Ethylene Diamine Tetra-Acetic Acid
FA	Fatty Acid
FS	Ferrous Sulphate
^{1}H-NMR	Proton Nuclear Magnetic Resonance Spectroscopy
KOH	Potassium hydroxide
PLS	Partial Least Square
PRESS	Predicted Residual Error Sum of Squares
RA	Roisn Acid
SFS	Sodium Formaldehyde Sulfoxylate
St	Styrene
THF	Tetrahydrofuran

Chapter 1 – Introduction

Polymers are macromolecules consisting of large quantities of small molecules (i.e., monomer) bound together by chemical reaction or polymerization. In chain-growth polymerization, polymers grow to high molecular weights at a very fast rate by way of a reactive centre. Different reactive centres such as free radicals, anions, or cations can be used. Free-radical polymerization can be applied under four classes of reaction conditions: bulk, suspension, solution and emulsion. Emulsion polymerization is a type of free radical polymerization with a typical recipe consisting of a dispersing medium (i.e., water), monomer(s), a water-soluble initiator, and an emulsifier. It has been widely used in various industries to produce latexes for different kinds of applications such as adhesives, coatings and synthetic rubber.

Emulsion polymerization often exhibits variability during the reaction process due to temperature fluctuations, the heterogeneity of the reaction medium, and due to competing particle nucleation mechanisms. In other words, it is a typical multiphase system which keeps changing during the process and is therefore hard to control, especially given the lack of robust on-line and in-line measurements of important product properties and process variables.

For effective industrial production under an appropriate process control scheme, it is often desirable to have a suitable means to monitor the emulsion polymerization process. Traditional polymerization monitoring is often performed by off-line sample analysis. It has the disadvantage of significant lag times between sampling and analysis which prevent the effective control of the process.

Attenuated Total Reflectance Fourier Transform Infrared (ATR-FTIR) spectroscopy has been demonstrated to be a very powerful tool for the on-line monitoring of changes in monomer concentration for a variety of polymerization systems in solution, emulsion and mini-emulsion (Hua and Dubé, 2001, 2002; Roberge and Dubé, 2005; Jovanovic and Dubé, 2007). To our knowledge, it has never been tested for the monitoring of the emulsion copolymerization of styrene/1,3 butadiene (SBR).

Emulsion polymerized SBR (E-SBR) is a very important polymer which has been produced at a rate of 772,000 metric tons per year in North America. Typical E-SBR applications include pneumatic tires and tubes; heels and soles for footwear; and gaskets. Thus, due to its economic importance and high levels of production, better control of the E-SBR process is desired to achieve more consistent properties. One evident solution is the use of in-line monitoring technology.

In this study, our objective was to demonstrate and validate the in-line monitoring of E-SBR batch emulsion copolymerization using ATR-FTIR spectroscopy by comparison to off-line monitoring techniques (i.e., gravimetry and ^{1}H-NMR spectroscopy)

1.1 Thesis Outline

This thesis consists of five chapters. Chapter 2 provides a theoretical background on emulsion polymerization kinetics and IR spectroscopy. As well, the special redox initiation system for "cold" E-SBR polymerization is described. The experimental design, apparatus, experimental procedures and the different methods used for the characterization of the latex are presented in Chapter 3. Chapter 4 contains a manuscript to be submitted for publication, which presents the results of the ATR-FTIR monitoring of the SBR emulsion polymerization. The final chapter provides a general discussion of the thesis as well as conclusions and recommendations based on the results obtained. Sample calculations are found in Appendix A while Appendix B contains information on the safe handling of butadiene gas monomer.

References

1. Hua, H., Dubé, M. A. "Terpolymerization monitoring with ATR-FTIR spectroscopy", J. Appl. Polym. Sci.: Part A: Polym. Chem., 39, 1860-1876, 2001.
2. Hua, H., Dubé, M. A. "In-line monitoring of emulsion homo- and copolymerizations using ATR-FTIR spectrometry", Polym. Reaction Eng. J., 10, 21-40, 2002.

3. Jovanovic, R., Dubé, M. A. "Butyl Acrylate/Vinyl Acetate Emulsion-Based Pressure-Sensitive Adhesives: Empirical Modeling of Final Properties", Can. J. Chem. Eng., 85, 341-349, 2007.
4. Roberge, S., Dubé, M. A. "The effect of particle size and composition on the performance of styrene/butyl acrylate miniemulsion-based PSAs", Polymer, 47, 799-807, 2006.

Chapter 2 - Background

In this section, the fundamentals of free-radical polymerization and emulsion polymerization are described. It is a guide to the emulsion polymerization of 1, 3 butadiene and styrene monomers. Next, Attenuated Total Reflectance-Fourier Transform Infrared (ATR-FTIR) spectroscopy is described.

Basic definitions. Polymers are composed of large quantities of small molecules, monomers, linked together by a chemical reaction termed polymerization. A requirement for polymerization is that each monomer must have a functionality of two (or higher) to be capable of being linked to two other monomers by chemical reaction. There are several classifications of polymers and polymerization reactions. The modern approach is to classify these according to two principal polymerization mechanisms. Step-growth polymerizations are polymerization in which the polymers form by the stepwise, intermolecular condensation of reactive groups. Chain-growth polymerizations are polymerizations in which the polymers form by the successive addition of unsaturated monomer units in a chain reaction promoted by an active centre. Free radical polymerization, a subclass of chain growth polymerization, is of interest in this study. Free radical polymerizations involve the addition of monomer to a free-radical reactive site located at the growing polymer chain end. Four polymerization techniques are commonly used industrially: bulk polymerization, solution polymerization, suspension polymerization and emulsion polymerization. These can be performed in batch, semi-batch or continuous reactors.

2.1 Free-radical Polymerization Kinetics

Free-radical polymerization is a chain-growth polymerization usually comprising the following steps: initiation, propagation, termination, and often, chain transfer and inhibition. Note that throughout this thesis, monomer 1 refers to styrene and monomer 2 to 1,3 butadiene.

Initiation

Initiation is the first stage of free-radical polymerization and it involves creation of the free-radical active centre which usually takes place in two steps. The first is the formation of free radicals (R•) from an initiator (I) and the second is the addition of a monomer molecule to one of these free radicals. In this work, free radicals were generated via the redox system (a pair of oxidizing agent and reducing agent), cumene hydroperoxide (CHP)/iron/sodium formaldehyde sulfoxylate (SFS), by the redox reaction:

$$ROOH + FeY^{-2} \xrightarrow{Ki} RO^{\bullet} + FeY^{-1} + OH^{-1} \qquad (2.1)$$

where *ROOH* represents CHP, FeY^{-2} represents the Fe^{2+}. FeY^{-1} represents the Fe^{3+}. K_r is the rate constant for the redox reaction.

The next step involves the addition of these free radicals to the first monomer molecule to produce the chain-initiating active centre $M_{r,i}$•.

$$RO^{\bullet} + M_1 \xrightarrow{k_{i,1}} M^{\bullet}_{1,1} \qquad (2.2)$$

$$RO^{\bullet} + M_2 \xrightarrow{k_{i,2}} M^{\bullet}_{1,2} \qquad (2.3)$$

where k_{ij} is the rate constant for the initiation step in which monomer j is added to the free radicals. $M_{r,i}$• denotes a free chain radical of chain length r ending in monomer unit j.

Propagation

The second stage in free-radical polymerization involves growth of the polymer chain by rapid addition of monomers to the active centre. Each addition simply moves the location of the active centre to the growing chain end. In copolymerization, where two monomers are present, the following reactions take place:

$$M^{\bullet}_{r,1} + M_1 \xrightarrow{k_{p,11}} M^{\bullet}_{r+1,1} \qquad (2.4)$$

$$M^{\bullet}_{r,1} + M_2 \xrightarrow{k_{p,12}} M^{\bullet}_{r+1,2} \qquad (2.5)$$

$$M^{\bullet}_{r,2} + M_1 \xrightarrow{k_{p,21}} M^{\bullet}_{r+1,1} \qquad (2.6)$$

$$M^{\bullet}_{r,2} + M_2 \xrightarrow{k_{p,22}} M^{\bullet}_{r+1,2} \qquad (2.7)$$

where $k_{p,ij}$ is the rate constant for propagation in which monomer unit j adds to the active centre $M_{r,i}$•. $M_{r+1,j}$• denotes a growing radical of chain length $r + 1$ ending in monomer unit j. Propagation with the growth of the chain to high-polymer proportions takes place very rapidly (<1s). When considering the kinetics of the propagation stage, the classical terminal model is employed in this thesis. The terminal model assumes that only the last monomer unit bound to the polymer chain affects the reactivity of the free-radical active centre.

Termination

In this step, growth of the polymer chain is terminated. There are two common mechanisms of termination which involve bimolecular reactions: combination and disproportionation. The first involves the coupling of two growing chains to form a single polymer molecule:

$$M_{n,1}^{\bullet} + M_{m,1}^{\bullet} \xrightarrow{k_{tc,11}} P_{n+m} \qquad (2.8)$$

$$M_{n,1}^{\bullet} + M_{m,2}^{\bullet} \xrightarrow{k_{tc,12}} P_{n+m} \qquad (2.9)$$

$$M_{n,2}^{\bullet} + M_{m,2}^{\bullet} \xrightarrow{k_{tc,22}} P_{n+m} \qquad (2.10)$$

where $k_{tc,ij}$ is the rate constant for termination stage by combination in which the terminal monomers for the radical chains are i and j, respectively. P_{n+m} denotes a dead polymer chain of length $m + n$. The second mechanism, termination by disproportionation, involves the abstraction of a hydrogen radical from one growing polymer chain to another, resulting in the formation of two dead polymer chains. One of these chains will contain a saturated end-group and the other an unsaturated end-group:

$$M_{n,1}^{\bullet} + M_{m,1}^{\bullet} \xrightarrow{k_{td,11}} P_n + P_m \qquad (2.11)$$

$$M_{n,1}^{\bullet} + M_{m,2}^{\bullet} \xrightarrow{k_{td,12}} P_n + P_m \qquad (2.12)$$

$$M_{n,2}^{\bullet} + M_{m,2}^{\bullet} \xrightarrow{k_{td,22}} P_n + P_m \qquad (2.13)$$

where $k_{td,ij}$ is the rate constant for termination by disproportionation in which the terminal monomers for the radical chains are i and j, respectively. In general, both termination

mechanisms can occur, but their extent depends upon the monomer and the polymerization conditions.

Chain Transfer

Chain transfer reactions to small molecules cause decreases in polymer molecular weight. This type of reaction is due to the transfer of a hydrogen or other atom to the growing polymer chain end in exchange for the active centre to a molecule present in the reaction system — the monomer, initiator, solvent. Thus, a dead polymer chain is formed and the free radical moves to a new molecule:

$$M_{n,1}^{\bullet} + M_1 \xrightarrow{k_{tr,11}} P_n + M_{1,1}^{\bullet} \qquad (2.14)$$

$$M_{n,1}^{\bullet} + M_2 \xrightarrow{k_{tr,12}} P_n + M_{1,2}^{\bullet} \qquad (2.15)$$

$$M_{n,2}^{\bullet} + M_1 \xrightarrow{k_{tr,21}} P_n + M_{1,1}^{\bullet} \qquad (2.16)$$

$$M_{n,2}^{\bullet} + M_2 \xrightarrow{k_{tr,22}} P_n + M_{1,2}^{\bullet} \qquad (2.17)$$

In the equations above, $k_{tr,ij}$ is the rate constant for chain transfer reaction in which the growing free-radical chain $M_{n,i}^{\bullet}$ transfers its radical to monomer unit j.

The free radical can also be transferred to a chain transfer agent, which is purposefully used to increase the probability of transfer reactions to lower the final polymer molecular weight:

$$M_n^{\bullet} + CTA \xrightarrow{k_{tr,CTA}} P_n + CTA^{\bullet} \qquad (2.18)$$

where $k_{tr,CTA}$ is the rate constant for chain transfer to CTA.

Rates of Polymerization

It is instructive to consider the rate of polymerization, R_p, when studying polymerizations. The rate of initiator decomposition is a rate-determining step which controls the rate of initiation, R_i, because the reaction of free radicals with monomer proceeds significantly faster than the formation of free radicals from the initiator. Considering that in the initiation stage only a certain quantity of free radicals will initiate a polymerization, an initiator efficiency factor, f, is usually employed. Hence, the rate of initiator dissociation can be expressed as:

$$R_i = 2f k_d [I] \qquad (2.19)$$

where k_d is the initiator decomposition rate constant and *[I]* is the initiator concentration.

Monomer disappears during the initiation stage as well as the propagation stage. The rate of polymerization which is synonymous with the rate of monomer disappearance can be expressed as:

$$\frac{-d[M]}{dt} = R_i + R_p \qquad (2.20)$$

However, comparing the number of monomer molecules reacting during the propagation stage, the number during the initiation stage can be ignored. Hence, the rate of polymerization can be simply expressed as the rate of propagation.

$$-\frac{d[M]}{dt} = R_p \qquad (2.21)$$

The rate of propagation, and also the rate of polymerization, is the sum of many individual propagation steps. It can be expressed as:

$$R_p = k_p[M][M^{\bullet}] \qquad (2.22)$$

where *[M]* is the monomer concentration and *[M •]* is the total concentration of all chain radicals.

At the start of the polymerization, the rate of initiation or free radical formation greatly exceeds the rate of termination, where free radicals are consumed. However, the rate of termination increases as the concentration of free radicals *[R •]* increases until they reach a balance where the two rates are more or less equal and the concentration of free radicals remains constant. This is referred to as the steady-state hypothesis for free radicals and can be expressed as:

$$\frac{d[R^{\bullet}]}{dt} = -\frac{d[M^{\bullet}]}{dt} \qquad (2.23)$$

According to the steady-state hypothesis, the rate of termination is equal to the rate of initiation and can be expressed as:

$$R_i = R_t = 2k_t[M^{\bullet}]^2 \qquad (2.24)$$

Hence, the rate of polymerization can be estimated from the combination of equations (19), (22) and (24) and can be expressed as:

$$R_p = k_p[M]\sqrt{\left(\frac{f k_d[I]}{k_t}\right)} \qquad (2.25)$$

Copolymer Composition and Reactivity Ratios

The composition of the copolymer formed at very low conversion (about 5%) is usually different from the composition of the co-monomer feed and is due to their monomer reactivity ratios (Odian, 2004). The terminal model of copolymerization will continue to be applied here to describe copolymer composition. The terminal model assumes that the chemical reactivity of the propagating chain in a copolymerization is dependent only on the identity of the monomer unit at the growing end and is independent of the chain composition preceding the last unit (Mayo et al., 1944). The monomers' reactivity is described by the reactivity ratios, r_1 and r_2:

$$r_1 = \frac{k_{p,11}}{k_{p,12}} \quad \text{and} \quad r_2 = \frac{k_{p,22}}{k_{p,21}} \qquad (2.26)$$

The Mayo-Lewis equation or the copolymer composition equation can be expressed in terms of mole fractions as

$$F_1 = 1 - F_2 = \frac{r_1 f_1^2 + f_1 f_2}{r_1 f_1^2 + 2 f_1 f_2 + r_2 f_2^2} \qquad (2.27)$$

where F_1 and F_2 are the instantaneous mole fraction of M_1 and M_2 chemically bound in the copolymer, and f_1 and f_2 are the instantaneous mole fractions of M_1 and M_2 in the reaction mixture.

2.2 Emulsion Polymerization Kinetics

Emulsion polymerization is a multiphase free-radical initiated chain polymerization in which a monomer or a mixture of monomers is reacted in an aqueous dispersion medium to form the final product – latex. The main ingredients for an emulsion polymerization usually consist of the dispersing medium (e.g., water), monomer(s), a water-soluble initiator, and an emulsifier. In addition, four phases are often presenting

during the emulsion polymerization: monomer droplets, micelles, polymer particles, and the aqueous phase.

Site of polymerization (Particle Formation)

The surfactant or emulsifier used in emulsion polymerization usually consists of both hydrophobic hydrocarbon chains and hydrophilic anionic head groups at two different ends. When the concentration of surfactant exceeds its critical micelle concentration (CMC), the excess surfactant molecules form into spherical colloidal aggregates referred to as micelles, which contain on the order of 100 molecules and typically are about 5 nm in diameter. In conventional emulsion polymerization processes, the micelles are the preferred site for particle nucleation.

Two major particle formation mechanisms are considered to dominate the emulsion polymerization process: micellar nucleation and homogeneous nucleation. The first step in particle nucleation occurs in the water phase as dissolved monomers react with the water-soluble initiators to form oligomeric radicals. Once these radicals reach a critical length, their solubility in the water phase decreases and they are susceptible to capture in an organic phase. Micellar nucleation occurs when the no longer water-soluble oligomeric radicals enter the monomer-swollen surfactant micelles. In the presence of monomer, these radicals initiate the polymerization, thus converting the micelles to monomer-swollen polymer particles. Homogeneous nucleation involves the precipitation or coagulation of the oligomeric radicals, to form particles (Fitch et al., 1969; Hansen and Ugelstad, 1978). The precipitated species will adsorb surfactant molecules to become stabilized and adsorb monomer to allow further propagation and growth. Nucleation of the monomer droplets, while possible, is highly unlikely due to the overwhelming surface area occupied by the micelles. Figure 2.1 shows particle formation mechanisms of emulsion polymerization.

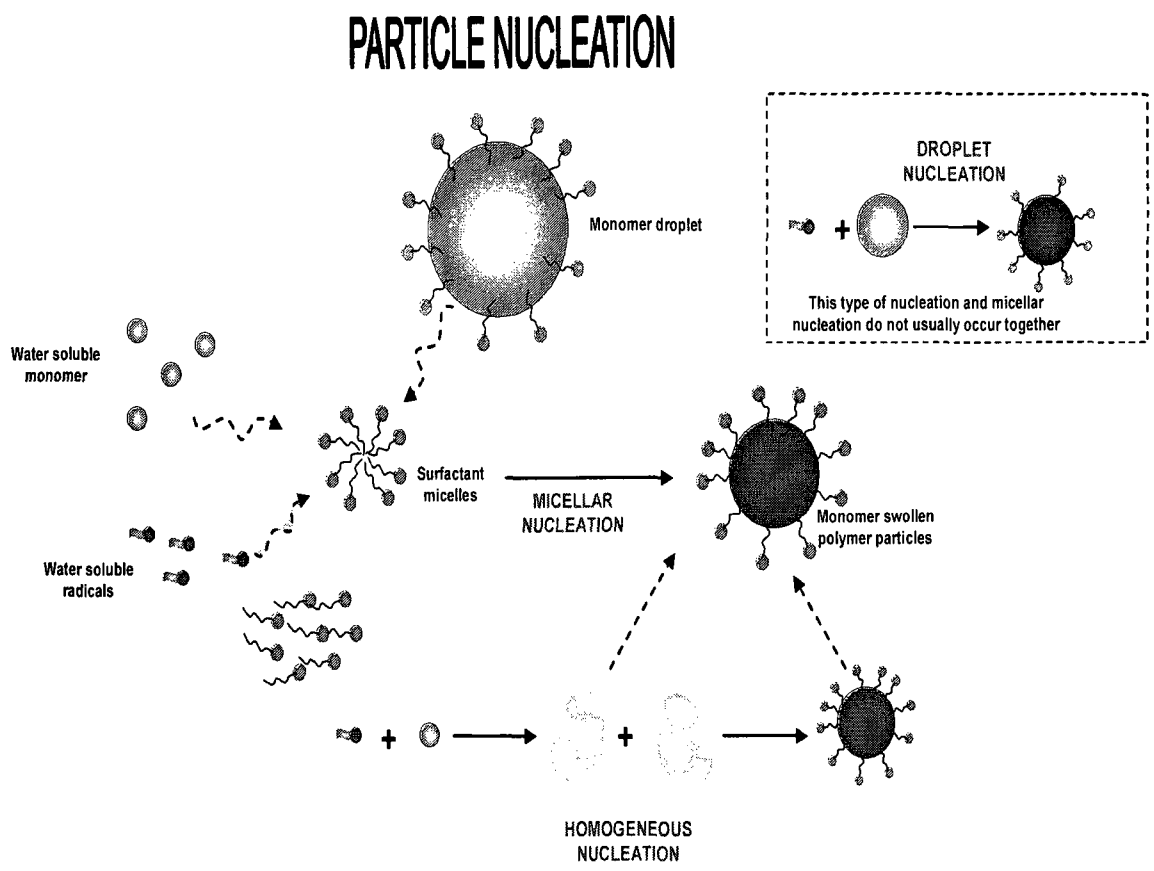

Figure 2.1: Emulsion polymerization particle formation mechanisms (Dubé, 2004)

Progress of Emulsion Polymerization

Conventional emulsion polymerization is commonly divided into three intervals as shown in Figure 2.2 (Harkins, 1947; Smith and Ewart, 1948).

Interval I: Particle nucleation occurs in this stage, with the reaction rate increasing with time as the number of particles increases. In this first stage, most of the monomer is dispersed in monomer droplets or micelles and there are few polymer particles. The end of interval I is identified as the point of disappearance of the micelles, most of which will have been converted to polymer particles.

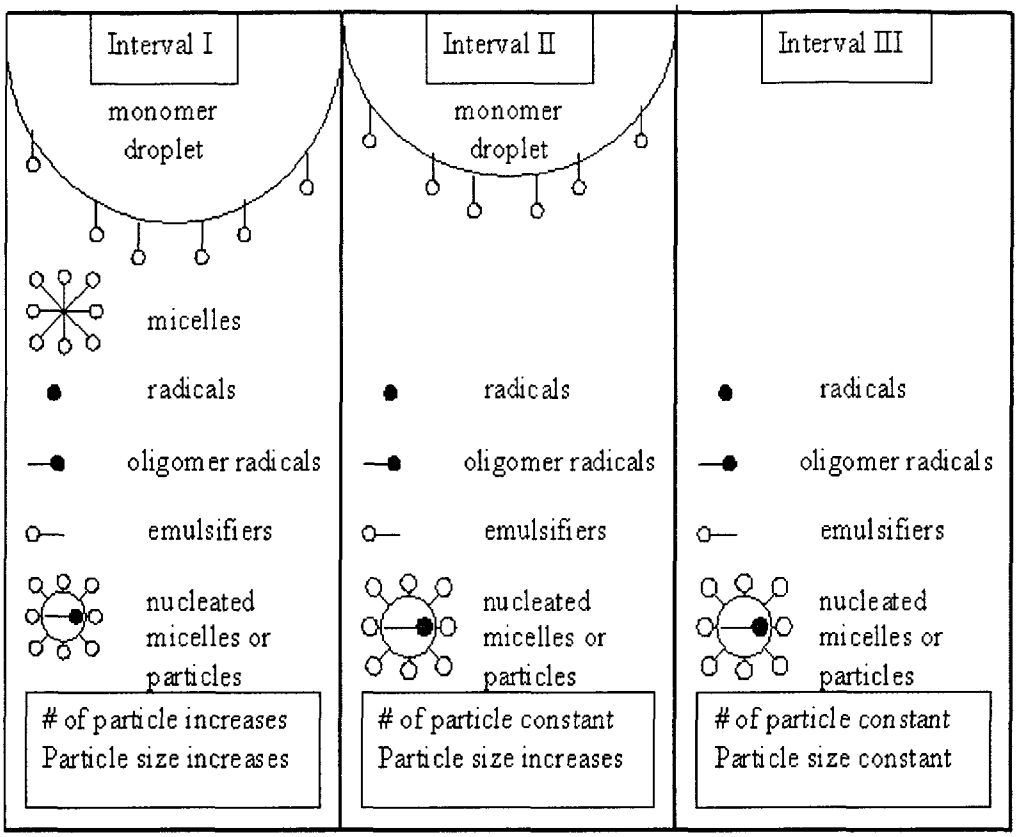

Figure 2.2: Three Intervals of an Emulsion Polymerization (Roberge, 2004)

Interval II: In the second stage, the unreacted monomer is found in the swollen polymer particles, in the monomer droplets and in limited amounts, dissolved in the aqueous phase. The monomer droplets act as reservoirs to maintain the polymerization within polymer particles. The concentration of monomer within a particle remains constant at their saturation point because the rate of monomer diffusion exceeds the rate of polymerization. As the number of particles remains constant, the rate of polymerization will remain constant too. The transition from Interval II to Interval III occurs when the monomer droplets are exhausted.

Interval III: Finally, in the last stage, no more monomer droplets are present and the residual monomer swells the polymer particles. The particle number remains the same in interval III as in the previous interval. The monomer concentration and the rate of polymerization decrease steadily as the remaining monomer within the particles is consumed.

2.3 Infrared IR Spectroscopy

Infrared (IR) spectroscopy is one of the most popular electromagnetic spectroscopic techniques applied in organic and inorganic chemistry. The principle of IR is to measure the absorption when an IR beam passes through a sample through different IR frequencies. Each chemical species contains different functional groups, and each of these groups has its own specific absorption corresponding to characteristic frequencies of IR radiation. This makes IR spectroscopic analysis a very effective and fast method for the determination of chemical functional groups in a sample. Comparing with other spectroscopic techniques, IR spectrometers can accept a wide range of sample types such as gases, liquids, solids and even multi-phase by using various sampling accessories. Thus, IR spectroscopy becomes more and more important in modern analytical techniques such as structural elucidation and compound identification.

Fundamentals of IR Spectroscopy

Infrared (IR) spectroscopy is a measurement of the adsorption of infrared light with matter. When temperatures are above absolute zero, all the atoms in molecules are in continuous vibration with respect to each other. The molecules will absorb radiation when both the frequency of a specific vibration and the IR radiation directed on the molecule are equal. The chemical bonds in the material start vibrating while absorbing infrared radiation. Functional groups, the characteristic fragments of molecules, have their own selectivity to absorb infrared radiation by the same wave number range regardless of the structure of the rest of the molecule. The width of an infrared band provides information about the strength and nature of the molecular interactions.

The primary limitations of IR spectroscopy are in quantitative measurements. Although IR measurements are precise in terms of identifying specific molecular structures, making accurate quantitative infrared measurements is a demanding process.

Quantitative Analysis

The electromagnetic spectrum of infrared radiation has a wide range: wavenumbers from roughly 13,000 to 10 cm^{-1}, or wavelengths from 0.78 to 1000 μm. It starts from

high frequencies as the red end of the visible region and ends with low frequencies at the microwave region.

Wavenumbers (ν) or wavelengths (λ) are two ways usually applied to present IR absorption positions. Wavenumber defines the number of waves per unit length. Thus, wavenumbers are directly proportional to frequency, as well as the energy of the IR absorption. Wavenumbers and wavelengths can be inter-converted using the following equation:

$$\nu(cm^{-1}) = \frac{1}{\lambda(\mu m)} \times 10^4 \qquad (28)$$

IR absorption information is generally presented in the form of a spectrum with wavelength or wavenumber as the x-axis and absorption intensity or percent transmittance as the y-axis (Figure 2.3).

Transmittance, T, is the ratio of radiant power transmitted by the sample (I) to the radiant power incident on the sample (I_0). Absorbance (A) is the logarithm to the base 10 of the reciprocal of the transmittance (T):

$$A = \log_{10}(1/T) = -\log_{10} T = -\log_{10} I / I_0 \qquad (29)$$

The transmittance spectra provide better contrast between intensities of strong and weak bands because transmittance ranges from 0 to 100%, whereas absorbance ranges from infinity to zero. Even the same sample will present obviously different results between the IR spectrum, which is linear in wavenumber, and the IR plot, which is linear in wavelength. It will appear as if some IR bands have been contracted or expanded. The IR region is commonly divided into three smaller areas: near IR, mid IR, and far IR (see Table 2.1).

Table 2.1: Different regions of IR spectrum

	Near IR	**Mid IR**	**Far IR**
Wavenumber	13,000-4,000 cm^{-1}	4,000-400 cm^{-1}	400-10 cm^{-1}
Wavelength	0.78-2.5 μm	2.5-25 μm	25-1,000 μm

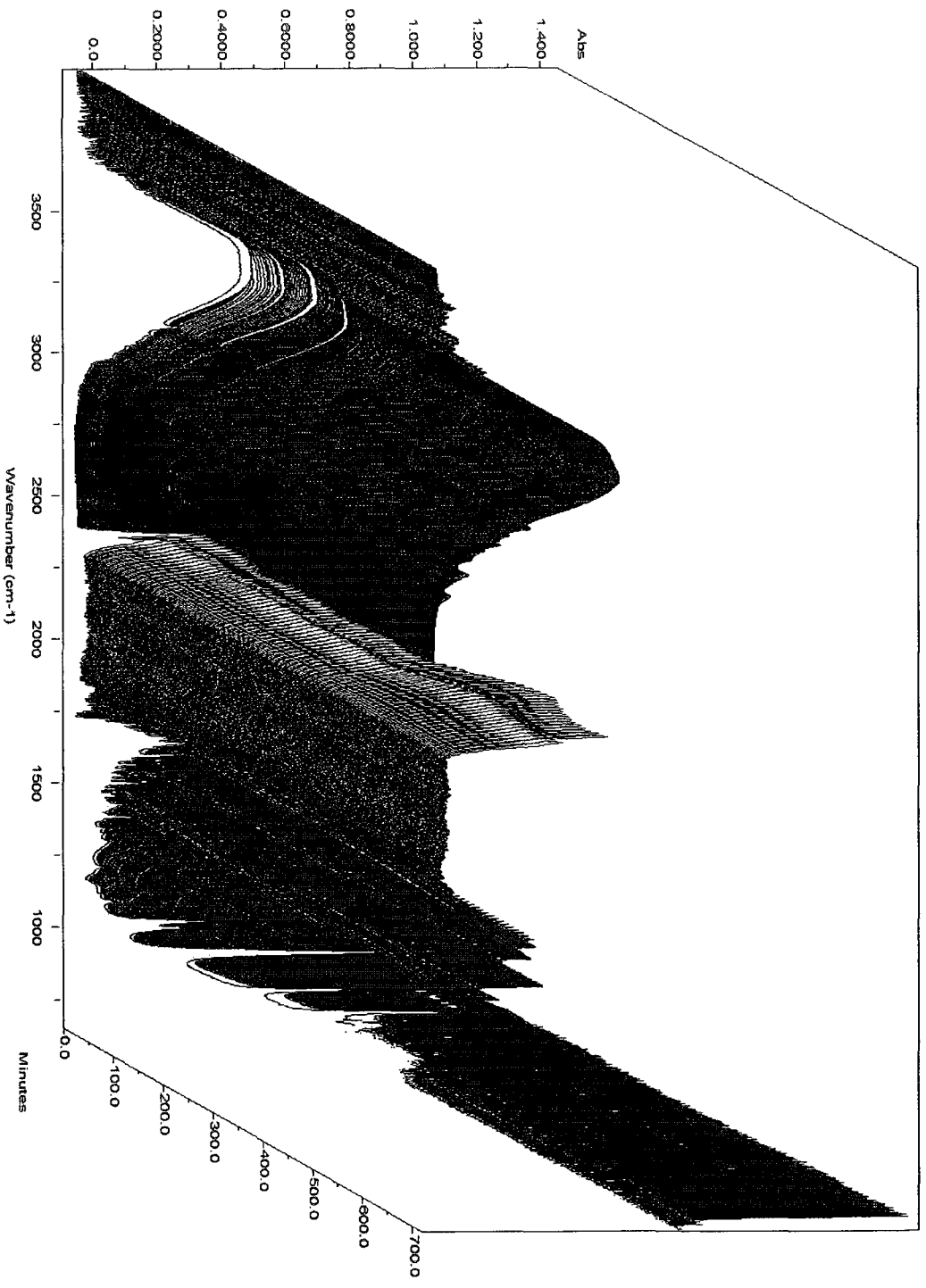

Figure 2.3: Reaction spectra of an E-SBR polymerization (St/Bd ratio: 40/60)

The far IR region provides useful information on sample molecular structure such as conformation and lattice dynamics of samples. The use of specialized optical materials

and sources are normally required for the technique. It has been widely used for the analysis of organic, inorganic, and organometallic compounds involving heavy atoms (mass number over 19). Near IR spectroscopy has gained increased interest, especially in process control applications because of its minimal or no sample preparation and its high-speed quantitative analysis without consumption or destruction of the sample. Near IR can be applied for remote analysis when it is combined with UV-visible spectrometers and coupled with fiber-optic devices.

In this project, we focus on the most frequently used mid IR region, between 4000 and 400 cm^{-1}(2.5 to 25 μm) which is also known as the "fingerprint region" for molecules due to its capture of just about all molecular features.

Fourier Transform Infrared Spectroscopy (FTIR)

Fourier Transform Infrared (FTIR) spectrometry was developed in order to overcome the limitations encountered with dispersive instruments (Smith, 1996). Fourier transform spectrometers have recently replaced dispersive instruments for most applications due to their superior speed and sensitivity. They have greatly extended the capabilities of infrared spectroscopy and have been applied to many areas that are very difficult or nearly impossible to analyze by dispersive instruments. Instead of viewing each component frequency sequentially, as in a dispersive IR spectrometer, all frequencies are examined simultaneously in Fourier transform infrared (FTIR) spectroscopy (Koenig, 1999).

Two of the many advantages that FTIR instruments have over dispersive spectrometers are:

- Better speed and sensitivity (Felgett advantage). A complete spectrum can be obtained during a single scan of the moving mirror, while the detector observes all frequencies simultaneously.
- Increased optical throughput (Jaquinot advantage). Energy-wasting slits are not required in the interferometer because dispersion or filtering is not needed.

FTIR spectrometers show their capability when samples that are energy-limited are analyzed or when increased sensitivity is desired.

Attenuated Total Reflectance (ATR)

Attenuated total reflectance (ATR) (also called internal reflection spectroscopy) accessories are especially useful for obtaining IR spectra of difficult polymer samples with low transmission (Harrick, 1967; Urban, 1996). They are suitable for studying thick or highly absorbing solid and liquid materials, including films, coatings, powders, threads, adhesives, polymers, and aqueous samples. ATR is one of the most versatile sampling techniques which require little or no sample preparation for most samples.

ATR occurs when a beam of radiation enters from a higher refractive index into a lower refractive index. The fraction of the incident beam reflected increases when the angle of incidence increases. All incident radiation is completely reflected at the interface when the angle of incidence is greater than the critical angle. The beam penetrates a very short distance beyond the interface and into the less-dense medium before complete reflection occurs. This penetration is called the evanescent wave and typically is at a depth of a few micrometers. Its intensity is reduced by the sample in regions of the IR spectrum where the sample absorbs. Figure 2.4 illustrates the basic ATR principles.

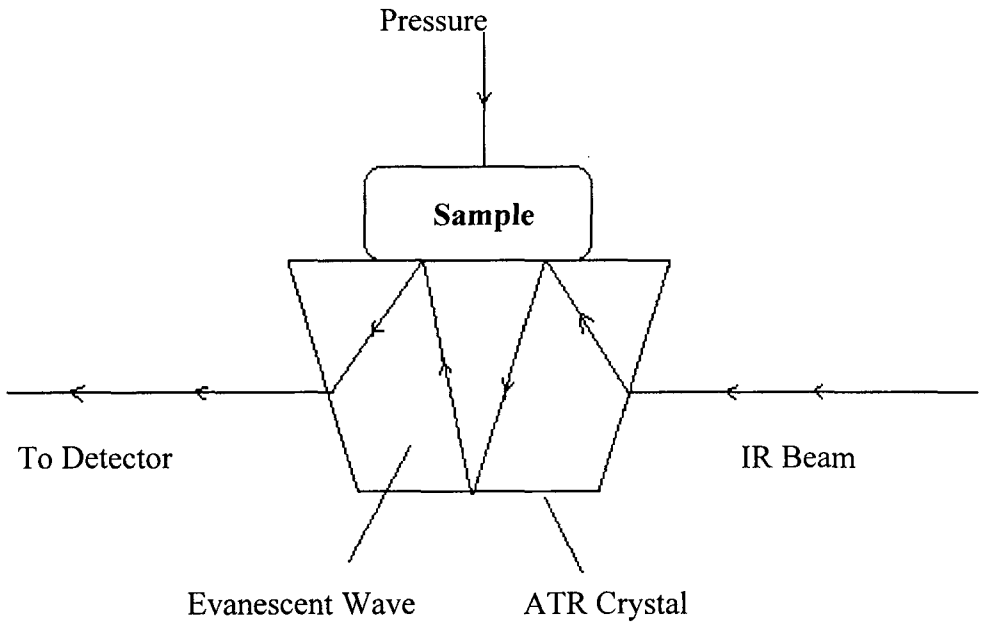

Figure 2.4: A schematic diagram of an attenuated total reflectance accessory (Roberge, 2004)

The sample is normally placed in close contact with a more-dense, high-refractive-index crystal, for which diamonds are the most commonly used IRE (internal reflection element) (Gunzler and Gremlich, 2002). The IR beam is directed onto

the bevelled edge of the ATR crystal and internally reflected through the crystal with a single or multiple reflections. Both the number of reflections and the penetration depth decrease with increasing angle of incidence. An ATR crystal gives higher numbers of reflections for each angle because of its higher length-to-thickness ratio.

The resulting ATR-FTIR spectrum resembles the conventional IR spectrum, but with some differences: The absorption band positions are identical in the two spectra, but the relative intensities of corresponding bands are different. Although ATR spectra can be obtained using either dispersive or FT instruments, FTIR spectrometers permit higher-quality spectra to be obtained in this energy-limited situation.

Applications of ATR-FTIR

Attenuated Total Reflectance Fourier Transform Infrared spectroscopy (ATR-FTIR) is one of the most often used spectroscopic methods for the study of polymers. It has been demonstrated that ATR-FTIR spectroscopic methods are reliable tools for on-line monitoring of polymerization processes. (Bauer et al., 2000; Roberge and Dubé, 2006)

As a result of the early work by Fahrenfort (1961), ATR-FTIR technology has been successfully applied to many polymerization systems. For example, Baranek et al. (1999) monitored batch and semi-batch isothermal and isoperibolic solution copolymerizations with ATR-FTIR spectroscopy. M'Bareck et al. (2004) monitored the compatibility of poly(acrylic acid) and poly(sodium styrene sulfonate). Hua and Dubé (2001) and Jovanovic and Dubé (2001) successfully monitored several solution polymerizations. Hua and Dubé (2001, 2002) and Jovanovic and Dubé (2007) successfully applied the technology, for the first time, to an emulsion polymerization. This was followed by its application to a styrene/butyl acrylate miniemulsion polymerization (Roberge and Dubé, 2006).

2.4 Emulsion Styrene-Butadiene Rubber (E-SBR)

Styrene-butadiene rubber (SBR) is an elastomeric copolymer consisting of styrene and 1,3 butadiene. It has been widely used in car tires where it is blended with natural rubber because of its good abrasion resistance and good ageing stability when protected by additives.

The emulsion-polymerized styrene-butadiene rubbers are produced using two different reaction methods:

1. The "hot" method, is distinguished by polymerization at temperatures in the region of 50°C using persulfates as initiator;
2. The "cold" method, refers to polymerization at temperatures in the region of 5°C using various redox systems as initiator.

Comparing these two methods, "cold" polymerized E-SBR has significantly better physical properties than hot polymerized E-SBR, for example, the tensile strength increases approximately linearly with decreasing polymerization temperature (Howland et al., 1951). Typical recipes for the "hot" and "cold" techniques are shown in Table 2.2.

Table 2.2: Typical recipe for "hot" and "cold" E-SBR (Lovell and El-Aasser, 1997)

Component	**Parts by Weight**	
	Cold	**Hot**
Styrene	25	25
Butadiene	75	75
Water	180	180
Emulsifier (Fatty Acid, Rosin Acid	5	5
Dodecyl mercaptan (DDM)	0.2	0.8
Cumene hydroperoxide (CHP)	0.17	-
$FeSO_4$ (FS)	0.017	-
Ethylene Diamine Tetra-acetic Acid (EDTA)	0.06	-
$Na_4P_2O_7 \cdot 10H_2O$	-	1.5
Potassium persulfate	-	0.3
SFS	-	0.1

Redox Initiation for "Cold" E-SBR Polymerization

In "cold" polymerization, the most widely used initiator system is the redox system, which employs cumene hydroperoxide (CHP)/iron/sodium formaldehyde sulfoxylate (SFS).

Free radicals are produced in the water phase by the redox reaction between CHP and a complex of Fe^{2+}- EDTA which is strictly water soluble. Because CHP exists between the aqueous and organic phases in an emulsion polymerization, it provides a constant source of peroxide in the water and consequently a relatively constant rate of radical generation. EDTA serves to form complexes with the iron which results in limiting the concentration of Fe^{2+} ion and preventing undesirable side reactions such as the formation of $Fe(OH)_3$ or iron-fatty acid salts.

The initiating mechanism is a redox reaction. The CHP is reduced to a radical and negatively charged hydroxide species while the iron (2+) is oxidized to the iron (3+) state. The function of SFS is to reduce iron (3+) back to iron (2+). Uraneck (1968) has summarized this mechanism as follows:

$$ROOH + FeY^{-2} \xrightarrow{K_1} RO^{\bullet} + FeY^{-1} + OH^{-1} \qquad (30)$$

$$FeY^{-1} + SFS \xleftrightarrow{K_2} FeY^{-2} + X^{+} \qquad (31)$$

$$RO^{\bullet} + M \xrightarrow{K_{pc}} ROM^{\bullet} \qquad (32)$$

where $ROOH$ represents CHP, FeY^{2} represents the Fe^{2+}. FeY^{1} represents the Fe^{3+}. EDTA complex, X^{+} represents the unknown oxidation products of SFS, RO represents the peroxide radical and M represents a monomer unit.

References

1. Adams, J. W., Messer, W. E., Howland, L. H. "MasterBatches from Carbon Blacks with GR-S Latices", Industr. Engng. Chem., 43(3), 754-765, 1951.
2. Baranek, B., Gottfried, M., Korfhage, K., Pauer, W., Schulz, K., Hans "Closed loop control of chemical composition in free radical copolymerization by Online reaction monitoring via calorimetry and IR-spectroscopy", RC User Forum Europe, Berne, Switzerland, 1999.

3. Bauer, C., Amram, B., Agnely, M., Charmot, D., Sawatzki, J., Dupuy, N., Huvenne, J.P. "On-Line Monitoring of a Latex Emulsion Polymerization by Fiber-Optic FT-Raman Spectroscopy. Part I: Calibration", Appl. Spect., 54, 528-535, 2000.
4. Dubé, M. A. CHG 8187 course notes. Department of Chemical and Biological Engineering, University of Ottawa, 2004
5. Fahrenfort, J. "A new principle for the production of useful infra-red reflection spectra of organic compounds", Spectrochim. Acta, 17, 698-709, 1961.
6. Fitch, R. M., Prenosil, M. B., Sprick, K. J. "The Mechanism of Particle Formation in Polymer. Hydrosols, I: Kinetics of the Aqueous Polymerization of Methyl. Methacrylate", J. Polym. Sci., C27, 95-118, 1969.
7. Günzler, H., Gremlich, H. U. "IR Spectroscopy: An introduction", Wiley-VCH; Germany, 1-361, 2002.
8. Hansen, F. K., Ugelstad, J. "Particle nucleation in emulsion polymerization: I. A theory for homogeneous nucleation", J. Polym. Sci., Polym. Chem. Ed., 16, 536-609, 1978.
9. Harkins, W. D. "A general theory of the mechanism of emulsion polymerization", J. Amer. Chem. Soc., 69, 1428-1444, 1947.
10. Harrick, N. J. "Internal Reflection Spectroscopy", Wiley-Interscience, New York, 1-342, 1967.
11. Hua, H., Dubé, M. A. "Off-line monitoring of butyl acrylate, methyl methacrylate and vinyl acetate homo- and copolymerizations in toluene using ATR-FTIR spectroscopy", Polymer, 42, 6009-6018, 2001.
12. Hua, H., Dubé, M. A. "Terpolymerization monitoring with ATR-FTIR spectroscopy" J. Polym. Sci.: Part A: Polym. Chem. 39, 1860-1876, 2001.
13. Hua, H., Dubé, M. A. "In-line monitoring of emulsion homo- and copolymerizations using ATR-FTIR spectrometry" Polym. Reaction Eng. J., 10, 21-40, 2002.
14. Jovanovic, R., Dubé, M. A. "Off-line monitoring of butyl acrylate and vinyl acetate homopolymerization and copolymerization in toluene" J. Appl. Polym. Sci., 82, 2958-2977, 2001.

15. Jovanovic, R., Dubé, M. A. "Butyl Acrylate/Vinyl Acetate Emulsion-Based Pressure-Sensitive Adhesives: Empirical Modeling of Final Properties", Can. J. Chem. Eng., 85, 341-349, 2007.
16. Koenig, J. L. "Spectroscopy of Polymers", 2nd Edition, Elsevier, New York, 1-491, 1999.
17. Lovell, P. A., El-Aasser, M. S., "Emulsion Polymerization and Emulsion Polymers", John Wiley and Sons, Inc.: England, 1-515, 1997.
18. Mayo, F. R., Lewis, F. M. "Copolymerization. I. A Basis for Comparing the Behavior of monomers in Copolymerization; The Copolymerization of Styrene and Methyl Methacrylate" J. Amer. Chem. Soc., 66, 1594–1601, 1944.
19. M'Bareck, C. O., Nguyen., Q. T., Metayer, M., Saiter, J. M., Garda, M. R. "poly (acrylic acid) and poly (sodium styrene sulfonate) compatibility by Fourier transform infrared and differential scanning calorimetry", J. Appl. Polym. Sci., 45, 4181-4187, 2004.
20. Odian, G. G. "Principles of Polymerization", 4th Edition; John Wiley and Sons Inc., New York, 1-374, 2004.
21. Roberge, S., Dubé, M.A. "In-line monitoring of styrene/butyl acrylate mini-emulsion polymerization with attenuated total reflectance/Fourier transform infrared spectroscopy", J. Appl. Polym. Sci., 103, 46-52, 2006.
22. Roberge, S., Thesis "Styrene/Butyl Acrylate Mini-Emulsion-Based Pressure Sensitive Adhesives", University Of Ottawa, 2004.
23. Smith, B. C. "Fundamentals of Fourier transform infrared spectroscopy", CRC Press: New York, 1-195, 1996.
24. Smith, W. V., Ewart, R.H. "Kinetics of emulsion polymerization", J. Chem. Phys., 16, 592-599, 1948.
25. Uraneck, C. A., Kennedy, J.P., Tornqvist, E.G.M. "Polymer Chemistry of Synthetic Elastomers", Chapter 4, Interscience Pub., New York, 1968.
26. Urban, M. W. "Attenuated total reflectance spectroscopy of polymers", Washington, DC; Amer. Chem. Soc., 1-256, 1996.

Chapter 3 – Paper on ATR-FTIR In-line Monitoring of St/Bd Emulsion Copolymerization

In-line Monitoring of SBR Emulsion Polymerization using ATR-FTIR Spectroscopy

Marc A. Dubé* and Liang Li
Department of Chemical and Biological Engineering, University of Ottawa
161 Louis Pasteur, Ottawa, ON, K1N 6N5 Canada
*Marc.Dube@uOttawa.ca

Abstract

The copolymerization of styrene/1,3-butadiene in emulsion was monitored in-line using an ATR-FTIR spectroscopic probe. The concentration of monomers was monitored to provide real-time conversion and copolymer composition data. Traditional off-line techniques, gravimetry and ^{1}H-NMR spectroscopy, were compared to the in-line ATR-FTIR data. A univariate method failed to achieve agreement between the in-line and off-line data. On the other hand, a multivariate calibration method using the full reaction spectra displayed no significant differences between the off-line and in-line data sets at a 95% confidence level. It was demonstrated that ATR-FTIR spectroscopy is a reliable tool for monitoring conversion and polymer composition in multi-phase emulsion polymerizations.

Keywords: styrene, 1,3-butadiene, emulsion polymerization, ATR-FTIR spectroscopy, ^{1}H-NMR spectroscopy, in-line monitoring.

Introduction

Styrene butadiene rubber (SBR) is a widely used synthetic rubber for the production of car and light truck tires and truck tire retread compounds. The most important industrial process for SBR manufacture is cold emulsion polymerization in a series of reactors which gives superior physical properties to other SBR products (Sayer et al., 1997).

SBR manufacturers continue to face the challenge of improving their product properties and reducing production costs (Hamielec and MacGregor, 1983). In order to better control the final product's properties and improve process control policies, it is essential to develop reliable and robust sensors to carry out real-time measurements for the polymerization processes (Chien et al., 1990; Baranek et al., 1999; Broadhead, 2003).

Emulsion polymerization is a typical multiphase reaction system in which several phases are usually present: monomer-swollen micelles, monomer droplets, polymer droplets and the aqueous phase. Typical emulsion polymerization recipes consist of a dispersing medium such as water, an emulsifier, monomer(s), initiator and other ingredients such as chain transfer agents, buffers, etc. It is the phase heterogeneity in the presence of water that typically poses the greatest challenge for monitoring emulsion polymerizations. Other challenges may arise such as the coagulation of the latex particles caused by the increasing viscosity during the later stages of the polymerization, run away potential and safety issues caused by the gaseous monomer. Thus, it is a difficult task to control emulsion polymerization processes, especially in light of the lack of robust on-line and in-line measurements for important product properties and key process variables (Lovell and EL-Aasser, 1997; Saenz et al., 1998; Reis et al., 2004). Traditional monitoring techniques, such as gravimetry and ^{1}H-NMR (proton nuclear magnetic resonance) spectroscopy, usually present significant time lags and pose serious challenges when real-time data are required.

In the last decade, several attempts were made to utilize various dielectric, acoustic, and spectroscopic techniques to monitor polymerization reactions (Jovanovic and Dubé, 2001; Fonseca et al., 2009). Recent developments in hardware sensors have been summarized by Dimitratos et al. for on-line conversion and copolymer composition monitoring (Dimitratos et al., 2004). Infrared (IR) and Raman spectroscopic techniques

have shown the most potential (Smith, 1996; Koenig, 1999; Fonseca et al., 2009). Attenuated Total Reflectance Fourier Transform Infrared (ATR-FTIR) spectroscopy is an attractive option because it is affordable, utilizes simple sampling techniques and has straightforward experimental operation. In addition, ATR-FTIR can offer much information about the reaction system at the molecular level while obtaining real-time structure and kinetic information on a polymerization process.

Recently, extensive research has been done on the application of ATR-FTIR spectroscopy to monitor different polymerization systems. The use of a ReactIR™ 1000 reaction analysis system (ASI Applied Systems, Mettler-Toledo Corp.) for the monitoring of solution (in toluene) homo- and copolymerization of monomers from the butyl acrylate/methyl methacrylate/vinyl acetate (BA/MMA/VAc) system has been reported (Jovanovic and Dubé, 2001; Hua and Dubé, 2002; Hua et al., 2004). This was extended to emulsion and miniemulsion polymerization monitoring (Hua and Dubé, 2002; Roberge and Dubé, 2006; Jovanovic and Dubé, 2007).

A number of applications of the ATR-FTIR spectroscopic technique to monitor styrene-containing systems have also been reported. Chatzi et al. reported on the monitoring of ethylhexyl acrylate/styrene emulsion polymerization (Chatzi et al., 1998). Pasquale and Long used the ReactIR™ 1000 to monitor stable free-radical polymerizations of styrene (Pasquale and Long, 1999).

The focus of this work, was to apply ATR-FTIR spectroscopy, coupled with a multivariate statistical approach, in-line to monitor the cold emulsion copolymerization of styrene and 1,3-butadiene. The concentration of each individual monomer and copolymer was collected to calculate the conversion and copolymer composition. ^{1}H-NMR spectroscopy was used for the off-line analysis of polymer composition data while the off-line conversion data were obtained using a conventional gravimetric method. In order to evaluate the monitoring ability of the ATR-FTIR spectroscopic technique, the in-line real-time kinetic data were compared to the off-line data.

Experimental Section

The reagents: Styrene (St), the chain transfer agent (CTA) n-dodecyl mercaptan, sodium formaldehyde sulfoxylate (SFS), cumene hydroperoxide (CHP), and ethylene diamine tetra-acetic acid (EDTA) (the above reagents are all from Sigma-Aldrich), 1,3-Butadiene (Bd) (BOC Gases), Fatty Acid (FA) (Westvaco), Rosin Acid (RA) (Westvaco), were used without any further purification. All components used to perform the characterizations, i.e., benzene-d (Sigma-Aldrich), chloroform-d (Sigma-Aldrich), and tetrahydrofuran (THF) (Sigma-Aldrich) were also used as received.

Experimental Design

"Cold E-SBR" experiments were designed to validate the adequacy of ATR-FTIR spectroscopy in-line monitoring for multiphase emulsion polymerizations by comparing with off-line ^{1}H-NMR data. All liquid-phase recipes were performed with pre-cooling the feed and a reaction temperature of 5°C at a pressure of 50 psig (345 kPa). The following concentrations of ingredients were also kept constant: RA = 2.5 phm, FA = 2.5 phm, KOH = 0.5 phm, CHP = 0.51 phm, SFS = 0.3 phm, CTA = 0.2 phm, and EDTA = 0.18 phm, where phm represents parts per hundred parts of monomer. Batch recipes are shown in the following Table 3.1. From Table 3.1, runs 1, 3, 4 and 8 which cover the whole region of the monomer and polymer concentrations were chosen to build the calibration curve for the ATR-FTIR analysis. Runs 2, 5, and 7, which are in the same concentration range were chosen to validate the model. Runs 7 and 8 employ a typical industrial monomer ratio.

Apparatus

Emulsion copolymerizations of St/1,3-Bd were performed in a Labmax™ setup (Mettler Toledo) which comprises a jacketed 1.2 L stainless steel batch reactor. Mixing at 100 rpm was applied to the reactor contents during the pre-cooling stage by an anchor stirrer and later, at 200 rpm during the reaction time. Due to the safety and run away potential of 1,3 butadiene monomer, the reactor was equipped with a nitrogen line to purge and/or pressurize the reactor, a bottom sampling valve (designed "in-house" using Swagelok™ quick connectors), an initiator-loading cell, a reflux condenser with a vent

line, and a port for the IR probe. The reaction temperature and stirring speed were controlled by Camille® software (Mettler-Toledo). The reaction pressure was adjusted by feeding nitrogen to the system.

Table 3.1: Batch recipes

		St (phm)[1]	Bd (phm)	Water (phm)
Runs used for calibration model	**Run 1**	**80**	**20**	**180**
	Run 3	**70**	**30**	**180**
	Run 4	**40**	**60**	**180**
	Run 8	**25**	**75**	**180**
Runs used for validation	**Run 2**	**75**	**25**	**220**
	Run 5	**60**	**40**	**140**
	Run 7	**25**	**75**	**160**

[1]phm = parts per hundred parts monomer

A ReactIR™ 1000 (ASI Applied Systems, Inc., Mettler Toledo) reaction analysis system was used in-line to collect mid-FTIR spectra (4000-650 cm^{-1}) of the multiphase emulsion copolymerization reactions. A light conduit and a diamond composite probe were inserted into the reactor for non-destructive in-line monitoring in a hostile reaction environment (Jovanovic and Dubé, 2001). The ATR-FTIR diamond composite probe (ReactIR™ 1000, Mettler-Toledo) was positioned about 2 mm above the blades of the agitator to ensure the monitoring of well-mixed latex. Figure 3.1 shows the experimental set-up for this reaction.

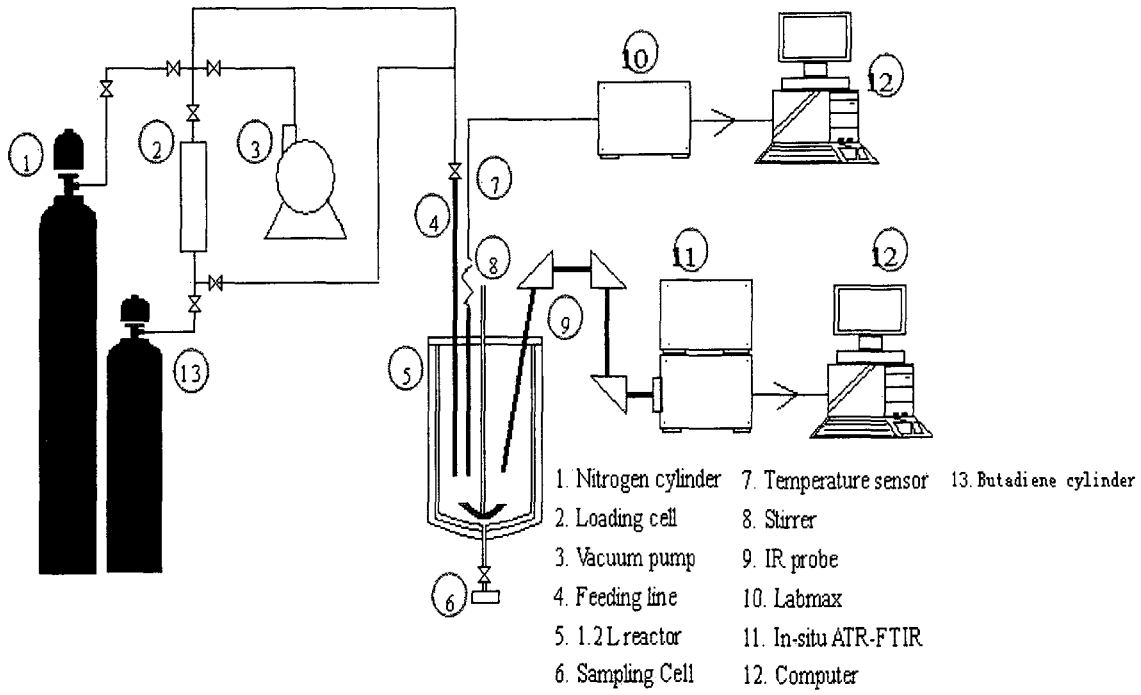

Figure 3.1: Reactor schematic

Experiment Preparation

The diamond composite probe of the IR was inspected and cleaned before connecting to the reactor. An air background spectrum was acquired before adding any ingredients into the reactor.

Water was added to the reactor and a water background spectrum was collected at this point. St, CHP, and DDM were poured into the reactor and purged with nitrogen gas for 1 h. Stirring at 100 rpm was applied to the reactor contents during this stage by an anchor stirrer.

The 1,3-butadiene gas cylinder was pre-cooled and transferred into a pre-cooled 1 L feed vessel. The feed vessel was weighed (the empty vessel was weighed previously). The weight of Bd gas inside the vessel was therefore known. The Bd gas monomer feed vessel was then connected to the reactor and a valve opened to transfer its contents to the reactor. The pressure of the reactor was typically at 40 psig (276 kPa) when the transfer was complete.

A mixed initiator solution consisting of SFS, $FeSO_4$, and water was purged with nitrogen for 2 min. It was then added to the reactor via a pressurized initiator-loading cell to start the reaction. The pressure in the reactor was at 50 psig (345 kPa) at this point.

The multiphase "cold" emulsion copolymerization of St/1,3-Bd was run at 5°C with an initial pressure of 50 psig (345 kPa). Reaction monitoring and process temperature monitoring were started simultaneously after the initiator had been charged. This corresponded to polymerization time zero. During the reaction, at suitable time intervals, samples were taken through a pre-weighed sampling vessel, which ended with Swagelok™ quick connectors. The sample vessel was then weighed and its contents poured into a pre-weighed dish in the fume hood and allowed to dry. The detailed experimental/sampling procedure is presented in Appendix C.

Characterization

The overall conversion of the "cold" E-SBR copolymerization, X (wt. fraction), was measured by gravimetry and was based on total monomer conversion. The overall conversions for all the runs are listed in Appendix B. The individual conversions for each monomer were calculated by the combination of overall conversion and individual copolymer composition, which were obtained from the results of ^{1}H-NMR spectroscopy.

Samples were taken from the reactor by a pre-weighed empty sample vessel and then reweighed for the total weight including the sample latex. Samples were poured into pre-weighed dishes, were dried in a fume hood at room temperature for at least one day, and then in a vacuum oven at about 30°C for another day. The following equation was used to calculate the weight fraction of solids:

$$weight\ fraction\ solids = \frac{(wt.of\ dried\ sample\ and\ dish - wt.of\ empty\ dish)}{(wt.of\ \text{vessel}\ and\ sample - wt.of\ empty\ \text{vessel})} \qquad (3.1)$$

The conversion was calculated after correcting for all the other reagents present in the sample using the following equation:

$$X(wt.fraction) = \frac{(wt.fr.\ solids - wt.fr.\ other\ solids)}{(wt.fraction\ monomers\ initially)} \qquad (3.2)$$

Proton nuclear magnetic resonance spectroscopy (^{1}H-NMR) has been widely applied to determine the average or cumulative composition of copolymers. Some research has

also been done with SBR samples (Li et al., 2006). The ^{1}H-NMR analysis was conducted using the ISO 21561 (2005) standard method.

Deuterated chloroform ($CDCl_3$) was used to dissolve the dried latex samples Analyses were carried out at room temperature. With a Bruker AMX-400 Fourier transform ^{1}H-NMR spectrometer. The acquisition time was 4.6 seconds and 16 scans were performed per readout. The areas under the appropriate absorption peaks of the spectra were used to estimate the relative amounts of monomer bound in the copolymer.

The signal intensities of the ^{1}H-NMR spectrum were integrated over each of areas A, B and C defined in Table 3.2. An example of a ^{1}H-NMR spectrum indicating the areas A, B and C is shown in Figure 3.2. As indicated in the table and figure, the 6.1-7.7 ppm range (area C) corresponds only to 5 protons of styrene, while the 4.3-5.0 ppm range (area A) is only related to 2 protons of 1,2-butadiene. The 5.0-6.1 ppm range (area B) represents the combined effect of 1 proton of 1,2- and 2 protons of 1,4-butadiene.

Table 3.2: Definition of signal integration areas

Area	**Signal integration range**
A	From 4.3 ppm to minimum intensity point around 5.0 ppm
B	From minimum intensity point around 5.0 ppm to minimum intensity point around 6.1 ppm
C	From minimum intensity point around 6.1ppm to 7.7 ppm

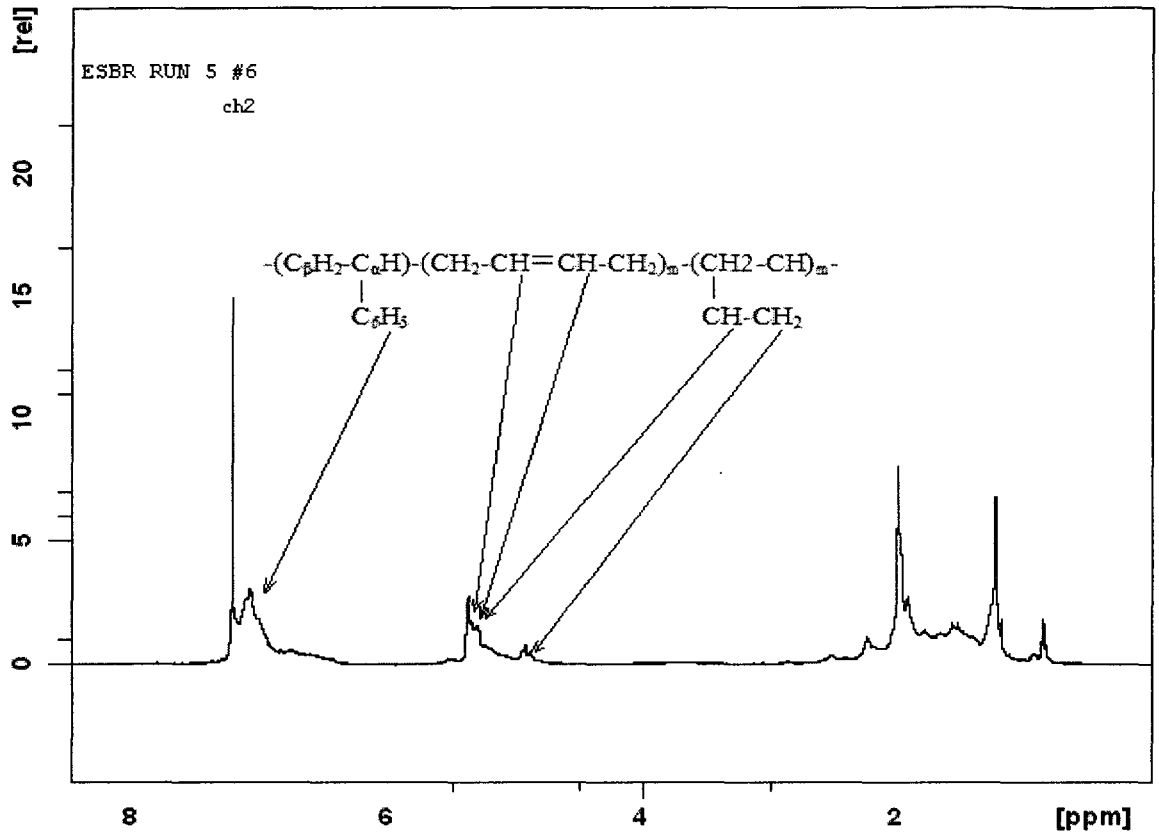

Figure 3.2: ^{1}H-NMR spectrum of cold emulsion styrene/1,3 butadiene copolymer showing relevant peak assignments

The relative composition of each monomer was calculated by the area ratios obtained by integration of the peaks over these ranges. The content of each component (1,4-bond and 1,2-vinyl bond) of the butadiene portion and the styrene content, were calculated using equations (3.3) to (3.6)

$$\%St = \frac{(C/5)\times 104}{(C/5)\times 104 + (B/2 + A/4)\times 54}\times 100 \qquad (3.3)$$

$$\%Bd = \frac{(B/2 + A/4)\times 54}{(C/5)\times 104 + (B/2 + A/4)\times 54}\times 100 \qquad (3.4)$$

$$\%Bd_{1,2} = \frac{A/2}{B/2 + A/4}\times 100 \qquad (3.5)$$

$$\%Bd_{1,4} = \frac{B/2 - A/4}{B/2 + A/4}\times 100 \qquad (3.6)$$

where %St is the styrene content of the SBR in mass%, %Bd is the butadiene content of the SBR in mass%, $\%Bd_{1,2}$ is the 1,2-vinyl bond content of the butadiene portion of the SBR in mol%, and $\%Bd_{1,4}$ is the 1,4 bond content of the butadiene portion of the SBR in mol%.

ATR-FTIR Spectroscopy (Multivariate method)

ATR-FTIR spectroscopy was used to monitor the overall and individual monomer conversions according to the multivariate statistical method described by Roberge and Dubé (2006). For this study, 128 scans and a resolution of 4 cm^{-1} were assumed to give a satisfactory signal to noise ratio and the reaction spectra were acquired every 2 min to ensure continuous monitoring.

The absorbance of different functional groups inside the monomers or polymers was monitored over the course of the reaction. Each functional group was associated with a characteristic peak and the concentration of a component was proportional to the absorbance, which could be measured as peak height, peak height ratio, and peak area or peak area ratio. Real-time peak profiles of monomers (changes in absorption for a specific component) were used to calculate the conversion and the copolymer composition. Figure 3.3 gives an example of an ATR-FTIR reaction spectrum showing some peaks corresponding to different functional groups.

The following expression was used to obtain the conversion of the individual monomers, x, in the reaction mixture:

$$x \text{ (mol fraction)} = 1 - \frac{\text{peak height at time } t}{\text{peak height at time } t = 0} \qquad (3.7)$$

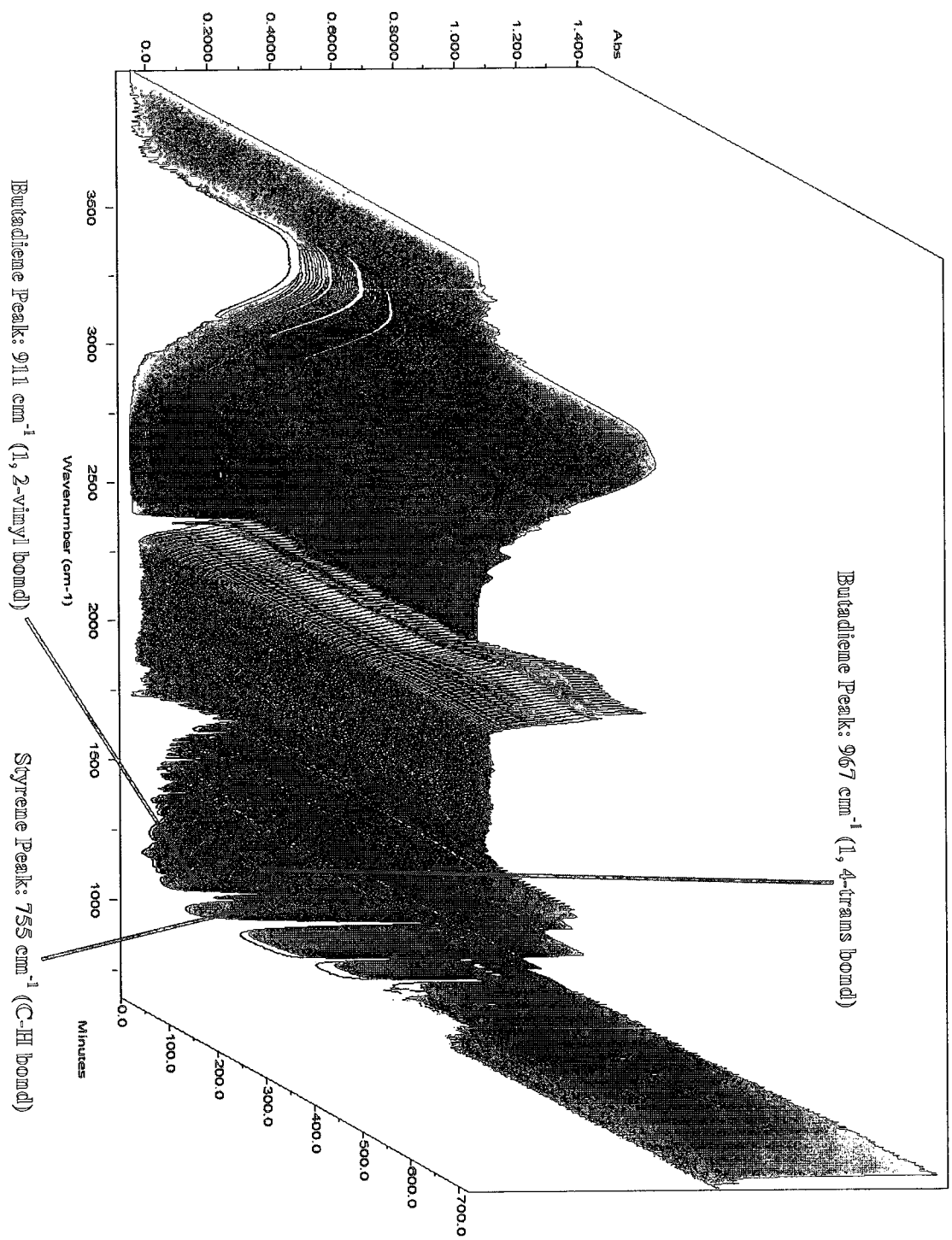

Figure 3.3: Common monomer peaks in the copolymerization of Styrene/1,3 Butadiene (weight ratio 40/60)

where peak height at time t = 0 represents the absorbance of the component in the reaction mixture prior to polymerization. Overall conversion, X, can be expressed in mol or mass fraction using the following expression:

$$X \text{ (mol fraction)} = \frac{n_1}{n_1 + n_2} x_1 \text{ (mol fraction)} + \frac{n_2}{n_1 + n_2} x_2 \text{ (mol fraction)} \qquad (3.8)$$

where $\frac{n_i}{n_i + n_j}$ represents the mole fraction of monomer i in the reaction mixture. The expression could also be written as a function of mass fraction:

$$X \text{ (mass fraction)} = \frac{m_1}{m_1 + m_2} x_1 \text{ (mol fraction)} + \frac{m_2}{m_1 + m_2} x_2 \text{ (mol fraction)} \qquad (3.9)$$

where $\frac{m_i}{m_i + m_j}$ represents the mass fraction of monomer i in the reaction mixture.

Results and Discussion

Typical reaction conversion data including overall conversion calculated by gravimetry and that of the individual monomers calculated by gravimetry and ^{1}H-NMR spectroscopy are shown in Figure 3.4. As was typical of most runs, complete conversion of St monomer was achieved while the conversion of Bd was not.

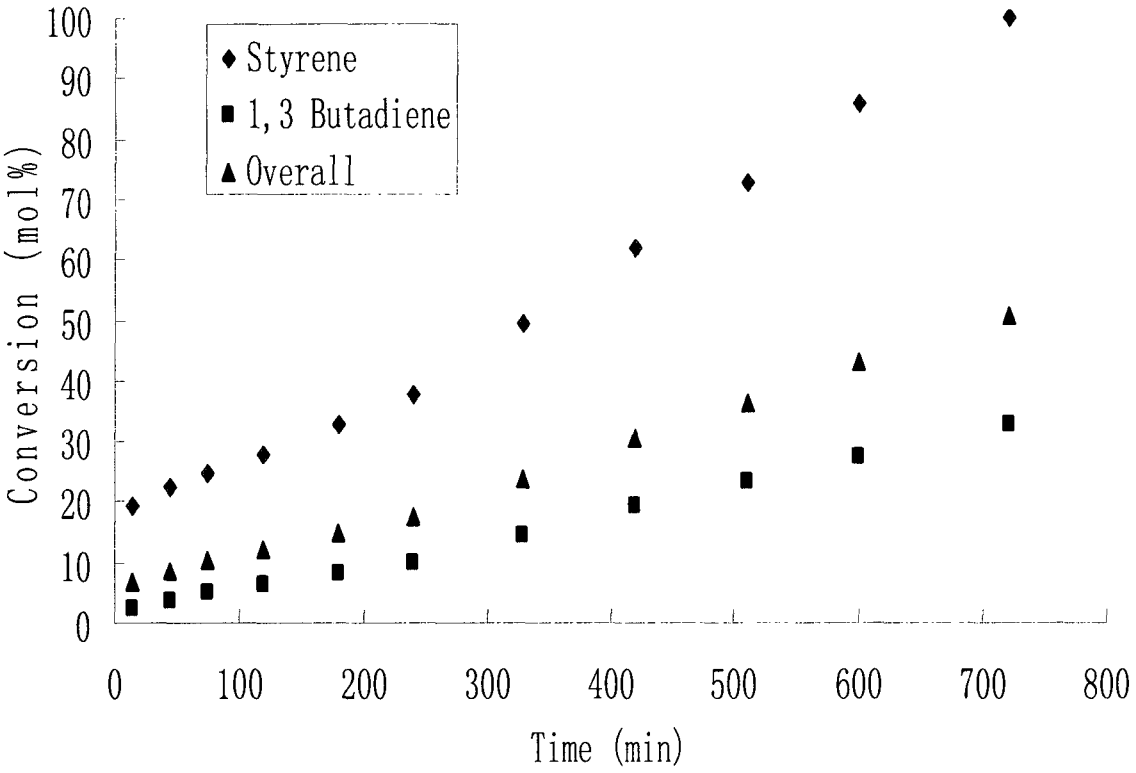

Figure 3.4: Conversion vs. time plot for Run 4 (St:Bd = 40:60 mol:mol)

The overall conversion for runs 1, 3, 4 and 8 are shown in Figure 4.5. The rate of polymerization (slope of the conversion vs. time plot) appears to increase, for the most part, with an increase in the St monomer concentration. This is due to the high monomer reactivity ratio for St relative to that of Bd. This is also evident from the individual monomer conversion plots (Figures 3.6 and 3.7).

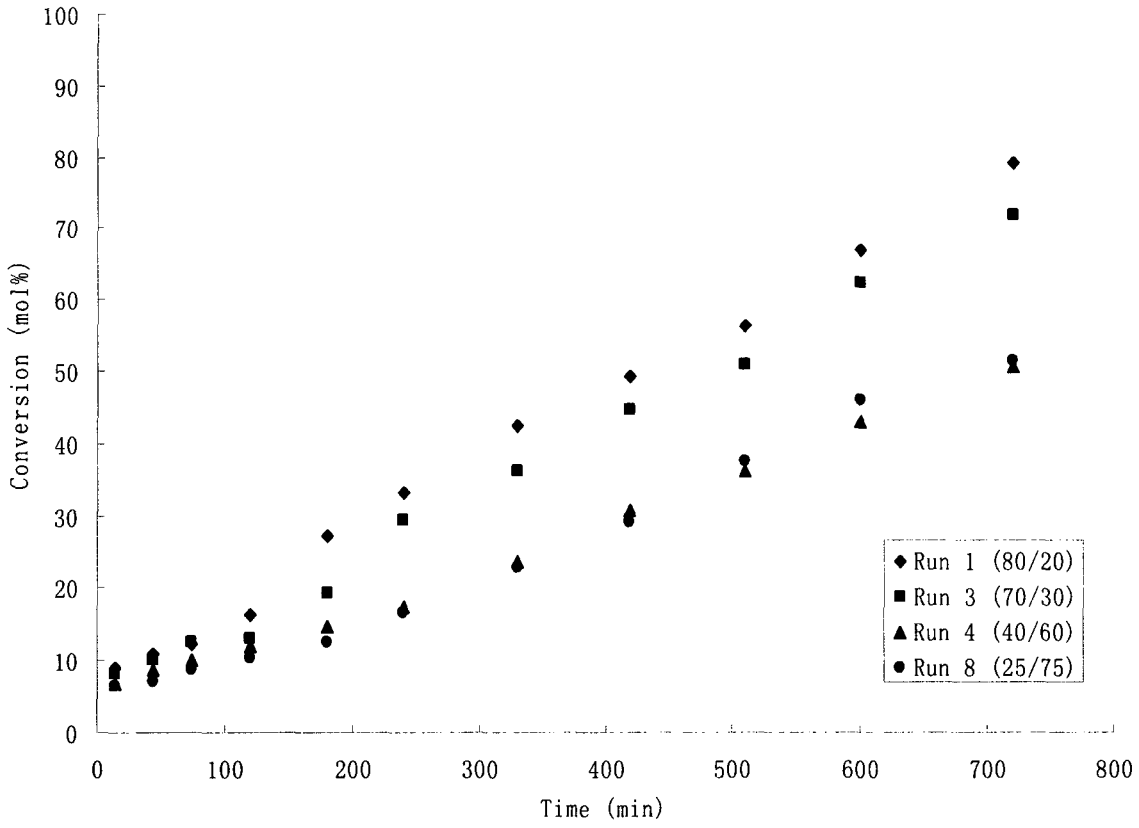

Figure 3.5: Overall monomer conversion vs. time for runs 1, 3, 4 and 8

Runs 7 and 8 were performed at the same monomer feed composition ratios but at different monomer:water ratios. Figures 3.8, 3.9 and 3.10 show the overall monomer, St monomer and Bd monomer conversions, respectively, vs. time. It is evident from these figures that the rate of polymerization of the Bd increased slightly with an increase in water concentration whereas that of St decreased slightly. For St, it may be because the decrease in monomer concentration. On the other hand, for Bd, it will increase the concentration of gaseous phase in the upper part of the reactor. The overall effect was an increase in the overall monomer conversion rate with an increase in water concentration. This may be because a more dispersed medium decreases the viscosity of the reaction system.

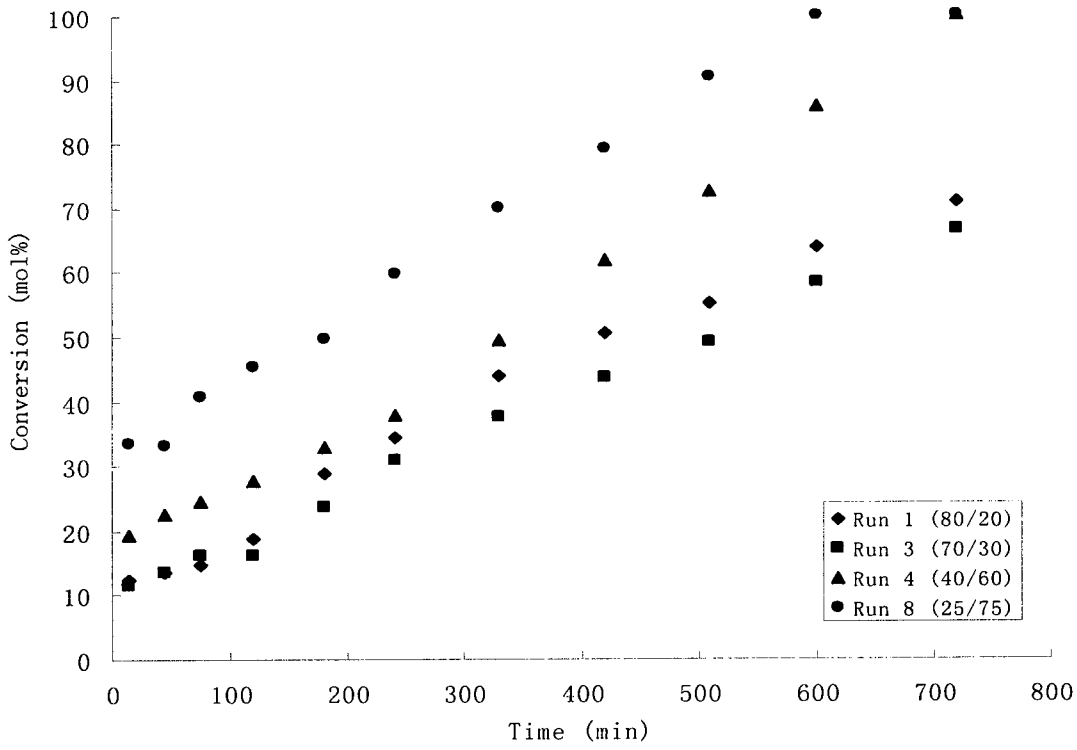

Figure 3.6: Styrene monomer conversion vs. time for runs 1, 3, 4 and 8

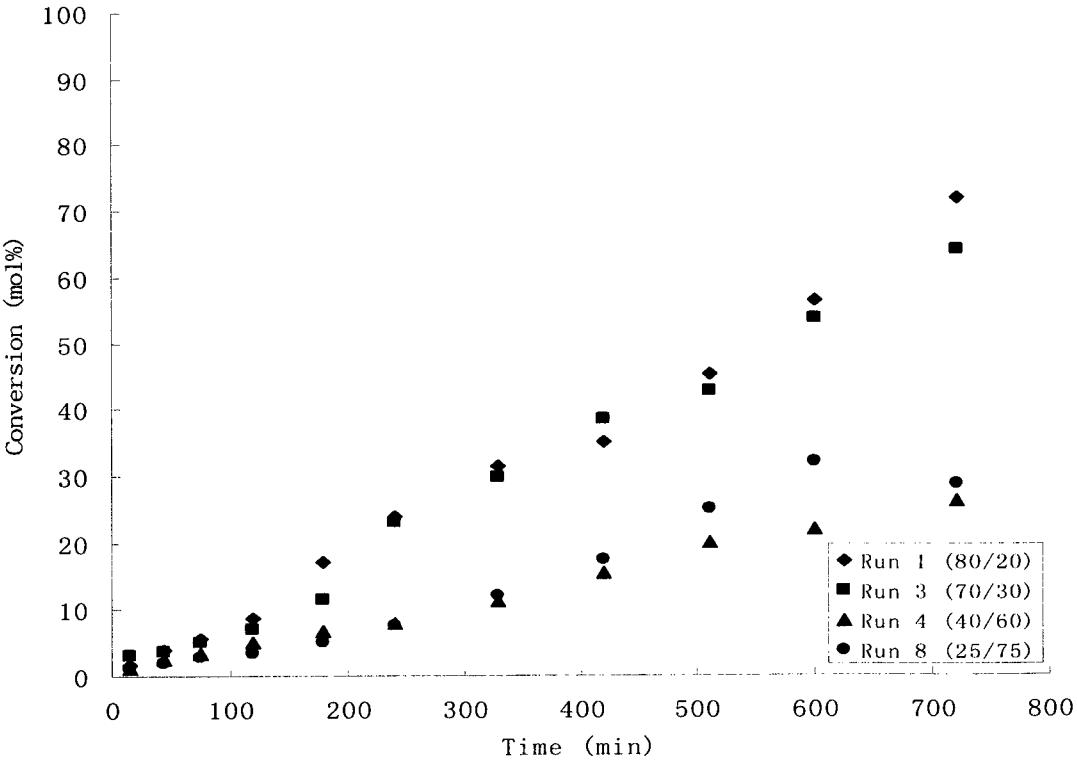

Figure 3.7: 1,3-butadiene monomer conversion vs. time for runs 1, 3, 4 and 8

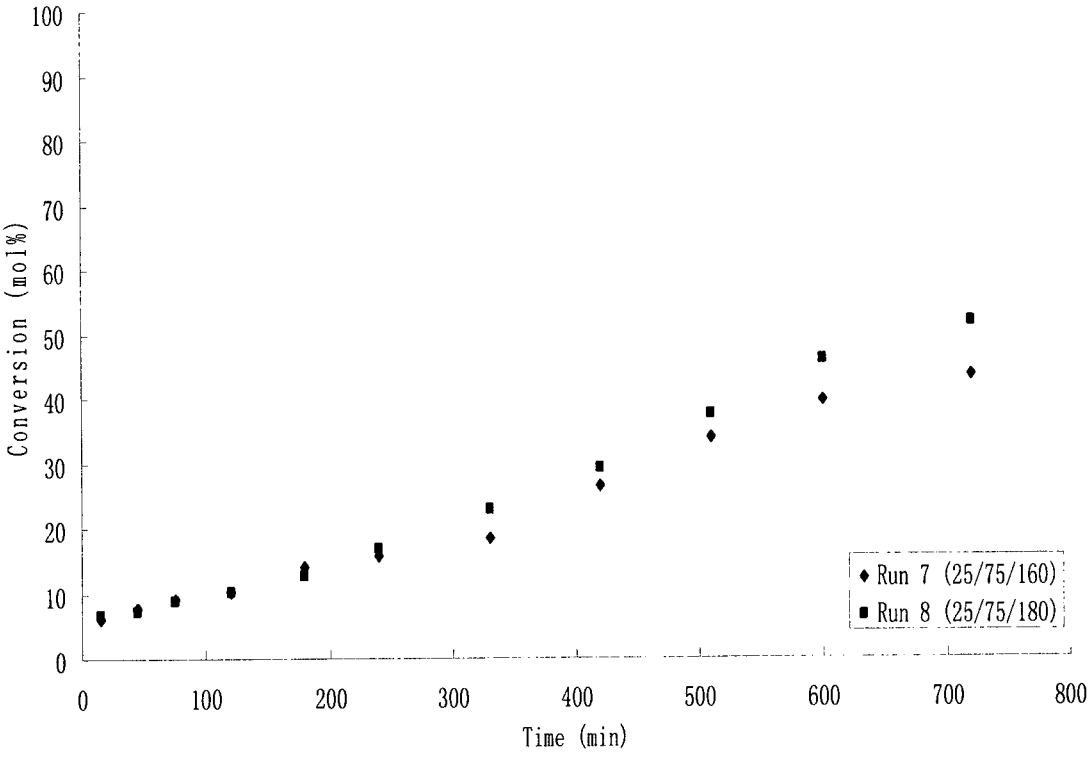

Figure 3.8: Overall monomer conversion vs. time for runs 7 and 8

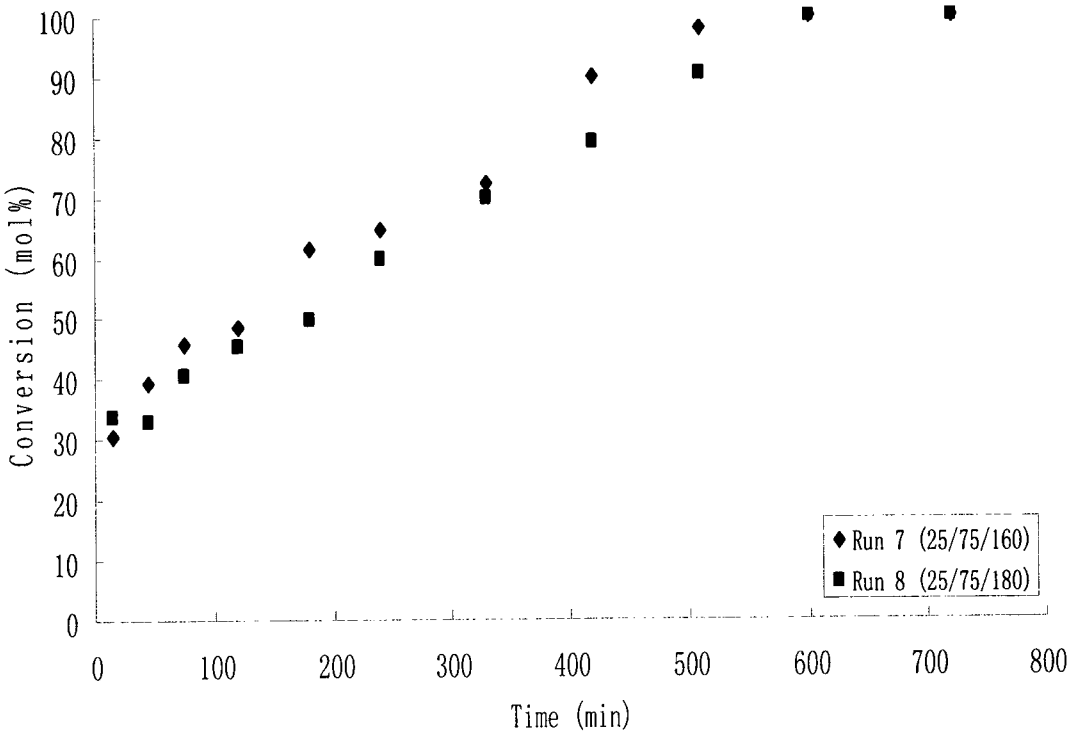

Figure 3.9: Styrene monomer conversion vs. time for runs 7 and 8

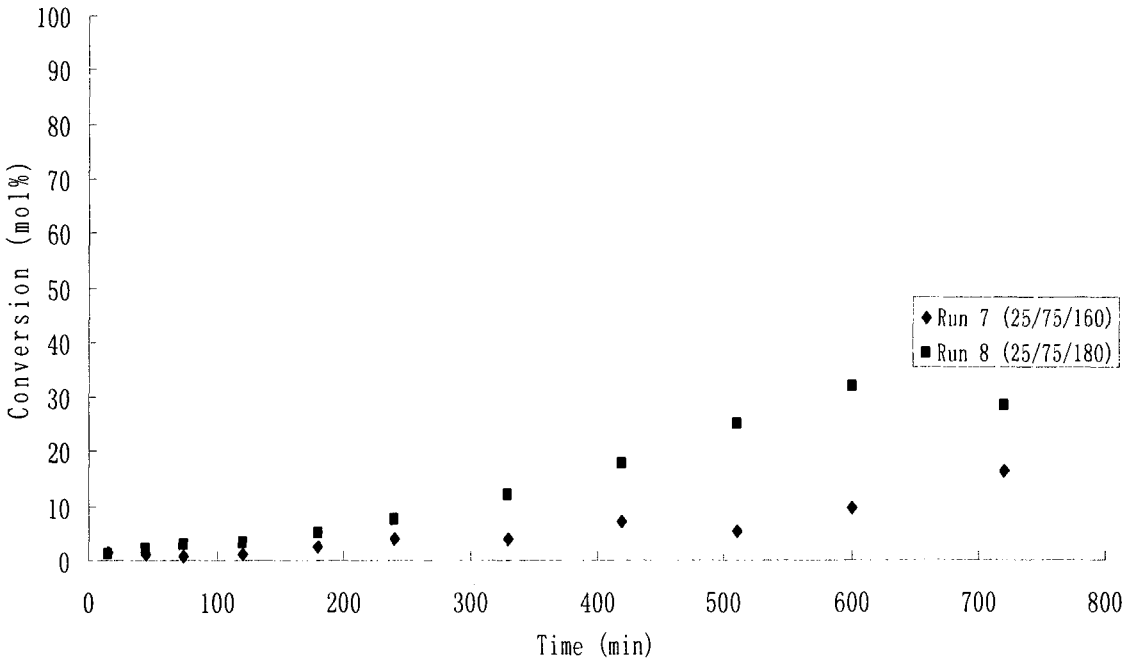

Figure 3.10: 1,3-butadiene monomer conversion vs. time for runs 7 and 8

Univariate method

All reactions were analyzed using a Univariate method. Because a single peak could not show all the variables contaminated by the reaction, poor results were achieved when tracking the absorbance of different monomer (or polymer) peaks for most of the reactions. Hence, it was decided to employ a multivariate method based on Partial Least Square (PLS) statistics.

Multivariate method

Forty-four off-line samples from the runs shown in Table 1 were used as standards to build a calibration model for the ATR-FTIR multivariate analysis. In order to develop a good calibration curve, a background spectrum of a mixture of water and emulsifiers was collected for each reaction. As part of the ReactIR™ 1000 system set up, the background spectrum (Figure 3.11) was automatically subtracted from the reaction spectra. Figure 3.12 shows a typical reaction spectrum of cold SBR emulsion polymerization.

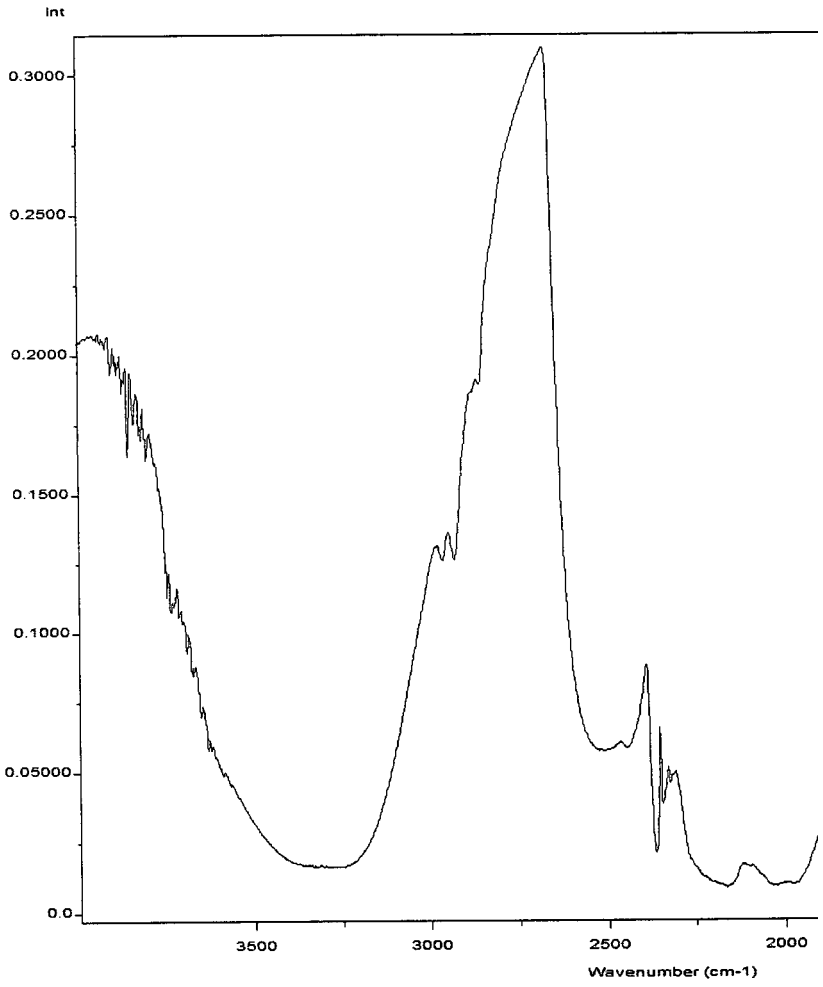
Int
0.3000
0.2500
0.2000
0.1500
0.1000
0.05000
0.0
3500
3000
2500
2000
Wavenumber (cm-1)

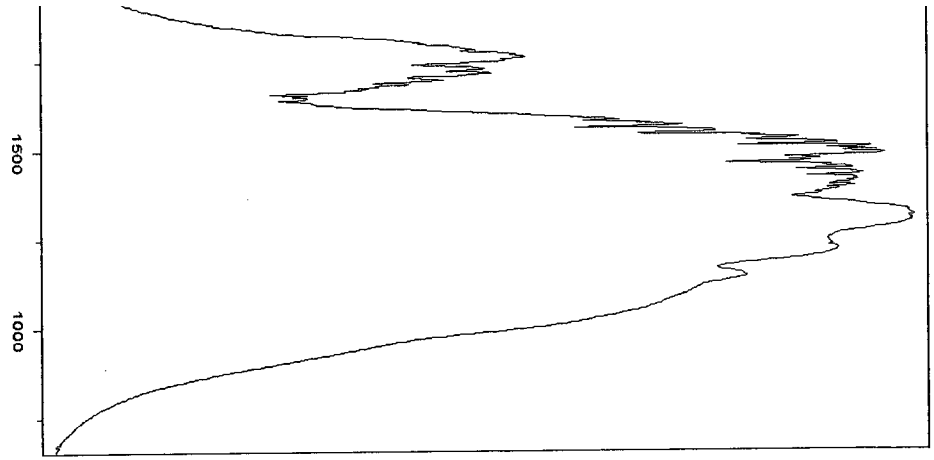

Figure 3.11: Typical background spectra for cold SBR emulsion polymerization

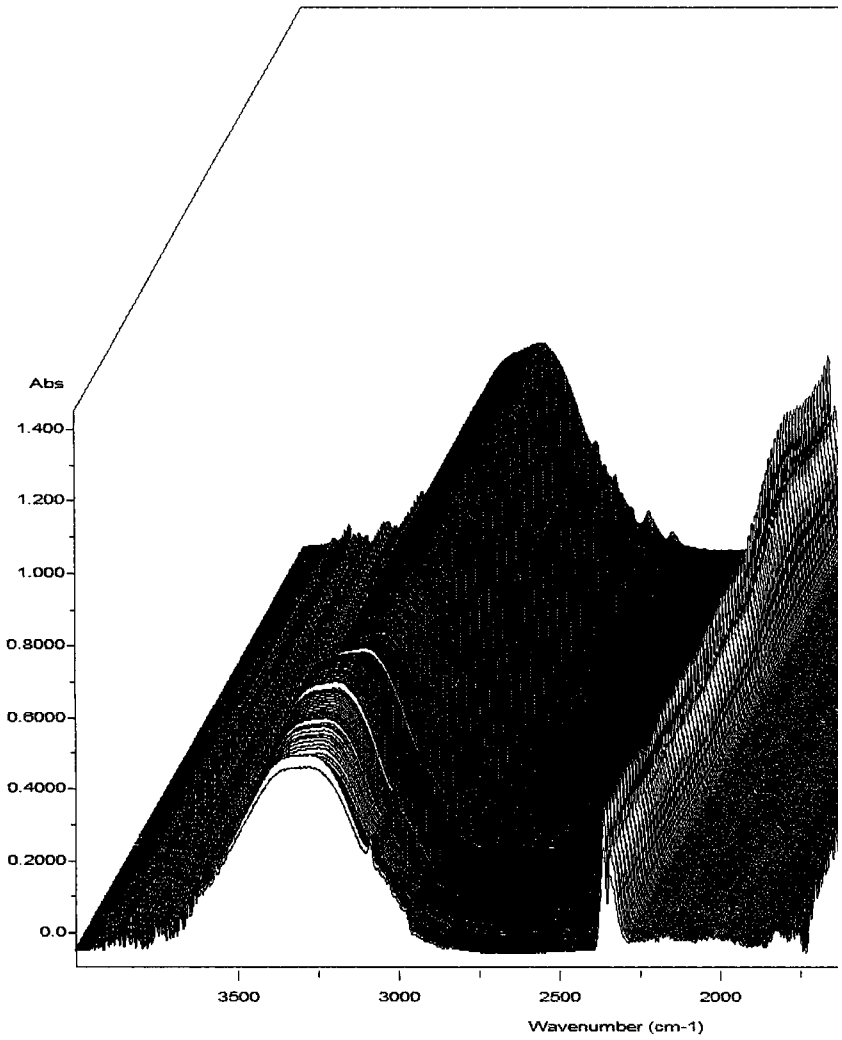
Abs
1.400
1.200
1.000
0.8000
0.6000
0.4000
0.2000
0.0
3500
3000
2500
2000
Wavenumber (cm-1)

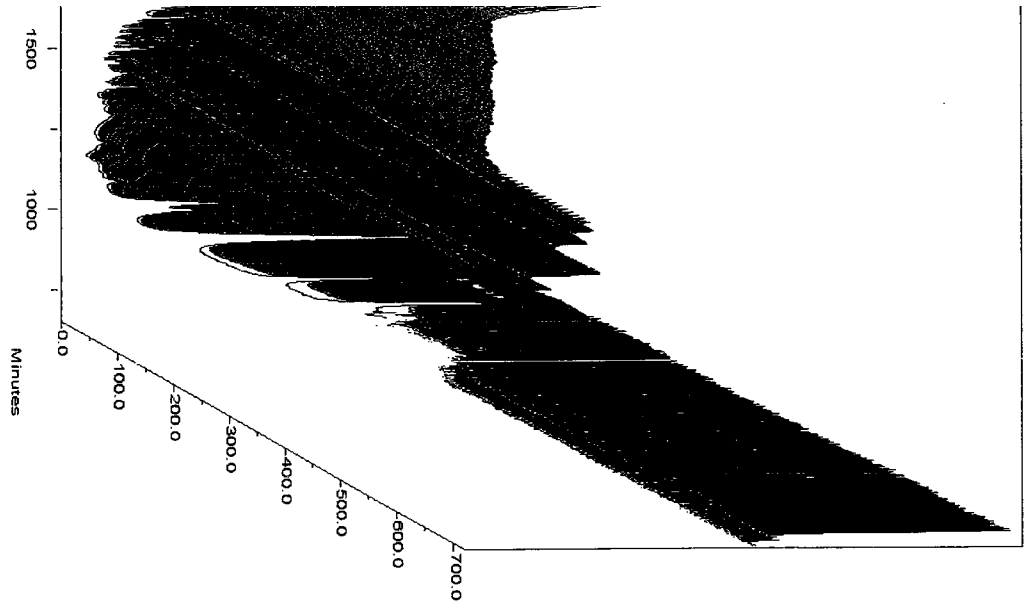

Figure 3.12: Typical reaction spectra for cold SBR emulsion polymerization (weight ratio 40/60)

A single sample reaction spectra is shown in Figure 3.13. Each spectra was selected corresponding to a real-time off-line sample and normalized. The calibration curve was then built from the normalized spectra. Figure 3.14 shows 77 normalized spectra used for calibration and validation.

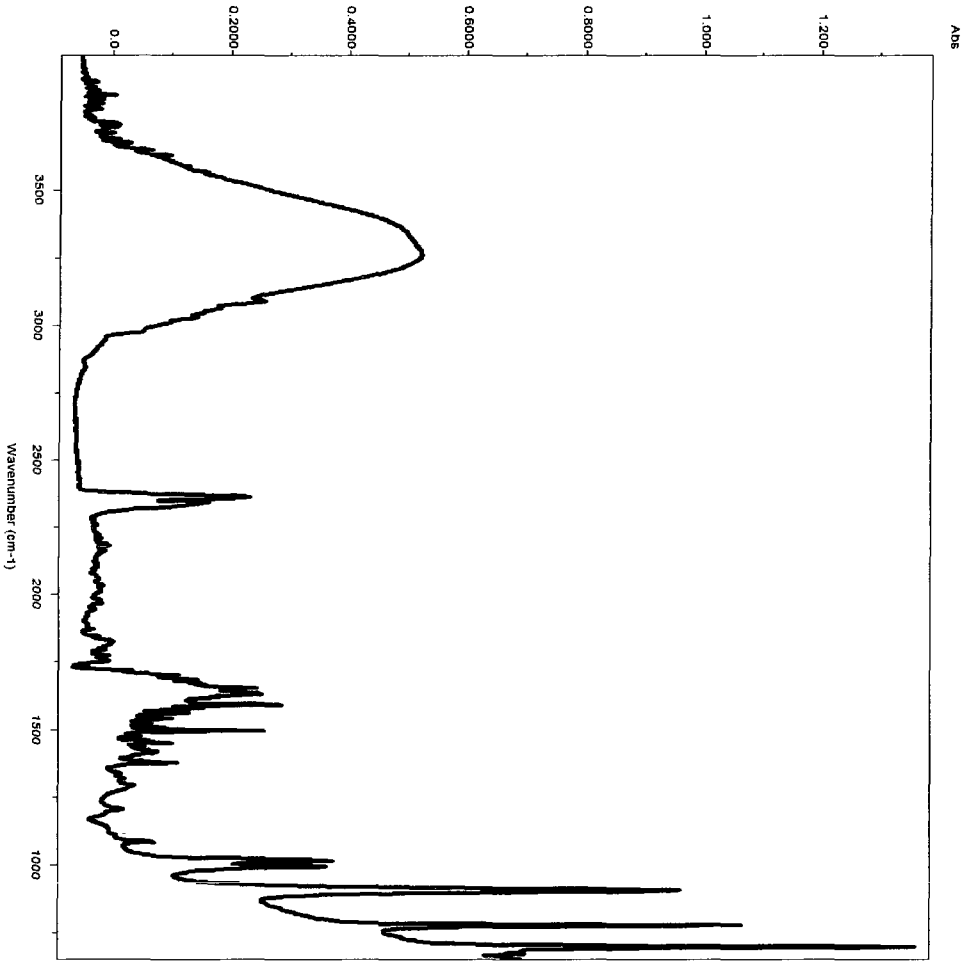

Figure 3.13: Single sample reaction spectra for cold SBR emulsion polymerization

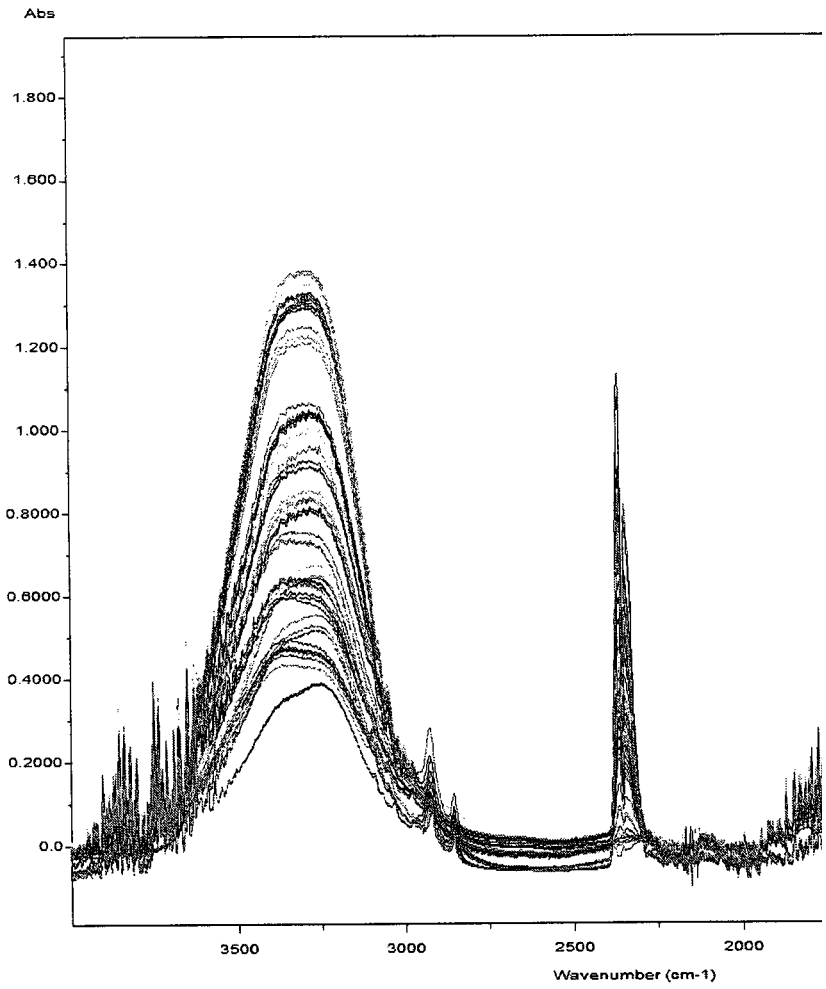
Abs
1.800
1.600
1.400
1.200
1.000
0.8000
0.6000
0.4000
0.2000
0.0
3500
3000
2500
2000
Wavenumber (cm-1)

Figure 3.14: All normalized standard spectra from real-time reaction

The calibration model was built with QuantIR version 2.1 software (ASI Applied Systems 1996, Mettler Toledo) by the Partial Least Squares (PLS) method. As required by the PLS method, a set of peak regions of interest needed to be chosen. These peak regions were identified *a priori* using information from an IR handbook. The peaks of interest are shown in Table 3.3 for Bd and Table 3.4 for St. A number of key spectra were then automatically selected, called factors, according to the selected peak regions. Some of the factors may be contaminated with noise or other information which is not related to the targets. Hence, the PRESS (Predicted Residual Error Sum of Squares) analysis was used to optimize the number of factors for the calibration. The PLS calibration error is improved when the PRESS value decreases, since factors contaminating useful information are added to the analysis. The factors resulting in the minimum PRESS value were used for calibration.

Table 3.3: Butadiene peak assignment

Butadiene Monomer	
Spectral Region (cm^{-1})	Absorbance Assignment
930	-CH= Stretching
1660	C=C Stretching
1800	$C=CH_2$ stretching
<3000	-C-H Stretching
>3000	-C=CH Carbon-Hydrogen Bond Stretching

(Source: http://www3.wooster.edu/chemistry/is/brubaker/ir/ir_spectrum.html)

Table 3.4: Styrene peak assignment (Rivard, 2002)

Styrene Monomer		**Poly(styrene)**	
Spectral Region (cm^{-1})	Absorbance Assignment	Spectral Region (cm^{-1})	Absorbance Assignment
3081	$=CH_2$ stretching		
3060	Ring C-H stretching vibration	3028	Ring -CH= stretching
3027	Ring C-H stretching vibration		$-CH_2$ asymmetric stretching
3010	-CH= stretching	2927	$-CH_3$ asymmetric stretching
1630	C=C stretching	2858	
1602	Ring quadrant stretching	1599	Ring quadrant stretching
1576	Ring quadrant stretching		
1495	Ring semi-circle stretching	1491	Ring semi-circle stretching
1449	Ring semi-circle stretching	1452	Ring semi-circle stretching
1412	$=CH_2$ deformation	1367	$-CH-CH_2$ wag
122	C-CH= stretching	1166	$-CH-CH_2$ wag
1082	Ring semi-circle stretching	1066	Ring semi-circle stretching
1021	Ring semi-circle stretching	1027	Ring semi-circle stretching
991.8	-CH= wag		
906.9	$-CH_2$ wag		
773.7	Ring C-H wag	758	Ring C-H wag
696.6	Ring bending	695.1	Ring bending

Several combinations of peak regions were tested. The set of peak regions shown in Table 3.5 gave the best results.

Table 3.5: Set of peak regions used for the multivariate calibration

Peak Regions	**1**	**2**	**3**	**4**	**5**	**6**
cm^{-1}	**650-1499**	**1580-1610**	**1860-1837**	**2300-2390**	**2790-3110**	**3695-3737**

Initially, a maximum number of 43 factors, which corresponded to the number of standard spectra less one, were chosen to establish the model. After the PRESS analysis, 22 factors were chosen to represent the St Concentration and 16 factors were chosen for the Bd concentration. Figure 3.15 shows a factor used in this analysis and Figure 3.16 shows the PRESS analysis.

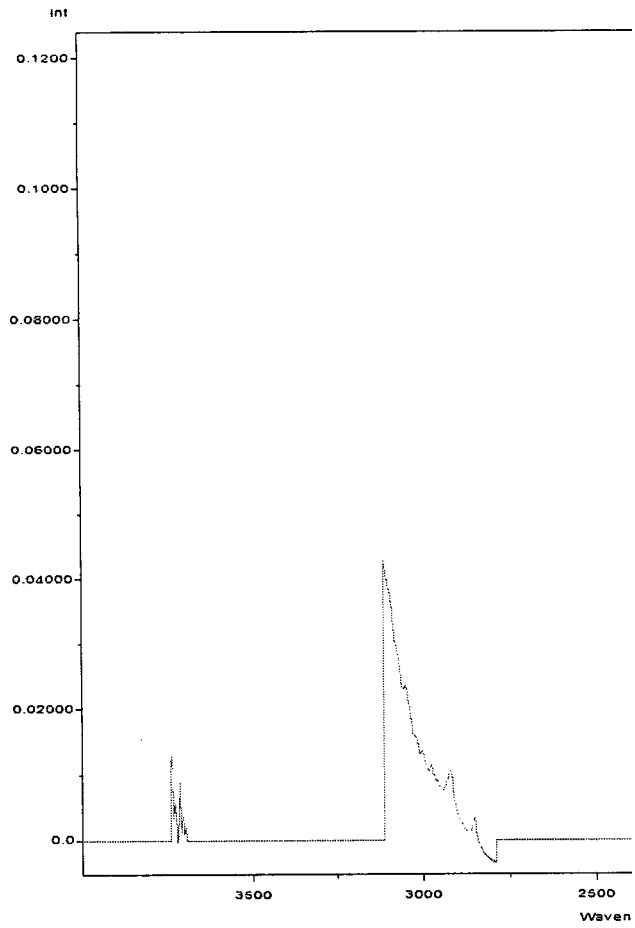
Int
0.1200
0.1000
0.08000
0.06000
0.04000
0.02000
0.0
3500
3000
2500
Waven

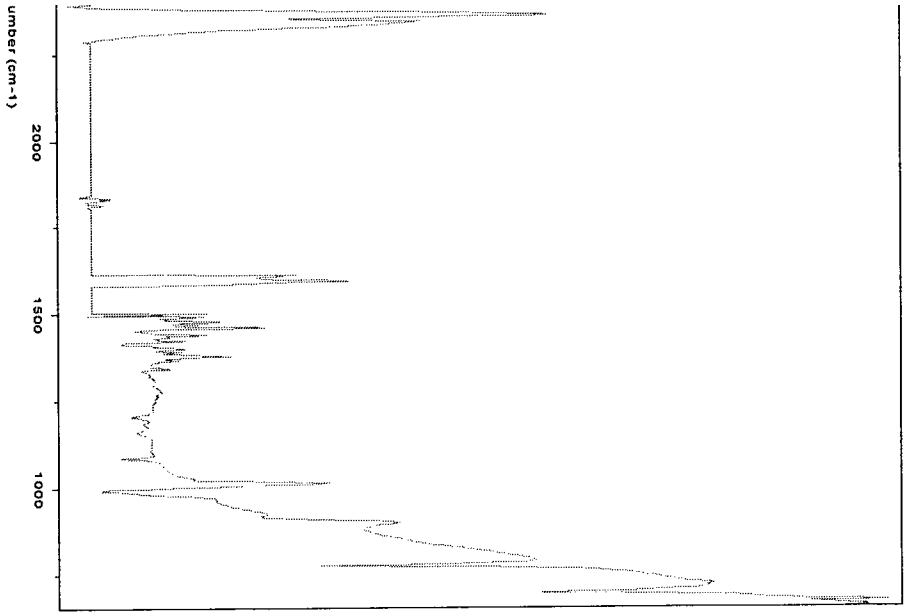

Figure 3.15: A factor for the PRESS analysis

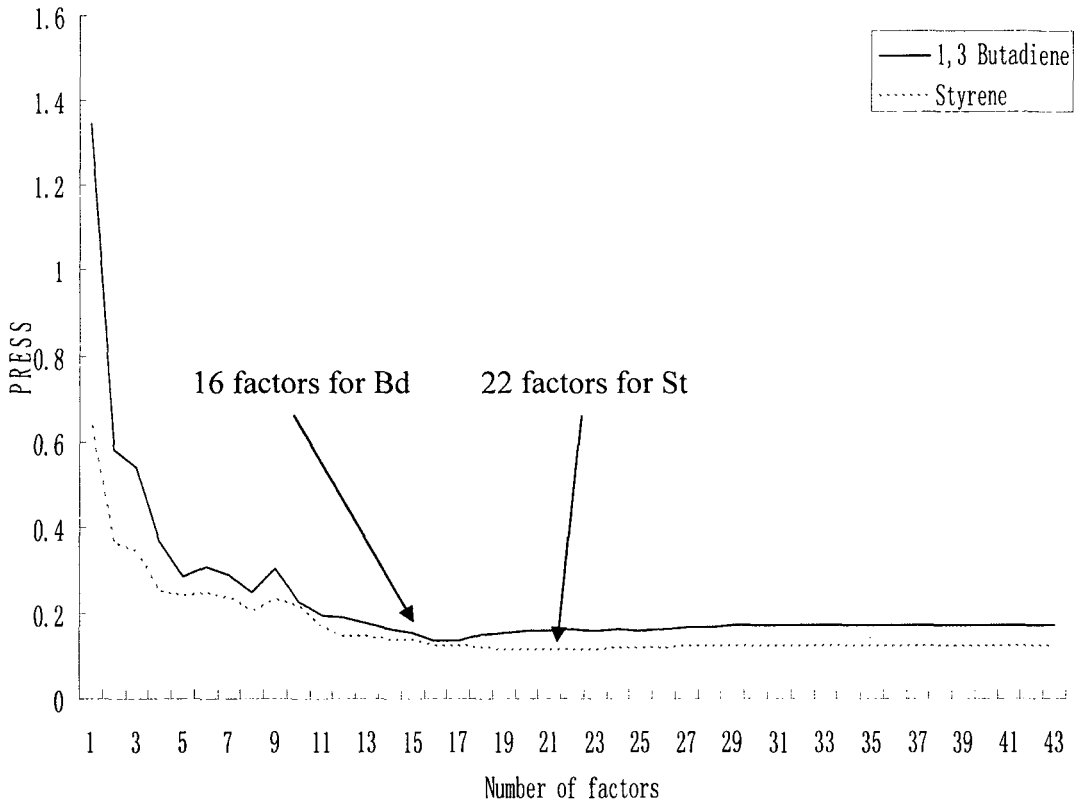

Figure 3.16: PRESS analysis for the PLS model

The calibration curves for St and Bd built using the PLS model are shown in Figures 3.17 and 3.18, respectively. The correlation coefficients were 0.9999 for St and 0.9993 for Bd, suggesting that successful calibration models were constructed. The models were then experimentally validated for both St and Bd using runs 2, 5 and 7 (see Table 3.1). Figures 3.19 and 3.20 show the model predictions vs. actual measurements for St and Bd, respectively, for runs 2, 5 and 7.

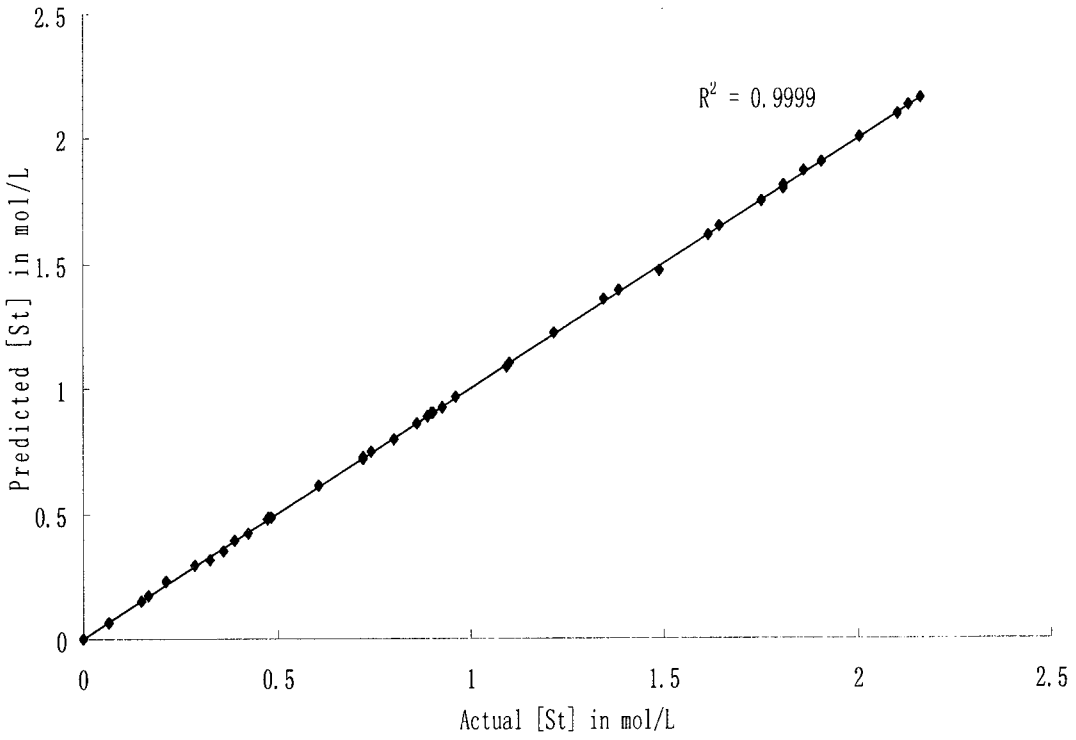

Figure 3.17: Styrene concentration calibration

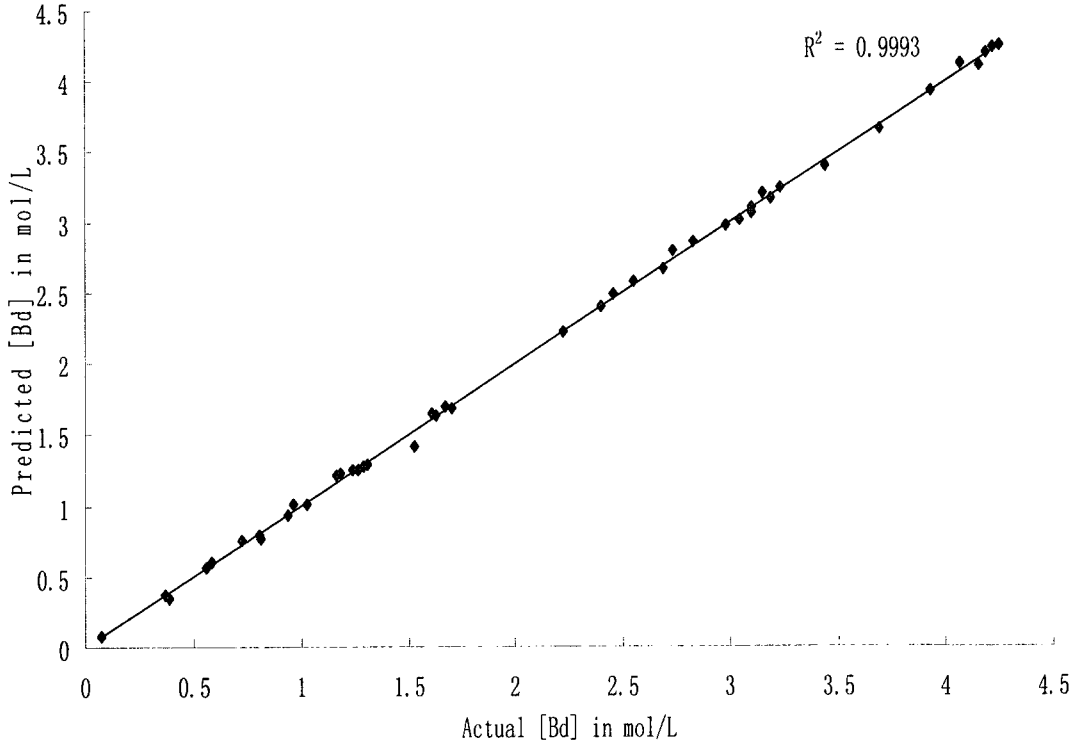

Figure 3.18: 1,3 Butadiene concentration calibration

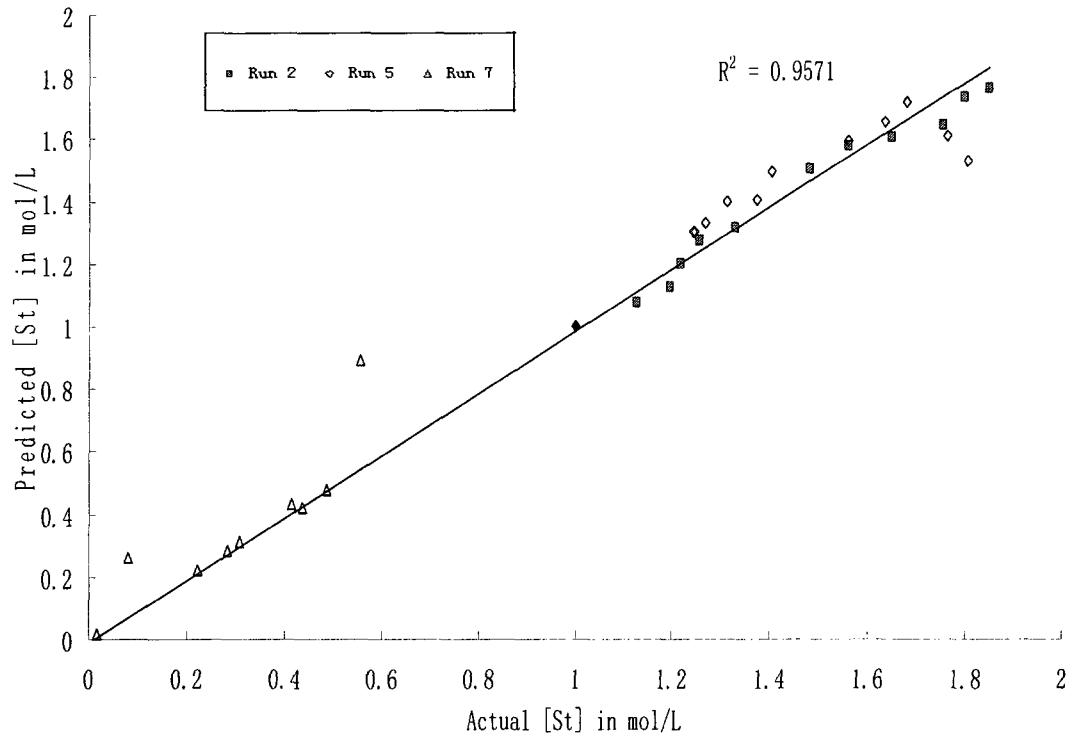

Figure 3.19: Styrene concentration validation

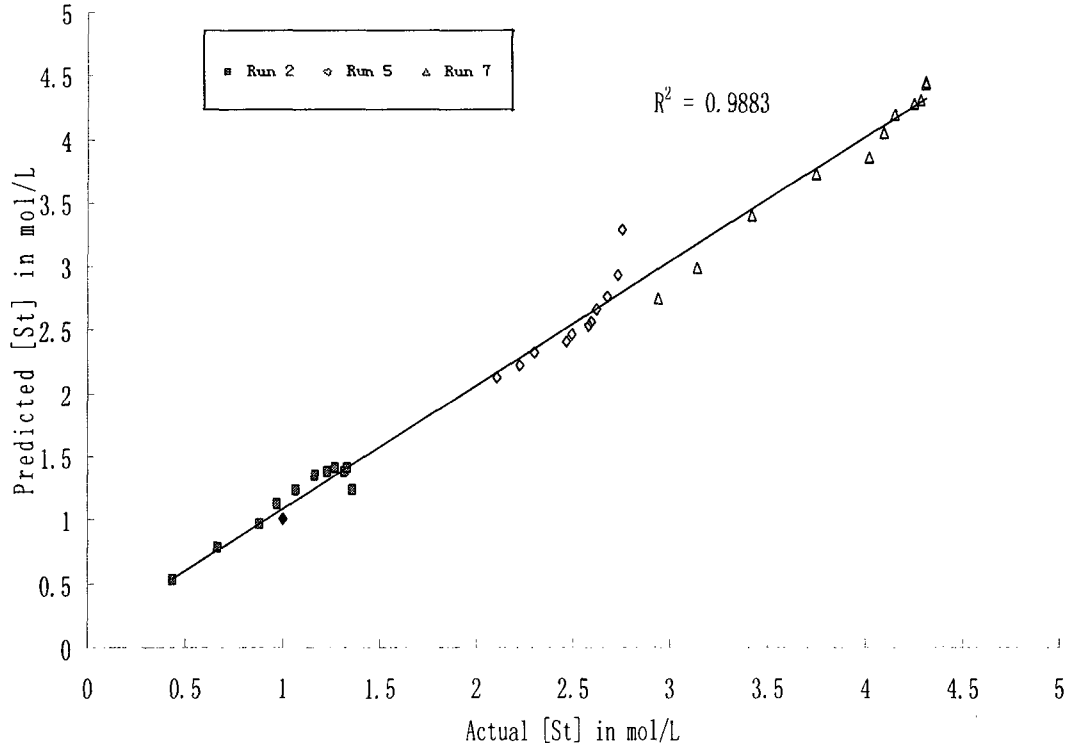

Figure 3.20: 1,3 Butadiene concentration validation

For further confirmation of the results, paired comparisons at a 95% confidence level were calculated between the monomer concentrations obtained by off-line measurements (gravimetry and ^{1}H-NMR spectroscopy) and the PLS model predictions. For all the samples used in the calibration, 95% confidence intervals for the difference between the two methods were found to be [-0.0017, 0.0017] in mol/L for St and [-0.0096, 0.0094] in mol/L for Bd. This showed that no significant differences existed between the two methods. For all the samples used in the validation (i.e., runs 2, 5 and 7), 95% confidence intervals were found to be [-0.0736, 0.0394] in mol/L for St and [-0.007, 0.106] in mol/L for Bd, further confirming that a successful calibration model was calculated.

The predicted concentrations of St and Bd from the PLS model were then used to calculate the individual and overall monomer conversions. The calculated conversions agreed well with the actual measurements. One example is shown in Figure 3.21 for individual conversions and in Figure 3.22 for overall conversions. Similar results were obtained for other runs.

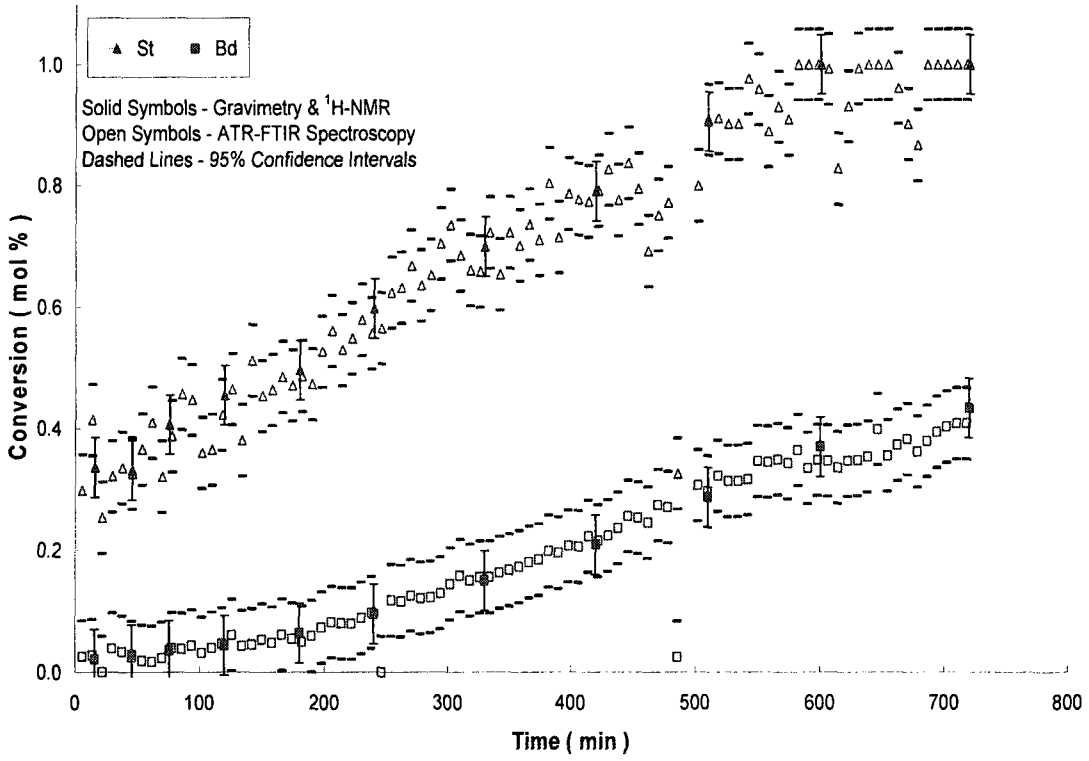

Figure 3.21: PLS individual conversion predictions for Run 8

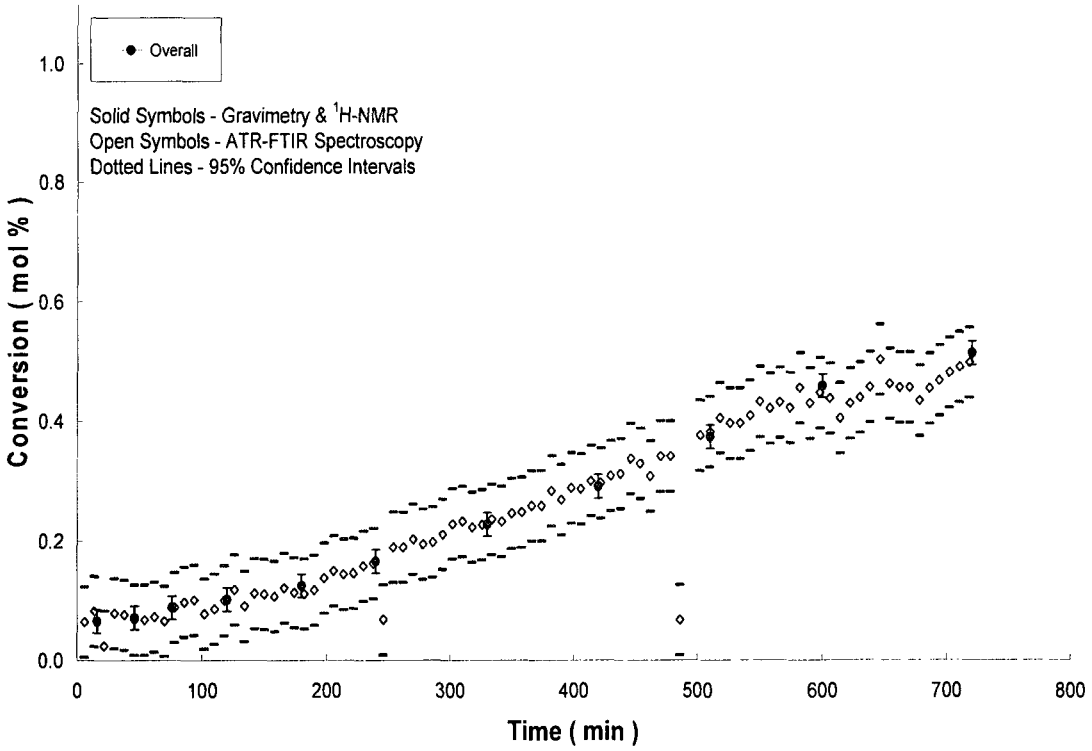

Figure 3.22: PLS overall conversion predictions for Run 8

Conclusions

A series of St/Bd emulsion copolymerizations was carried out in a 1.2 L stainless steel reactor. Conversions were monitored off-line using gravimetry and in-line monitoring was performed using ATR-FTIR spectroscopy. It was found that the air background and the signal to noise ratio were both appropriate for this kind of system. A multivariate or PLS method using the full spectra of reactions provided excellent results for the in-line emulsion polymerization monitoring. No significant differences were found between the off-line (gravimetry and ^{1}H-NMR spectroscopy) results and the ATR-FTIR spectroscopy data coupled with the PLS method confirming that ATR-FTIR spectroscopy is a reliable tool for monitoring individual monomer concentrations and conversions. Future work could consider integrating a feedback control policy to such a system.

Acknowledgements

The authors wish to gratefully acknowledge the financial support from Omnova Solutions, U.S.A. and the Natural Sciences and Engineering Research Council of Canada.

References

1. Baranek, B., Gottfried, M., Korfhage, K., Pauer, W., Schulz, K., Hans "Closed loop control of chemical composition in free radical copolymerization by Online reaction monitoring via calorimetry and IR-spectroscopy", RC User Forum Europe, Berne, Switzerland, 1999.
2. Broadhead, T. O., Hamielec, A. E., MacGregor, J. F. "Dynamic modelling of the batch, semi-batch and continuous production of styrene/butadiene copolymers by emulsion polymerization", Die Makromolekulare Chemie, 10, 105 – 128, 2003.
3. Chien, D. C. H., Penlidis, A. "On-line Sensors for Polymerization Reactors", J. Macromol. Sci. – Rev. Macromol. Chem. Phys., C30, 1-42, 1990.
4. Dimitratos, J., Eliçabe, G., Georgakis, C. "Control of Emulsion Polymerization Reactors", AIChE J., 40, 1993-2021, 2004.
5. Fonseca, G. E., Dubé, M.A., Penlidis, A. "A Critical Overview of Sensors for Monitoring Polymerizations", Macromol. Reaction Eng., in press, 2009.
6. Hamielec, A. E., MaGregor, J. F., Modelling Copolymerizations in "Polymer Reaction Engineering", K.H. Reichert and W. Geiser's Edition, Hauser Publishers, 1983.
7. Hua, H., Dubé, M.A. "In-line monitoring of emulsion homo- and copolymerizations using ATR-FTIR spectrometry", Polym. Reaction Eng. J., 10, 21-40, 2002.
8. Hua, H., Rivard, T., Dubé, M. A. "Off-Line Monitoring of Styrene/Butyl Acrylate Copolymerizations in Toluene using ATR-FTIR Spectroscopy", Polymer, 45, 345-354, 2004.
9. ISO 21561:2005 "Styrene-Butadiene rubber (SBR) – Determination of the microstructure of solution-polymerized SBR", 2005.

10. Jovanovic, R., Dubé, M.A. "Off-line monitoring of butyl acrylate and vinyl acetate homopolymerization and copolymerization in toluene" J. Appl. Polym. Sci., 82, 2958-2977, 2001.
11. Jovanovic, R., Dubé, M.A. "Butyl Acrylate/Vinyl Acetate Emulsion-Based Pressure-Sensitive Adhesives: Empirical Modeling of Final Properties", Can. J. Chem. Eng., 85, 341-349, 2007.
12. Koenig, J. L. "Spectroscopy of Polymers", 2nd Edition, Elsevier, New York, 1-491, 1999.
13. Li, D., Sudol, E.D., El-Aasser, M.S. "Miniemulsion and conventional emulsion copolymerization of styrene and butadiene: Effect of process on gel content", J. Appl. Polym. Sci., 102, 4626-4622, 2006.
14. Lovell, P.A., El-Aasser, M.S. "Emulsion Polymerization and Emulsion Polymers", John Wiley and Sons, Inc.: England, 1-515, 1997.
15. Pasquale, A. J., Long, T. E. "Real-time monitoring of the stable free radical polymerization of styrene via in-situ mid-infrared spectroscopy", Macromolecules, 32, 7954-7957, 1999.
16. Reis, M. M., Araujo, P. H. H., Sayer, C., Giudici, R. "Development of calibration models for estimation of monomer concentration by Raman spectroscopy during emulsion polymerization: Facing the medium heterogeneity", J. Appl. Polym. Sci., 93, 1136-1150, 2004.
17. Rivard, T. M.A.Sc. thesis, Department of Chemical Engineering, University of Ottawa, 2002.
18. Roberge, S., Dubé, M.A. "In-line monitoring of styrene/butyl acrylate mini-emulsion polymerization with attenuated total reflectance/Fourier transform infrared spectroscopy", J. Appl. Polym. Sci., 103, 46-52, 2006.
19. Saenz De Buruaga, I., Arotçarena, M., Armitage, P. D., Gugliotta, L. M., Leiza, J. R., Asua, J. M. "On-line calorimetric control of emulsion polymerization reactors", Chem. Eng. Sci., 51, 2781-2786, 1998.
20. Sayer, C., Lima, E. L., Pinto, J. C. "Dynamic modeling of SBR emulsion polymerization reactors refrigerated by thermosyphons", Chem. Eng. Sci., 52, 341-356, 1997.

21. Smith, B.C. "Fundamentals of Fourier transform infrared spectroscopy", CRC Press: New York, 1-195, 1996.
22. Source: http://www3.wooster.edu/chemistry/is/brubaker/ir/ir_spectrum.html

Chapter 5 – Conclusions and Recommendations

Styrene butadiene rubber (SBR) is a widely used synthetic rubber for the production of car and light truck tires and truck tire retread compounds. SBR manufacturers continue to face the challenge of improving their product properties and reducing production costs (Hamielec and MacGregor, 1983). Much research has been done on the chemical modification of SBR because of the great demand for new materials (De Sarkar et al. 1998; Halasa et al., 2005; Khoee and Sorkhi, 2007)

In order to better control the final product's properties and improve process control policies, it is essential to develop reliable and robust sensors to carry out real-time measurements for polymerization processes (Chien and Penlidis, 1990; Broadhead et al., 2003). Traditional polymerization monitoring is often carried out using off-line characterization of samples from a process flow line or using the data for thermal changes during reaction time. Traditional off-line techniques suffer primarily from time lags between sampling and analytical results. Thus, in-line or on-line monitoring techniques can provide a more effective means to control the polymerization process. Compared to bulk and solution polymerization, emulsion polymerization may at first appear to be simpler for in-line monitoring due to its lower viscosity, however, due to its heterogeneous nature, it can pose significant challenges (Saenz De Buruaga et al., 1998).

In the last decade, several attempts were made to utilize various dielectric, acoustic, and spectroscopic techniques to monitor polymerization reactions (Jovanovic and Dubé, 2001). Infrared (IR) and Raman spectroscopic techniques have shown the most potential (Koenig, 1999; Smith, 1996). Attenuated Total Reflectance Fourier Transform Infrared (ATR-FTIR) spectroscopy is an attractive option because it is affordable, utilizes simple sampling techniques and has straightforward experimental operation. In addition, ATR-FTIR can offer much information about the reaction system at the molecular level while obtaining real-time structure and kinetic information on a polymerization process.

The focus of this work, was to apply ATR-FTIR spectroscopy, coupled with a multivariate statistical approach, in-line to monitor the cold emulsion copolymerization of styrene and 1,3-butadiene. A series of SBR emulsion copolymerizations were performed in a jacketed 1.2 L stainless steel batch reactor. The concentration of each

individual monomer and copolymer was monitored via ATR-FTIR spectroscopy to calculate the conversion and copolymer composition. ^{1}H-NMR spectroscopy was used for the off-line analysis of polymer composition data while the off-line conversion data were obtained using a conventional gravimetric method. In order to evaluate the monitoring ability of the ATR-FTIR spectroscopic technique, the in-line real-time kinetic data were compared to the off-line data. A multivariate or PLS method using the full spectra of reactions provided excellent results for the in-line emulsion polymerization monitoring. No significant differences were found between the off-line (gravimetry and ^{1}H-NMR spectroscopy) results and the ATR-FTIR spectroscopy data coupled with the PLS method confirming that ATR-FTIR spectroscopy is a reliable tool for monitoring individual monomer concentrations and conversions.

Future work regarding to cold SBR emulsion polymerization should include the following:

1. In order to reduce the risk of coagulation of the copolymerization, Additional reaction conditions including a different emulsifier system should be investigated.
2. An upgrade to the existing ATR-FTIR probe may prove beneficial for future experiments. The probe used in this project often developed a thin layer of latex on its surface towards the end of some reactions. Newer probe models exist with reduced probabilities for fouling.
3. An alternative solvent for the NMR analyses would be desirable. Some samples, usually the last two samples in some reactions, had difficulty dissolving in chloroform-d. Alternatively, a solid-state NMR approach may also be of value.
4. The next step in this study would be to implement a feedback control policy integrated with the ATR-FTIR spectroscopy system. By manipulating the co-monomer feed rates, one would be able to provide excellent composition control. This would ultimately allow the tailoring of desired latex properties.

References

1. Broadhead, T. O., Hamielec, A. E., MacGregor, J. F. "Dynamic modelling of the batch, semi-batch and continuous production of styrene/butadiene copolymers by emulsion polymerization", Die Makromolekulare Chemie, 10, 105 – 128, 2003.
2. Chien, D. C. H., Penlidis, A. "On-line Sensors for Polymerization Reactors", J. Macromol. Sci. – Rev. Macromol. Chem. Phys., C30, 1-42, 1990.
3. De Sarkar, M., De, P. P., Bhowmick, A. K. "Influence of styrene content on the hydrogenation of styrene-butadiene copolymer", J. Appl. Polym. Sci., 71, 1581-1595, 1998.
4. Halasa, A. F., Prentis, J., Hsu, B., Jasiunas, C. "High vinyl high styrene solution SBR", Polymer, 46, 4166-4174, 2005.
5. Hamielec, A. E., MacGregor, J. F., Modelling Copolymerizations in "Polymer Reaction Engineering", K.H. Reichert and W. Geiser's Edition, Hauser Publishers, 1983.
6. Jovanovic, R., Dubé, M.A. "Off-line monitoring of butyl acrylate and vinyl acetate homopolymerization and copolymerization in toluene" J. Appl. Polym. Sci.,. 82, 2958-2977, 2001.
7. Khoee, S., Sorkhi, M. "Microstructure analysis of brominated styrene-butadiene rubber", Polym. Eng. Sci., 47, 87-94, 2007.
8. Saenz De Buruaga, I., Arotçarena, M., Armitage, P. D., Gugliotta, L. M., Leiza, J. R., Asua, J. M. "On-line calorimetric control of emulsion polymerization reactors", Chem. Eng. Sci., 51, 2781-2786, 1998.
9. Smith, B.C. "Fundamentals of Fourier transform infrared spectroscopy", CRC Press: New York, 1-195, 1996.

Appendix A – Experimental Design and Procedure

A.1 Reagent

The reagents: styrene (St) (Sigma-Aldrich), 1,3-butadiene (Bd) (BOC GASES), fatty acid (FA) (Westvaco), rosin acid (RA) (Westvaco), the chain transfer agent (CTA) n-dodecyl mercaptan (DDM) (Sigma-Aldrich), sodium formaldehyde sulfoxylate (SFS) (Sigma-Aldrich), ferrous Sulphate(FS) (Sigma-Aldrich), potassium hydroxide (KOH) (Sigma-Aldrich), cumene hydroperoxide (CHP) (Sigma-Aldrich), and ethylene diamine tetra-acetic acid (EDTA) (Sigma-Aldrich)were used without any further purification. All components used to perform the characterizations, i.e., benzene-d (Sigma-Aldrich), chloroform-d (Sigma-Aldrich), and tetrahydrofuran (THF) (Sigma-Aldrich) were also used as received.

A.2 Experimental Design

"Cold E-SBR" experiments were designed to validate the adequacy of ATR-FTIR spectroscopy in-line monitoring method for multiphase emulsion polymerization by comparing with off-line ^{1}H-NMR data. All liquid-phase recipes were performed with pre-cooling, a reaction temperature of 5°C at a pressure of 50 psig (245 kPa). The following concentrations of ingredients were also kept constant: RA = 2.5 phm, FA = 2.5 phm, KOH = 0.5 phm, CHP = 0.51 phm, SFS = 0.3 phm, FS = 0.06 phm, CTA = 0.2 phm, and EDTA = 0.18 phm, where phm represents parts per hundred parts of monomer. Batch recipes are showing in the following table A.1.

Table A.1: Batch recipes

		St (phm)[1]	Bd (phm)	Water (phm)
Runs used for the model	**Run 1**	**80**	**20**	**180**
	Run 3	**70**	**30**	**180**
	Run 4	**40**	**60**	**180**
	Run 8	**25**	**75**	**180**
Runs used for the validation	**Run 2**	**75**	**25**	**220**
	Run 5	**60**	**40**	**140**
	Run 7	**25**	**75**	**160**

[1]phm = parts per hundred parts monomer

A.3 Apparatus

Emulsion copolymerizations of St/1,3-Bd were performed in a Labmax™ setup (Mettler Toledo) which comprises a jacketed 1.2 L stainless steel batch reactor. Mixing at 100 rpm was applied to the reactor contents during the pre-cooling stage by an anchor stirrer and later on at 200 rpm during the reaction time. The reactor was equipped with a nitrogen line to purge and/or pressurize the reactor, a bottom sampling valve (designed "in-house" using Swagelok™ quick connectors), an initiator-loading cell, a reflux condenser with a vent line, and a port for the IR probe. The ATR-FTIR diamond composite probe (ReactIR™ 1000, Mettler-Toledo) was positioned about 2 mm above the blades of the agitator to ensure the monitoring of well-mixed latex. The reaction temperature and stirring speed were controlled by Camille® software (Mettler-Toledo). The reaction pressure was adjusted by feeding nitrogen. Figure A.1 shows the Labmax™ reactor setup.

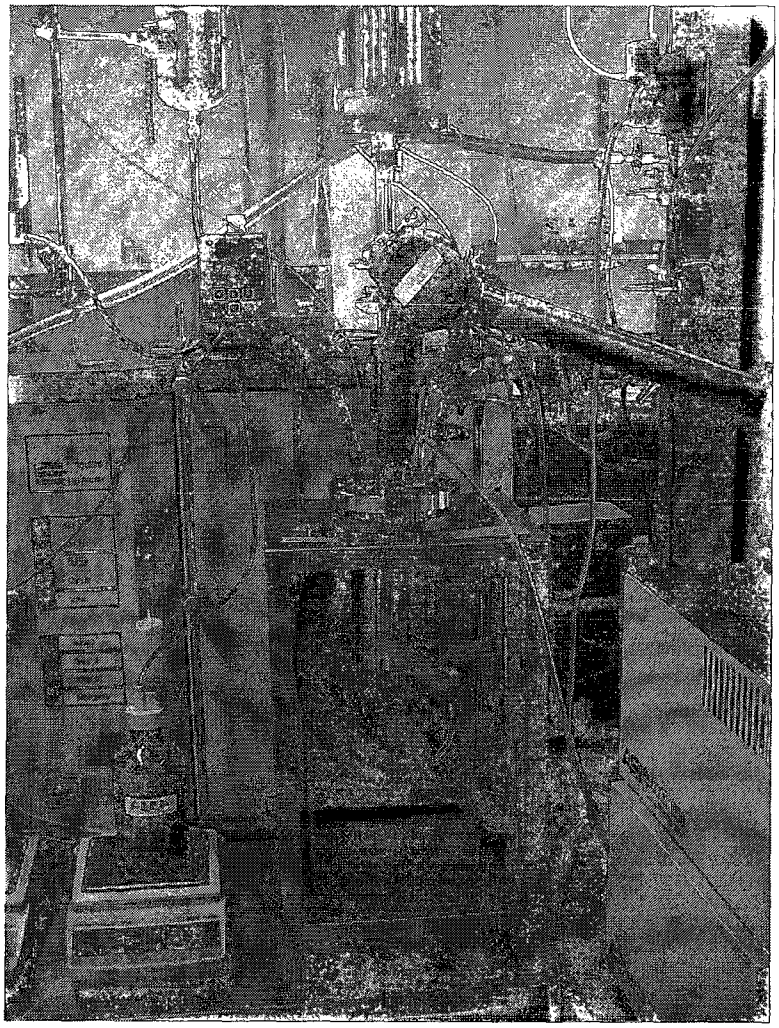

Figure A.1: 1.2 L stainless steel batch reactor

A ReactIR™ 1000 (ASI Applied Systems, Inc., Mettler Toledo) reaction analysis system was used in-line to collect mid-FTIR spectra (4000-650 cm^{-1}) of the multiphase emulsion copolymerization reactions. A light conduit and a diamond composite probe were inserted into the reactor for non-destructive in-line monitoring in a hostile reaction environment (Jovanovic and Dubé, 2001). The IR apparatus is shown in Figure A.2.

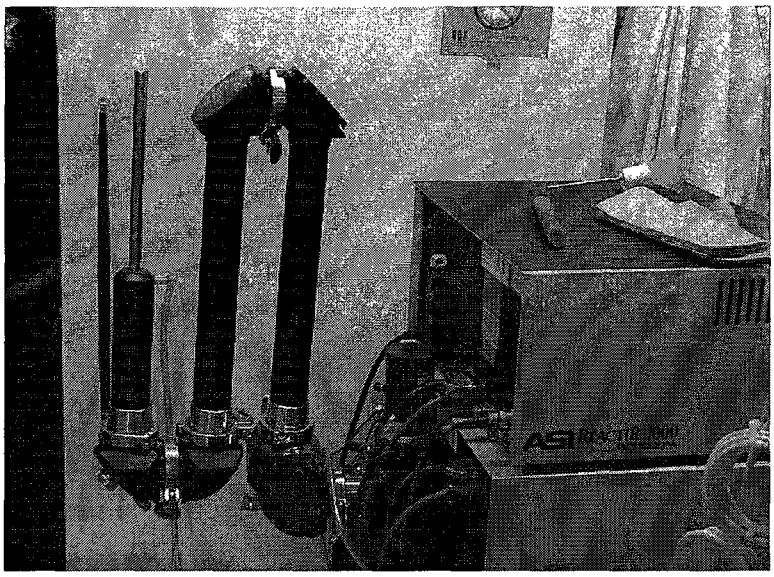

Figure A.2: ReactIR™ 1000

A.4 Experiment Preparation

Emulsifier

The emulsifier solution was prepared by mixing the FA and RA with water a day before the reaction. The hard solid RA was placed in a 100 mL beaker with the FA suspension and potassium hydroxide pellets. Water and EDTA were poured in the beaker later and mixed with a magnetic agitator at a temperature of about 50°C for 1 h. The well-mixed emulsifier solution in the beaker was sealed with parafilm and kept in a refrigerator for 12 h.

ATR-FTIR Spectroscopy

The diamond composite probe of the IR was inspected and cleaned before connecting it to the reactor. Its position was adjusted according to the user guide of the probe to reach the maximum peak height and contrast number. Clearance between the probe and the agitator was ensured to protect the probe. This was done by manually turning the agitator shaft. The probe's position was then fixed. An air background spectrum was acquired before adding any ingredients into the reactor.

Other ingredients

Water was added to the reactor first and a water background spectrum was collected at this point. St, CHP, and DDM were poured in a 250 mL beaker and mixed with a magnetic agitator for 15 min. The mixed solution was then poured into the reactor and purged with nitrogen gas for 1 h. Stirring at 100 rpm was applied to the reactor contents during this stage by an anchor stirrer.

1, 3 – Butadiene

The 1,3 butadiene gas cylinder was stored in a 20 L bucket. Before transferring Bd gas to a 1 L feed vessel, the bucket was filled with ice to pre-cool the Bd gas. The Bd gas monomer transfer-feed 1 L vessel was kept in another 20 L bucket, containing a mixture of water and ethylene glycol (weight ratio: 1:4). The bucket was connected to two cooling baths and a thermometer. When the temperature of the water-ethylene glycol mixture reached 0°C, the valve of the Bd cylinder was opened to transfer the Bd into the 1 L feed vessel. Then the feed vessel was weighed (the empty vessel was weighed previously). The weight of Bd gas inside the vessel was therefore known.. Usually, ~2.5 h was needed for the feed vessel to achieve the desired temperature. The Bd gas monomer feed vessel was then connected to the reactor and a valve opened to transfer its contents to the reactor. The pressure of the reactor was typically at 40 psig (276 kPa) when the transfer was complete.

Initiator

The mixed initiator solution was prepared 15 min prior to the reaction. Measured amounts of SFS, $FeSO_4$, and water were poured in a 50 mL beaker and mixed with a magnetic agitator for 15 min. The prepared solution was purged with nitrogen for 2 min. It was then added to the reactor via a pressurized initiator-loading cell to start the reaction. The pressure in the reactor was at 50 psig (345 kPa) at this point.

A.5 Polymerization

The multiphase "cold" emulsion copolymerization of St/1,3-Bd was run at 5°C with an initial pressure of 50 psig (345 kPa). The reactor was pre-cooled with two cooling baths for 2 h in order to reach the reaction temperature, 5°C. After leak testing by

pressurizing the reactor with nitrogen, the position of the IR diamond composite probe was adjusted to match the maximum peak height and contrast number and then the air background spectrum was collected. Next, the water, the well-mixed and pre-cooled emulsifier solution and the styrene monomer with CHP and DDM were poured into the reactor. The background spectrum was collected after each solution was added for later data analysis. Then, the reactor was closed and stirring at 100 rpm was started. The temperature control program was then activated to keep the reaction mixture at the reaction temperature, 5°C. Before the Bd and the initiator solution were injected, the whole system was purged of oxygen by bubbling N_2 through the mixture for 1 h. The ATR-FTIR probe data collection was begun at this point to monitor the system for any potentially early reaction of styrene monomer. The liquefied Bd monomer was then transferred to the reactor from its feeding vessel. The Bd liquid monomer was then injected into the reactor by the pressure of nitrogen gas on the back end of the feed vessel. When the pressure reached about 35 psig, the initiator dissolved in de-ionized water was deoxygenated by bubbling N_2 through it and charged into the loading cell. The initiator solution was then charged into the reactor by the pressure of nitrogen gas. The reaction system reached its set point pressure of 50 psig (345 kPa) and temperature of 5°C. Reaction monitoring and process temperature monitoring were started simultaneously after the initiator had been charged. This corresponded to polymerization time zero. During the reaction, at suitable time intervals, samples were taken through a pre-weighed sampling vessel, which ended with Swagelok quick connectors. The sample vessel then weighed and then was poured into a pre-weighed dish in the fume hood and allowed to dry. The detailed experimental/sampling procedure is in Appendix C.

A.6 Experimental Procedure

1. Turn on the tap water before turning on the LabMax system.
2. Ensure all valves are closed.
3. Switch on LabMax system.
4. Start the computer, go START/PROGRAMS/LABMAX to start the program.
   User name: alr; Password: labmax.

5. In main menu

   Go to INITIAL SETTINGS: Tj = 5oC; Stirrer speed R: 0 rpm.

   Go to DEFINE METHOD/SET UP/CONTROLLER UNIT/OK/Return to method menu

   Go to SAFETY PARAMETERS

	Minimum	Maximum
T_r	-30	230
T_j	-30	230
R (stirrer speed, rpm)	0	300
pH input	-9999	9999
In 1 input	-9999	9999
In 2 input	-9999	9999
In 3 input	-9999	9999
T_{safe} (^{o}c)	5	
(T_j-T_r)(^{o}c)	15	

   Go to RECIPE

Stage#	Stage type	Duration (min)	Final temp. (^{o}c)	Stirrer speed (rpm)	Control loop
1	T_r	40	5	200	N/A
2	T_r	720	5	200	N/A
3	End	1	5	0	N/A

   Go to CONSISTENCY CHECK

   Go to SAVE METHOD (select your own directory in the hard disk)

   Go to RETURN TO MAIN MENU

   Go to EXECUTE EXPERIMENT (select your own directory in the hard disk to store experimental data)

6. Install the ASI ReactIR 1000 Probe into the reactor. Adjust its position according to the user guide of the probe and ensure there is CLEARANCE between the probe and the agitator. This can be done by MANUALLY turning the agitator shaft. Then tighten up the screw underneath to fix the probe's position.

7. Follow the ReactIR 1000 Operating Procedures to acquire the background spectrum before adding water, styrene, and emulsifier into the reactor.
8. Add water and emulsifier into the reactor. Bring to reaction temperature and acquire another background spectrum.
9. In LabMax program, start the experiment.
10. Add styrene into the reactor.
11. Degas the water, styrene, and emulsifier. Turn on the nitrogen and keep the pressure at 5 psi (Gauge Pressure) and the temperature at 5 oc. Open V1, partially open V7 and V9 so that N2 is bubbled slowly into the reactor to prevent foaming. Then open V11 to drive the air out of the reactor; the reading from the pressure gauge should increase. This stage takes 40 minutes.
12. Initiator charging to load cell. During the first stage of the experiment, dissolve FeSO4 into water according to the recipe. Purge the initiator solution with nitrogen: open V2 toward the nitrogen; partially open V4 and V6; place the plastic charging tube into the initiator solution container. Let the nitrogen purge the initiator solution slowly to drive oxygen out. Then close V2, V4, and V6. Turn on the vacuum pump, open V3 and V4, keep the pump on for about 3 minutes to make vacuum inside the loading cell, close V3 and V4. Turn off the vacuum pump. Place the plastic charging tube into the initiator solution container. Slowly open V6; the contents should begin to charge into the cell. Do not allow air to enter as it will weaken the vacuum and if the polymerization is being performed under nitrogen, the air will act as an impurity in the system. Close V6 when the contents are charged.
13. Inject Butadiene in the reactor. First, close V1, V9, V7, and V11. Make sure the V13 is open V12 is close, and then open V14. Next, adjust V13 and keep the out pressure at 10 psi (Gauge pressure). Then, open V12, V10 and V7, adjust the flow rate by manipulating V12. When required amount has been charged, close V14, V13, V12, and V10.
14. Pressurize the reactor with N2 while simultaneously injecting the initiator. Open V2 and V4; slowly open V5, V8, and V7.The contents will charge quickly in less than 10 seconds. Close V7, then V8 and V5. Open V6; let nitrogen flush the line.

Close V6, V4 and V2. Finally open V1 and V9, keep the pressure at 2 atm (29.8 psi).

15. Start to collect reaction spectra, following the ReactIRTM 1000 Operating Procedure.
16. Taking samples. Weigh empty sampling cell. Before collecting the samples, connect the vacuum pump with cell to the reactor. Keep closing V15 and open V16, evacuate the part under V15 (include sample cell, elbow, and quick connector). Open V15; flush the bottom latex (about 5-6mL) into cell1, remove cell1 to the fume hood. Then close V15, and connect to cell2. Partially open V15, allow the latex to fill the cell2. Then close V15. Remove the cell2 and weigh it. Open the ball valve of cell2, let butadiene escape into the fume hood, and then reweigh sampling cell. Calculate the amount of butadiene which was released.
17. Sample analysis (gravimetry). Take several drops of the sample latex and add them into the weighing dish, weigh the dish and the sample latex. Put the dish onto shelf over night. The next day put sample dishes into vacuum oven evaporate water and residual monomer until their weights do not change any more, and then weigh it again.
18. When the experiment ends, in the LabMax program input the experiment terminating parameters: Tj=5oC, stirrer speed = 0 rpm.
19. Reactor cleaning. Fill the reactor with DDI water, heat the reactor to 50oC:
20. In LabMax MAIN MENU
21. Go to INITIAL SETTINGS: Tj=50 oc; Stirrer speed R: 300 rpm.
22. Open V8, turn on and off V10 several times to flush the dipping tube for 3 seconds. Close V10 and V8. Repeat the above cleaning steps with DDI water twice; add soap into the reactor if it is hard to clean with only water. Repeat the above cleaning steps with acetone once; recycle the acetone for washing. Repeat the above cleaning steps with toluene once if necessary.
23. Disassemble the dip tube and sampling tube for further cleaning. DO NOT disassemble all the valves, but clean all latex left inside the valves.

Figure A.3 Reactor Part

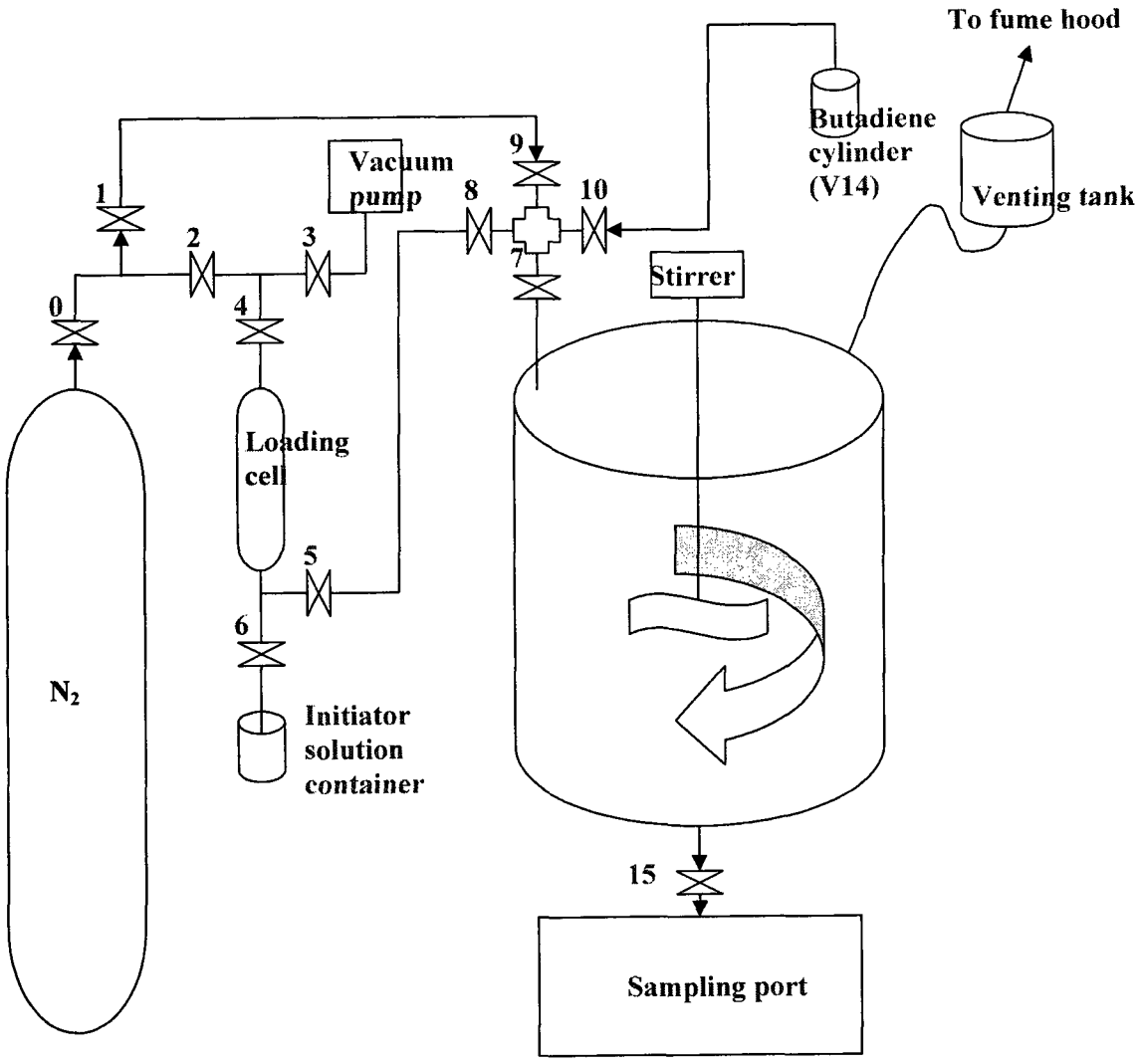

Figure A.4 Bottom of the reactor

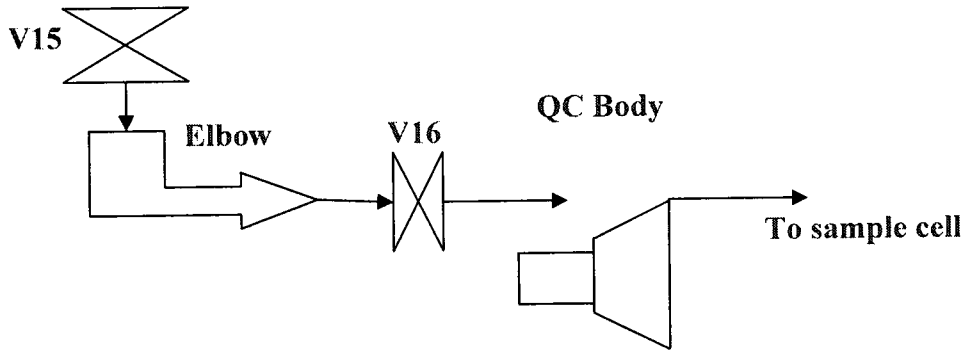

Figure A.5 Sampling cell

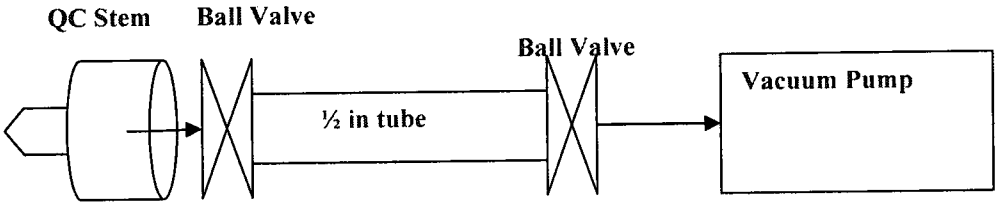

Appendix B – Sample Calculations

St/BA (25/75 wt fr.) cold emulsion copolymerization at 5°C is selected to illustrate the calculation procedures throughout Appendix A.

Polymerization recipe

Table B.1: Polymerization Recipe

	Ingredient	Weight (g)	phm	Wt. Fraction
monomer #1	St	69.46	23.97	0.0856
monomer #2	Bd	220.30	76.03	0.2716
medium	Water	501.20	172.97	0.6180
emulsifier #1	Fatty Acid	6.87	2.37	0.0085
emulsifier #2	Rosin Acid	6.90	2.38	0.0085
emulsifier #3	KOH	1.67	0.58	0.0021
initiator #1	CHP	1.44	0.50	0.0018
initiator #2	FS	0.15	0.05	0.0002
initiator #3	SFS	0.87	0.30	0.0011
initiator #4	EDTA	0.50	0.17	0.0006
CTA	n-dod. merc.	1.67	0.58	0.0021
Total		811.03		1

*phm = parts per hundred monomers

Parts per hundred monomers for a given ingredient

$$\text{phm(i)} = \frac{\text{weight of ingredient}}{\text{total weight of monomers}} \qquad \text{phm(St)} = \frac{69.46}{69.46 + 220.30} = 23.97$$

Weight fraction for a given ingredient

$$\text{w(i)} = \frac{\text{weight of ingredient}}{\text{total weight}} \qquad \text{w(St)} = \frac{69.46}{811.03} = 0.0856$$

Experimental calculations for gravimetric data

Table B.2: Experimental values for gravimetric data

Time(min)	Empty Disk (g)	Cell + Latex (g)	Empty Cell (g)	Dry latex + disk (g)	Solids	Conversion (mass fr.)
15	30.8146	254.49	249.58	31.1059	0.0593	0.0968
45	29.9238	254.41	249.52	30.2216	0.0609	0.1012
75	31.1959	254.02	249.49	31.5009	0.0693	0.1248
120	31.0675	254.57	249.50	31.4513	0.0757	0.1426
180	31.2329	254.45	249.50	31.6518	0.0846	0.1676
240	30.5274	254.73	249.49	31.0607	0.1018	0.2156
330	30.2071	254.70	249.54	30.8457	0.1255	0.2820
430	30.6201	254.71	249.56	31.3889	0.1493	0.3486
510	30.2645	254.67	249.59	31.1799	0.1802	0.4351
600	30.8656	254.76	249.64	31.9456	0.2109	0.5212
720	31.1116	254.74	249.68	32.2669	0.2283	0.5698

Solids for a given time

$$\text{Solids} = \frac{(\text{wt. of dry latex and disk - wt. of empty disk})}{(\text{wt. of cell and latex - wt. of empty cell})}$$

$$\text{Solids} = \frac{(31.1059 - 30.8146)}{(254.49 - 249.58)} = 0.0593$$

Conversion for a given time X

$$X(\text{mass fr.}) = \frac{\text{Solids - wt. fr. emulsifiers - wt. fr. initiators - wt. fr. CTA}}{\text{initial wt. fr. monomers}}$$

$$X(\text{mass fr.}) = \frac{0.0593 - 0.0085 - 0.0085 - 0.0021 - 0.0018 - 0.0002 - 0.0011 - 0.0006 - 0.0021}{0.2716 + 0.0855}$$

$$= 0.0968$$

Experimental calculations for ^{1}H-NMR data

Table B.3 Experimental values for 1H-NMR data

Time (min)	C	B	A	C(St)	C(Bd)
15	83.9299	10.0896	5.9805	0.7196	0.2804
45	80.3323	14.2957	5.3719	0.6542	0.3458
75	80.3919	15.1893	4.4188	0.6489	0.3511
120	19.0268	16.4508	4.5224	0.6282	0.3718
180	74.1463	20.9388	4.8969	0.5591	0.4409
240	70.0029	24.4460	5.5511	0.5071	0.4929
330	63.4982	30.0893	6.4125	0.4327	0.5673
420	59.6208	35.3640	6.2727	0.3825	0.6175
510	54.8484	39.7455	5.4061	0.3407	0.6593
600	50.9965	42.9582	6.3120	0.3067	0.6933
720	49.6316	43.5594	18.1550	0.2739	0.7261

Relative composition of each monomer C(i)

$$C(St) = \frac{(C/5)\times 104}{(C/5)\times 104 + (B/2 + A/4)\times 54}$$

$$C(Bd) = \frac{(B/2 + A/4)\times 54}{(C/5)\times 104 + (B/2 + A/4)\times 54}$$

$$C(St) = \frac{(83.9299/5)\times 104}{(83.9299/5)\times 104 + (10.0896/2 + 5.9805/4)\times 54} = 0.7196$$

$$C(Bd) = \frac{(10.0896/2 + 5.9805/4)\times 54}{(83.9299/5)\times 104 + (10.0896/2 + 5.9805/4)\times 54} = 0.2804$$

Appendix C – Additional Figures and Tables

Figures C.1 to C.14: PLS results for conversion predictions

Figures C.15 to C.28: Conversions by gravimetry and copolymer compositions

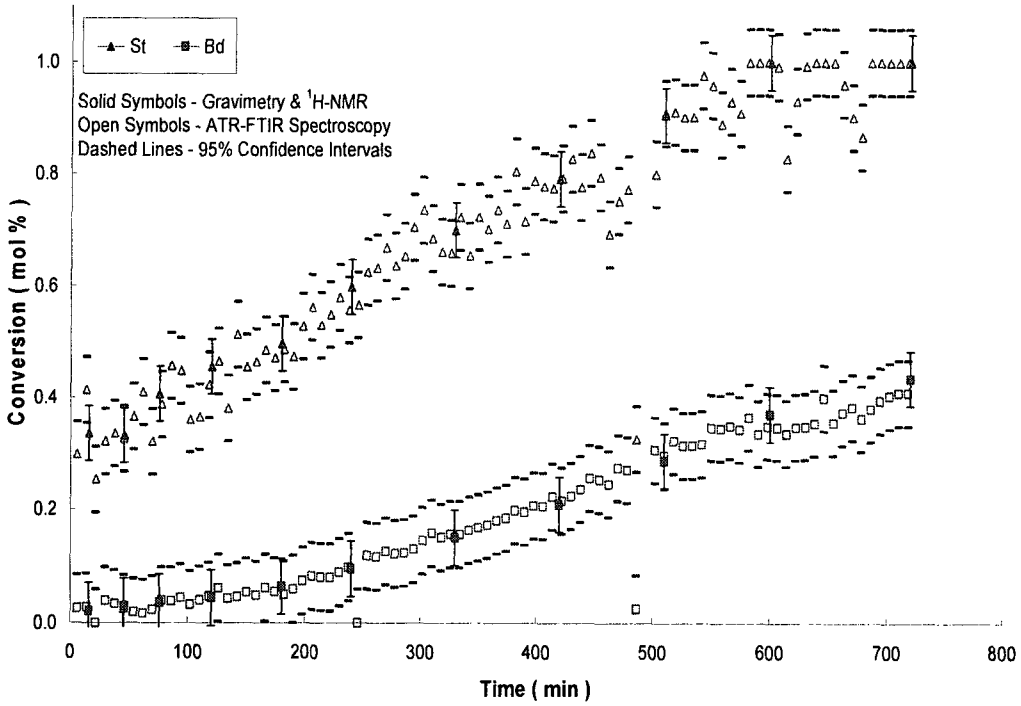

Figure C.1: PLS individual conversion predictions for Run 8

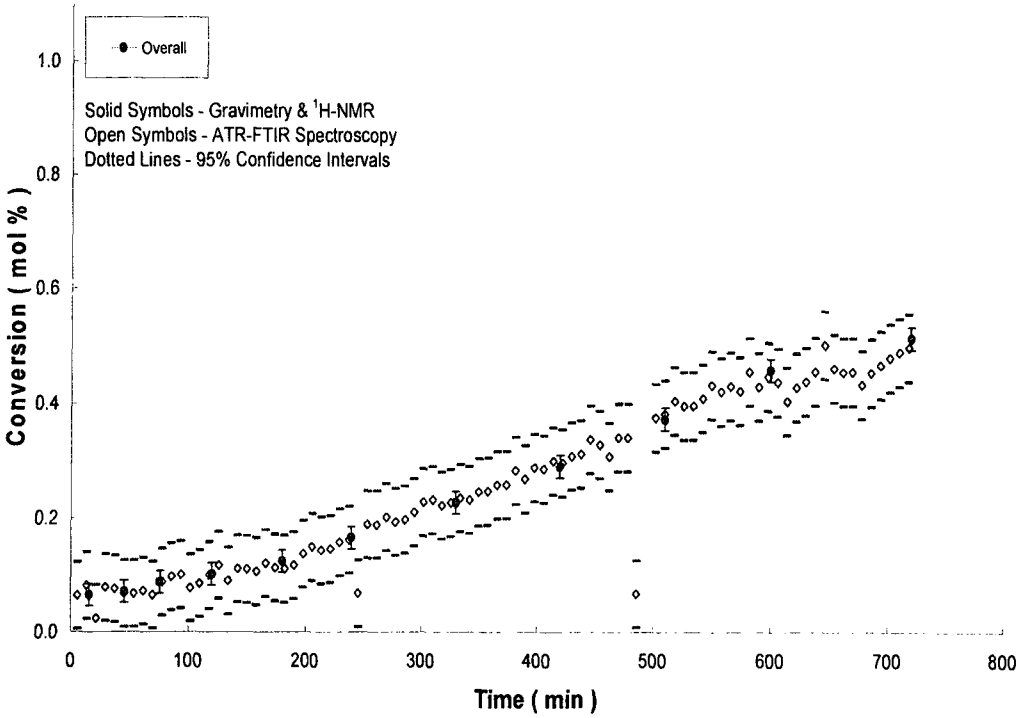

Figure C.2: PLS overall conversion predictions for Run 8

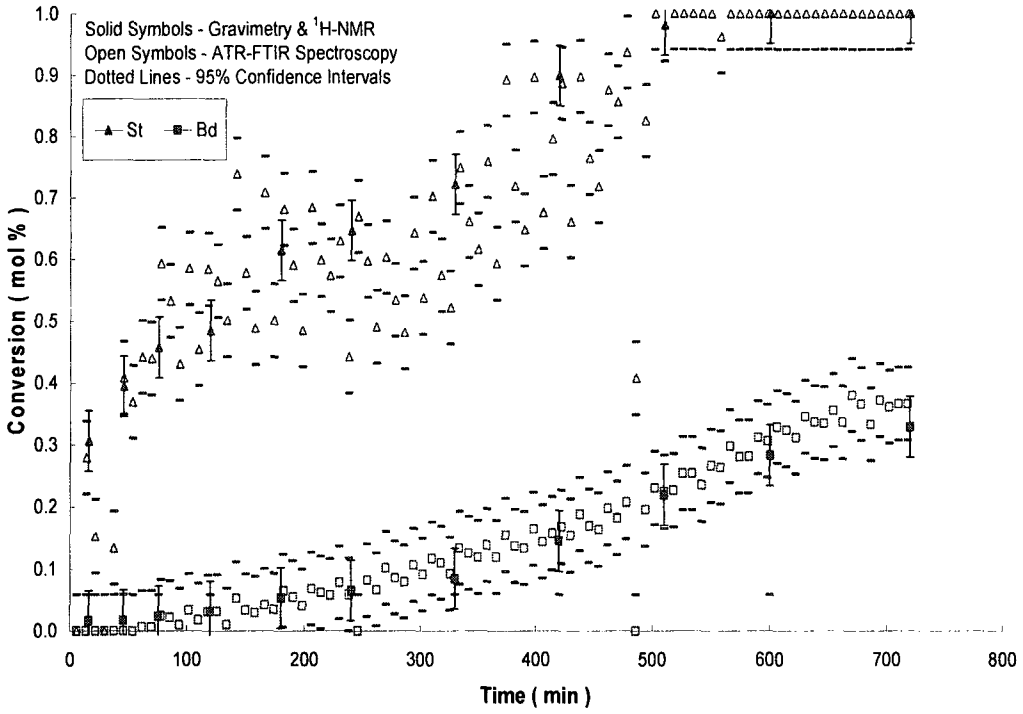

Figure C.3: PLS individual conversion predictions for Run 7

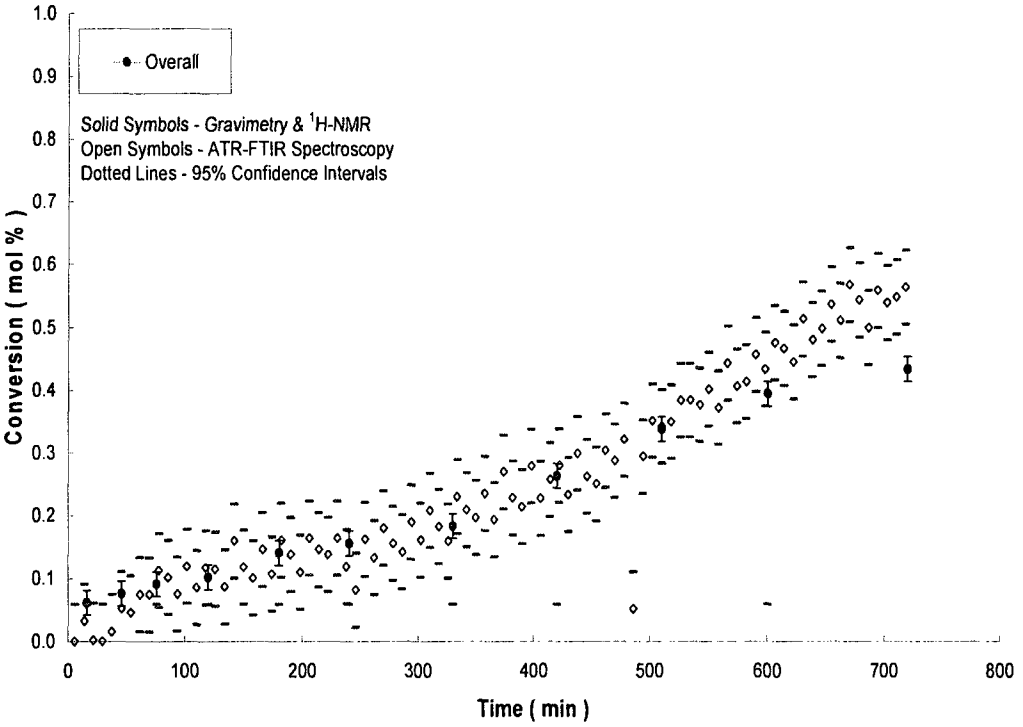

Figure C.4: PLS overall conversion predictions for Run 7

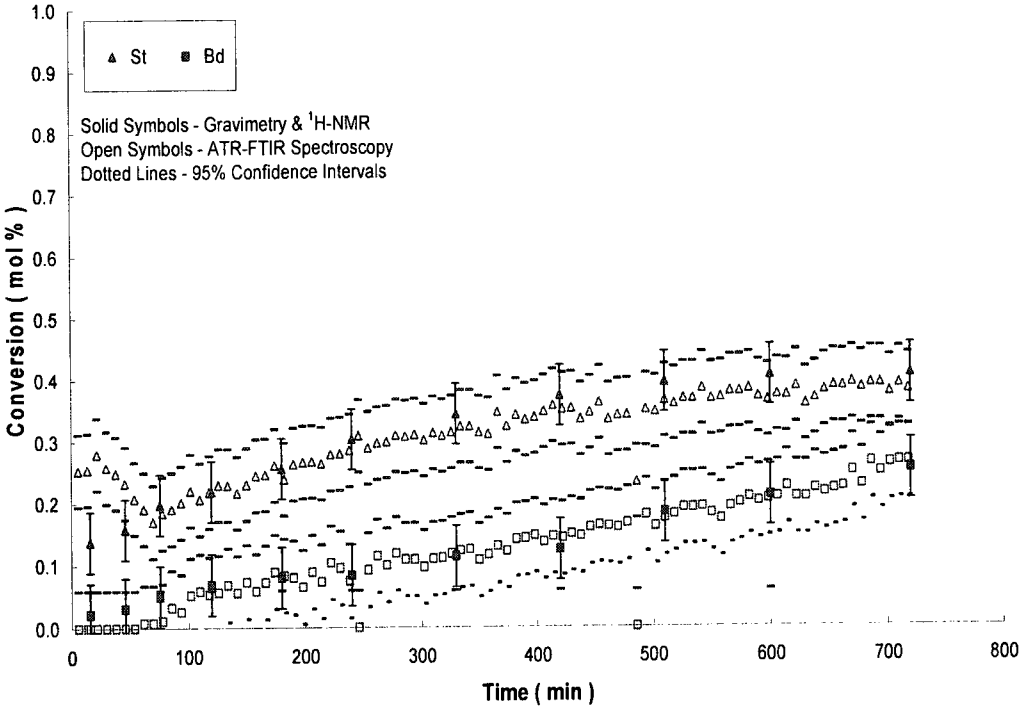

Figure C.5: PLS individual conversion predictions for Run 5

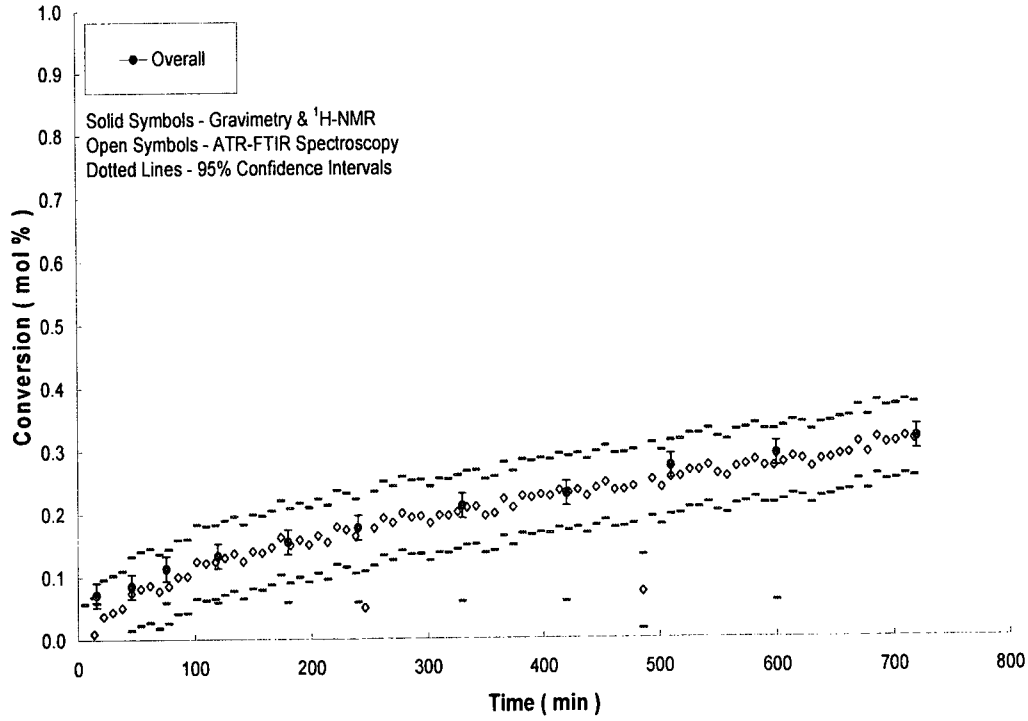

Figure C.6: PLS overall conversion predictions for Run 5

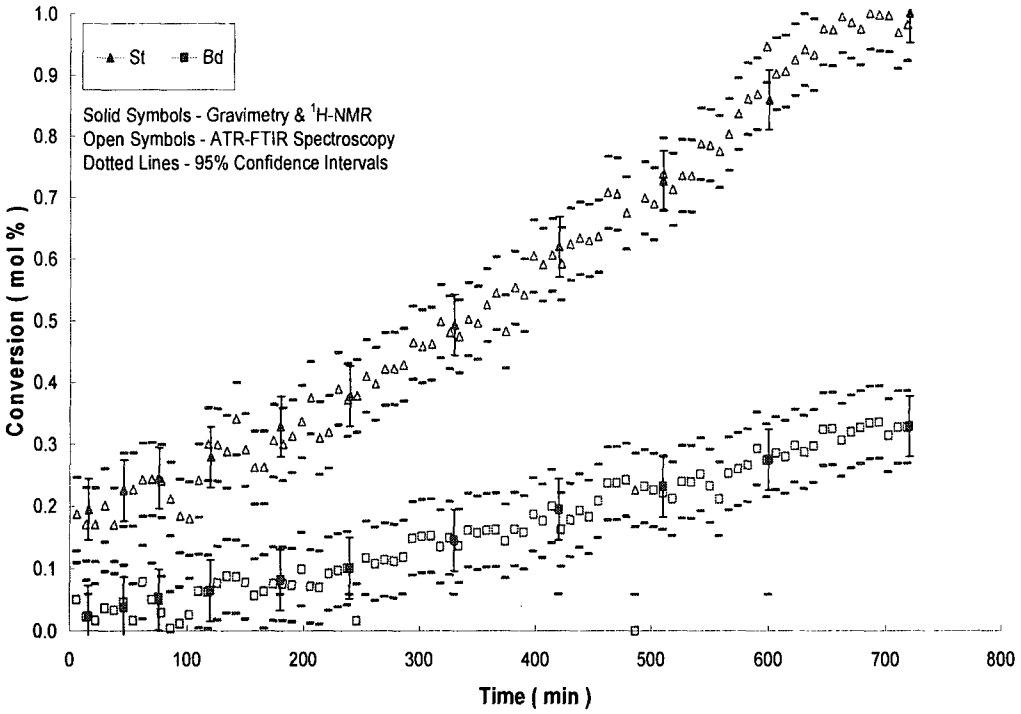

Figure C.7: PLS individual conversion predictions for Run 4

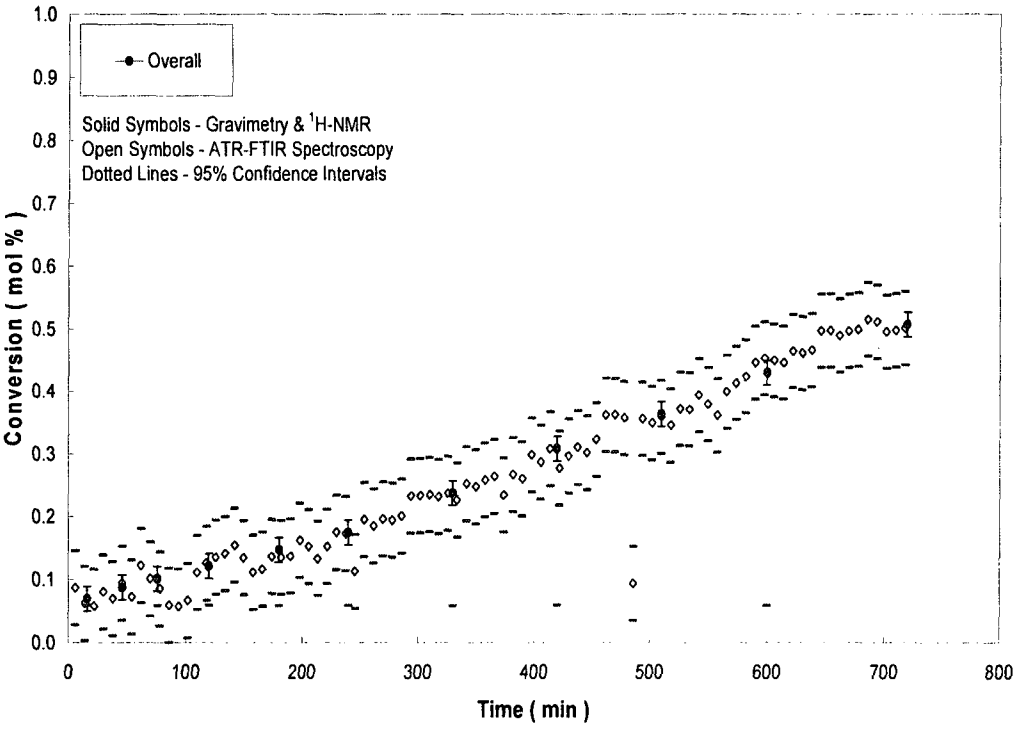

Figure C.8: PLS overall conversion predictions for Run 4

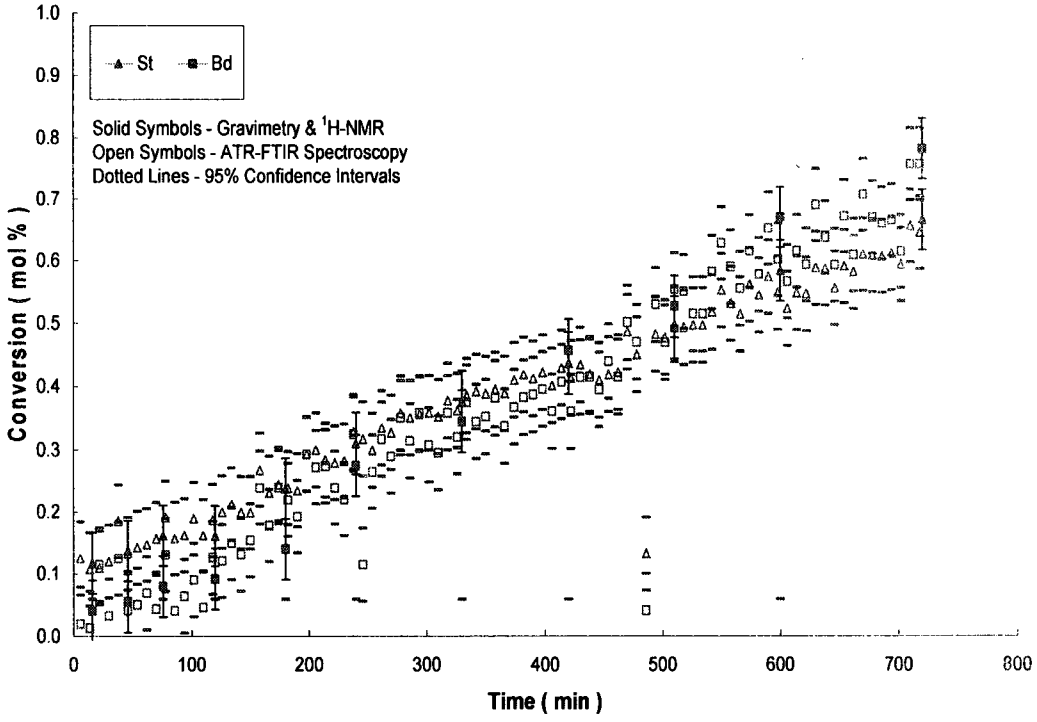

Figure C.9: PLS individual conversion predictions for Run 3

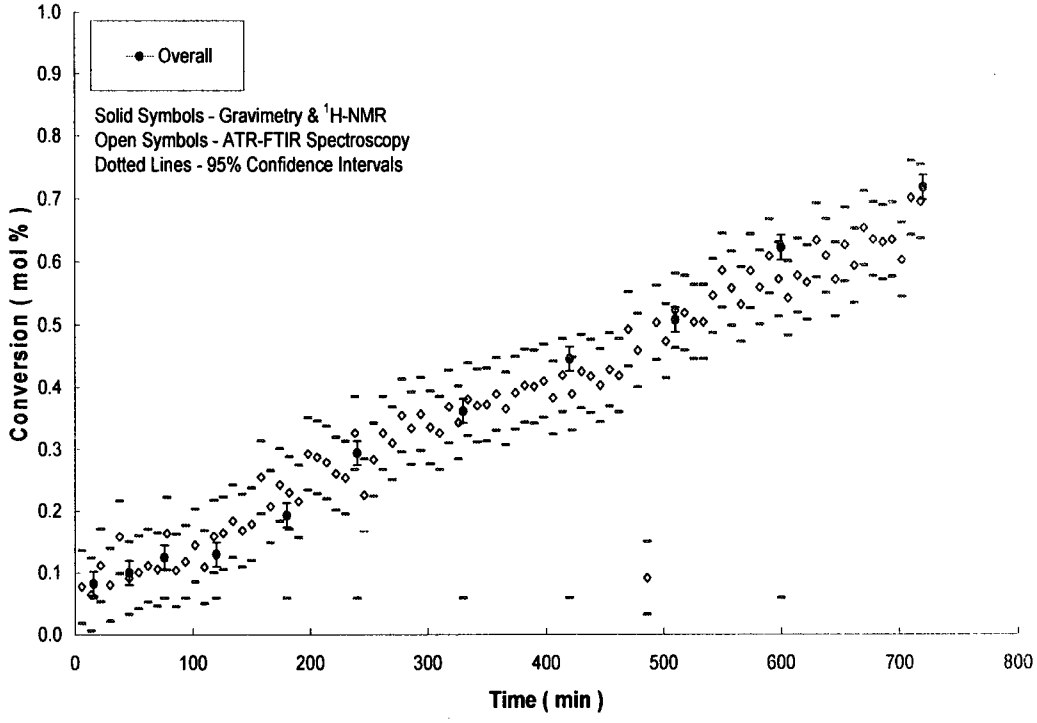

Figure C.10: PLS overall conversion predictions for Run 3

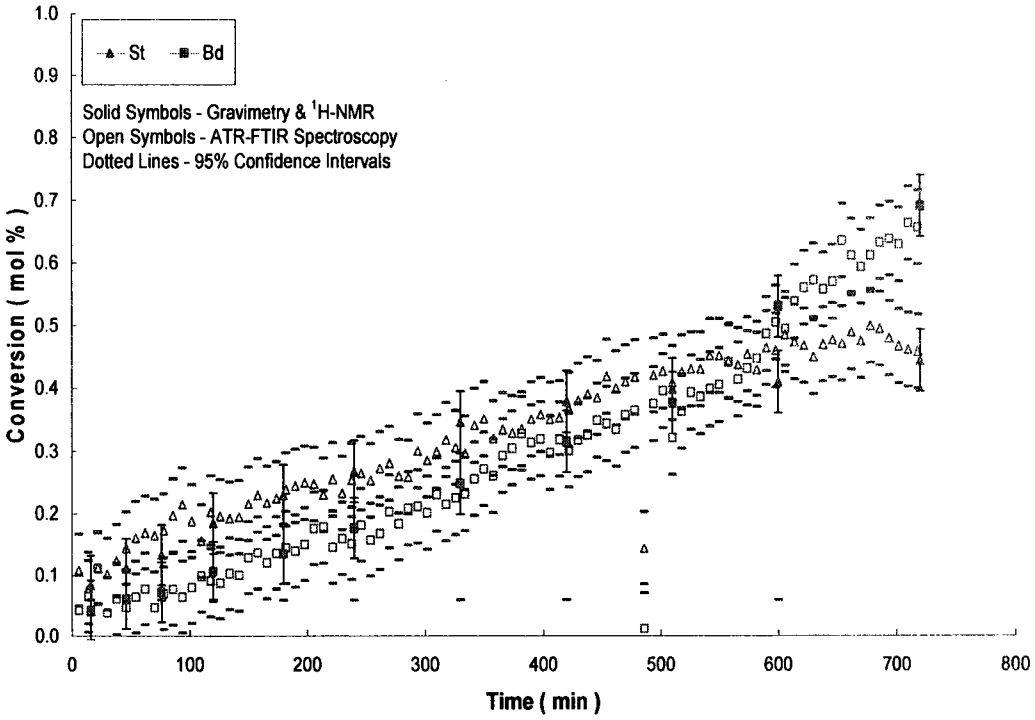

Figure C.11: PLS individual conversion predictions for Run 2

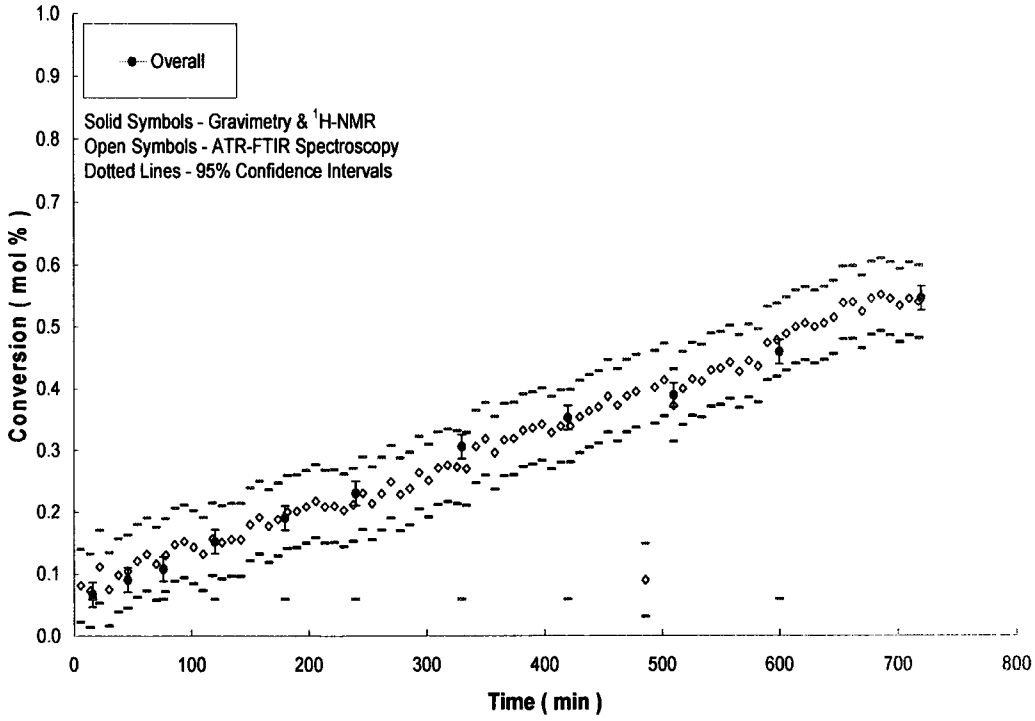

Figure C.12: PLS overall conversion predictions for Run 2

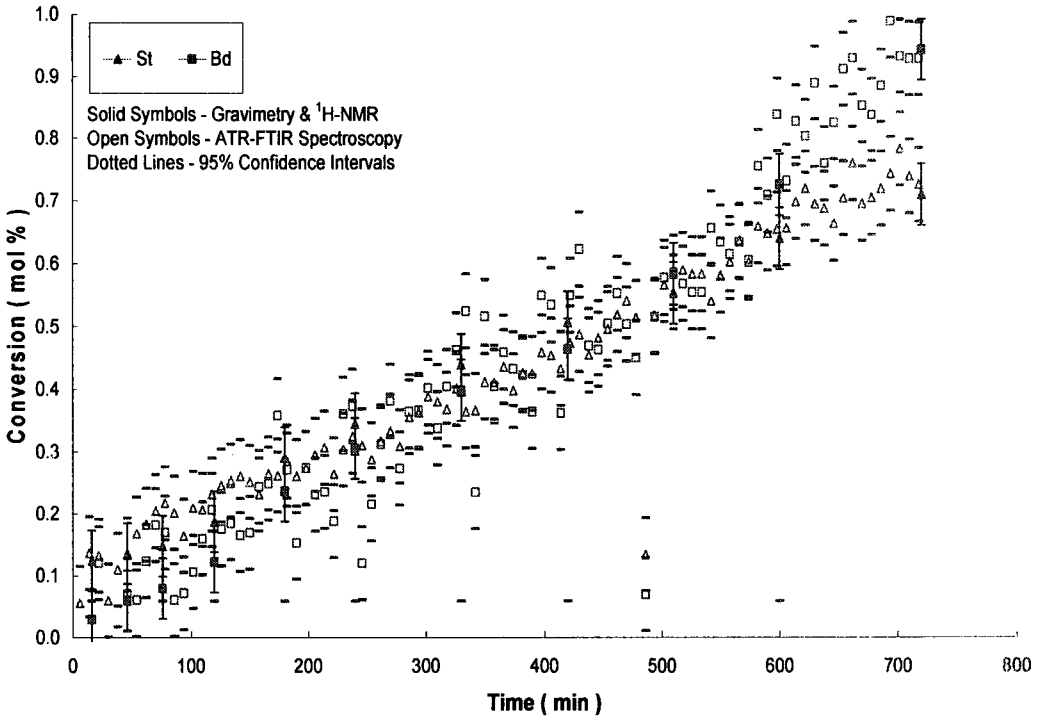

Figure C.13: PLS individual conversion predictions for Run 1

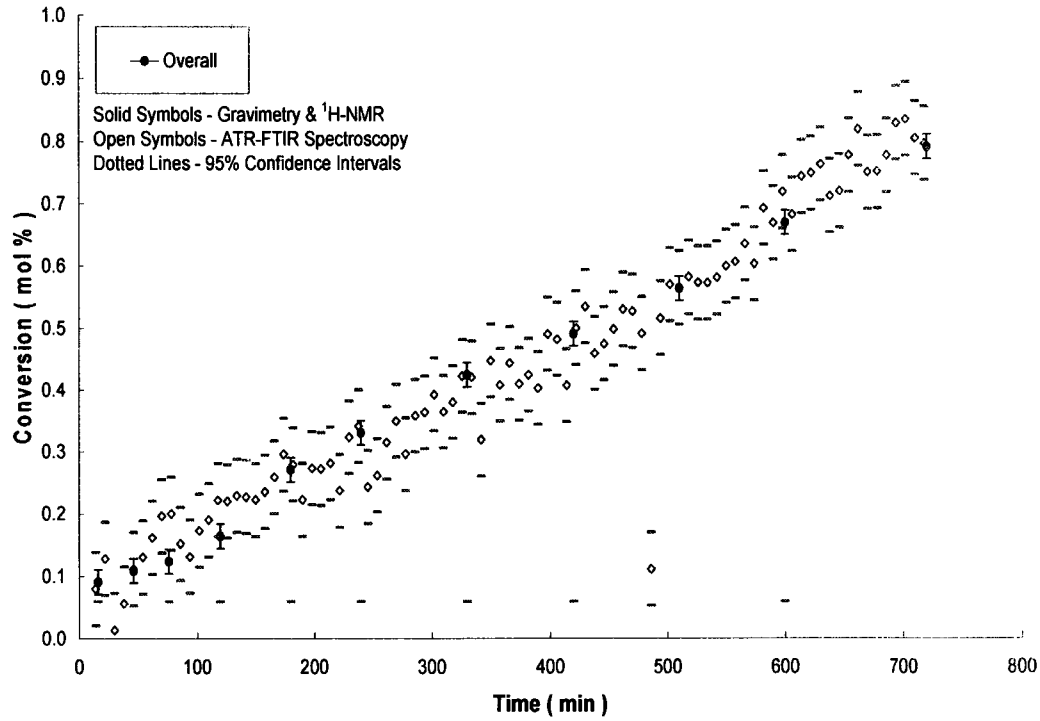

Figure C.14: PLS overall conversion predictions for Run 1

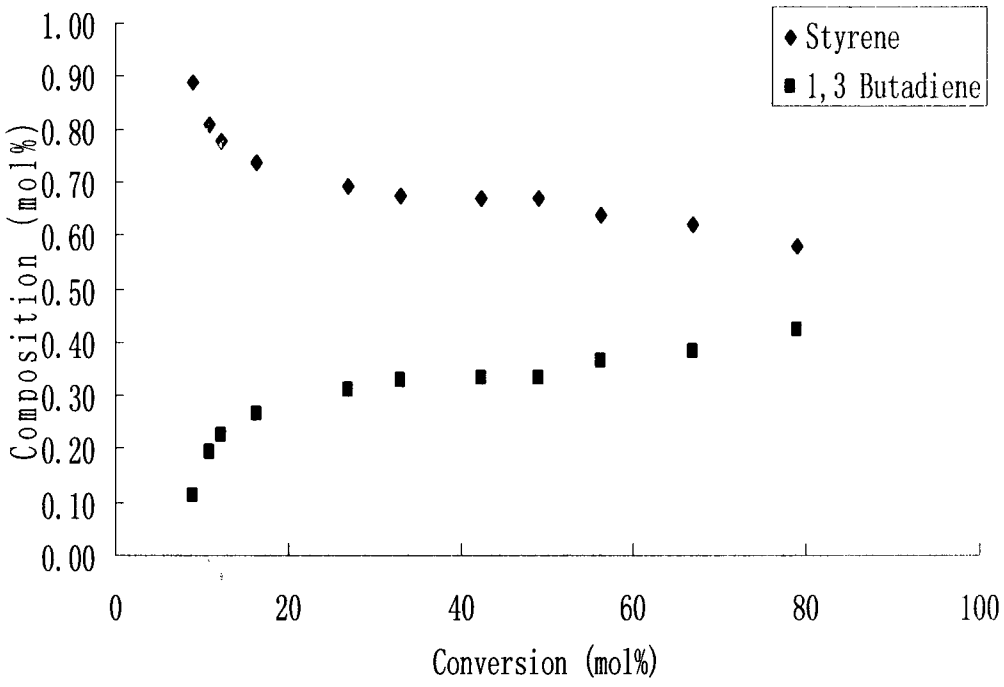

Figure C.15: Cumulative copolymer composition for Run 1

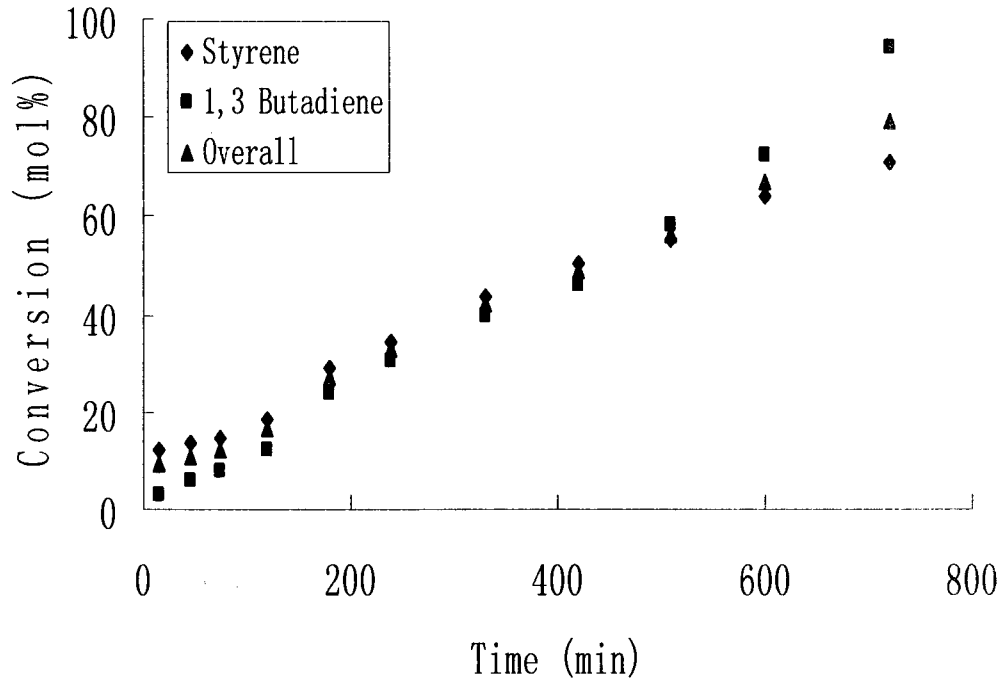

Figure C.16: Conversion versus time for Run 1

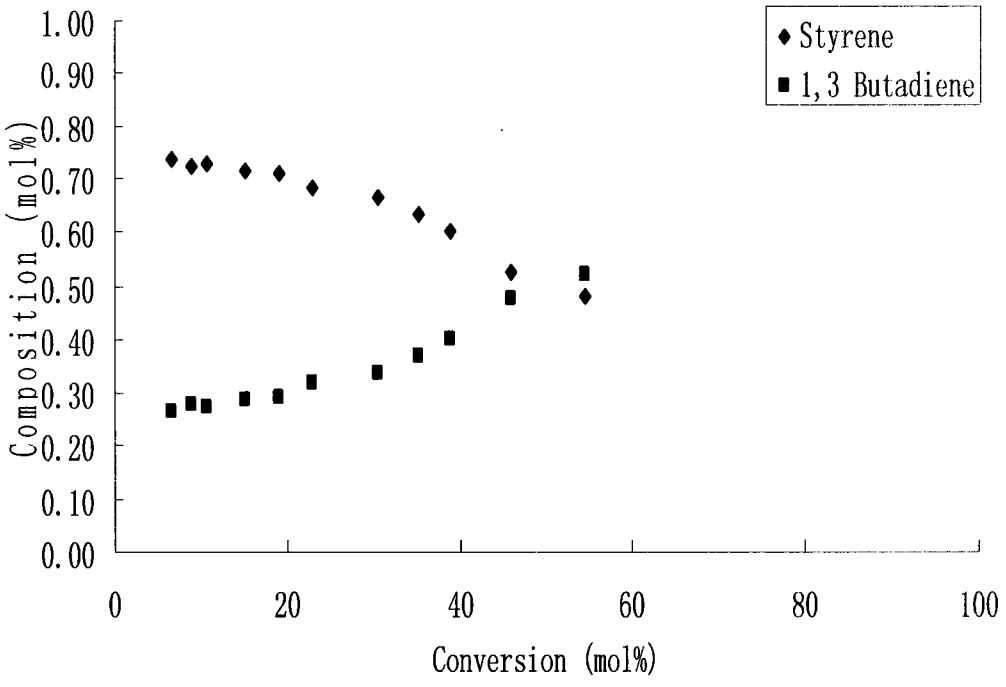

Figure C.17: Cumulative copolymer composition for Run 2

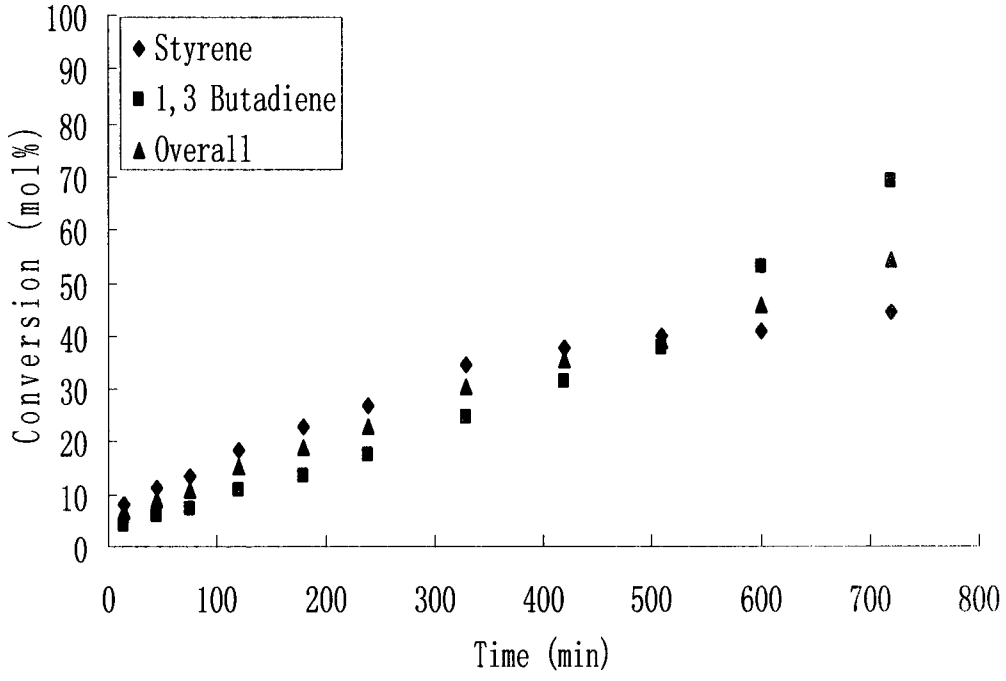

Figure C.18: Conversion versus time for Run 2

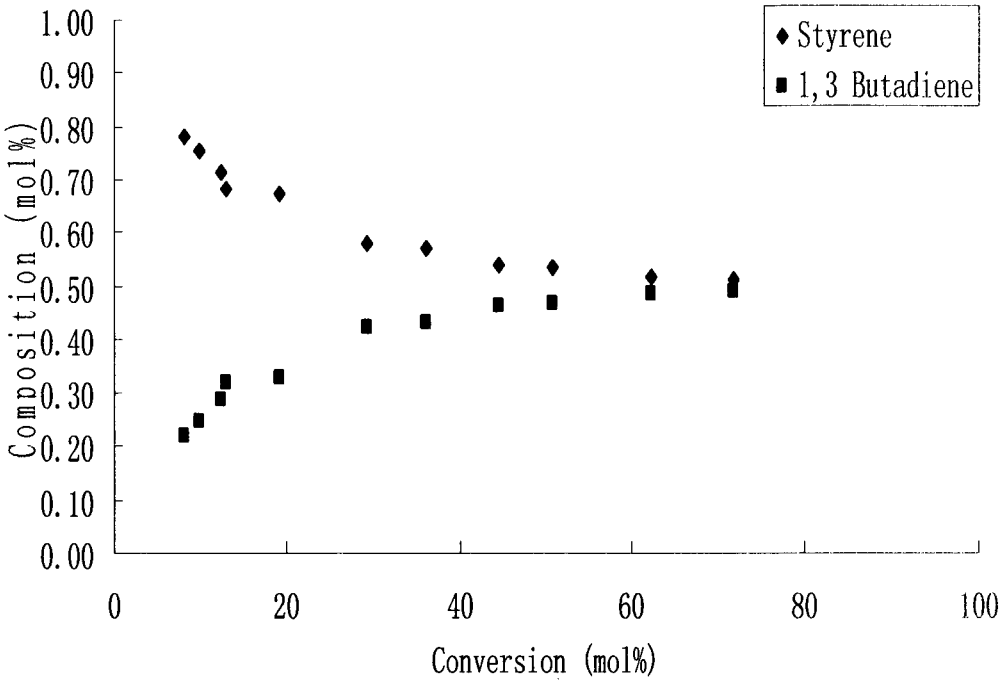

Figure C.19: Cumulative copolymer composition for Run 3

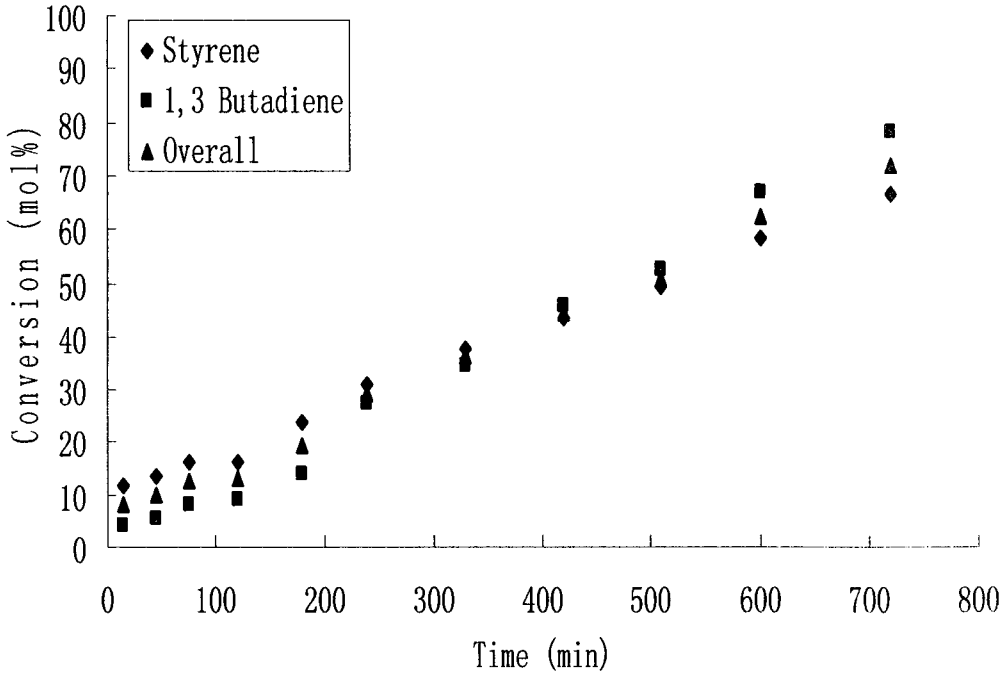

Figure C.20: Conversion versus time for Run 3

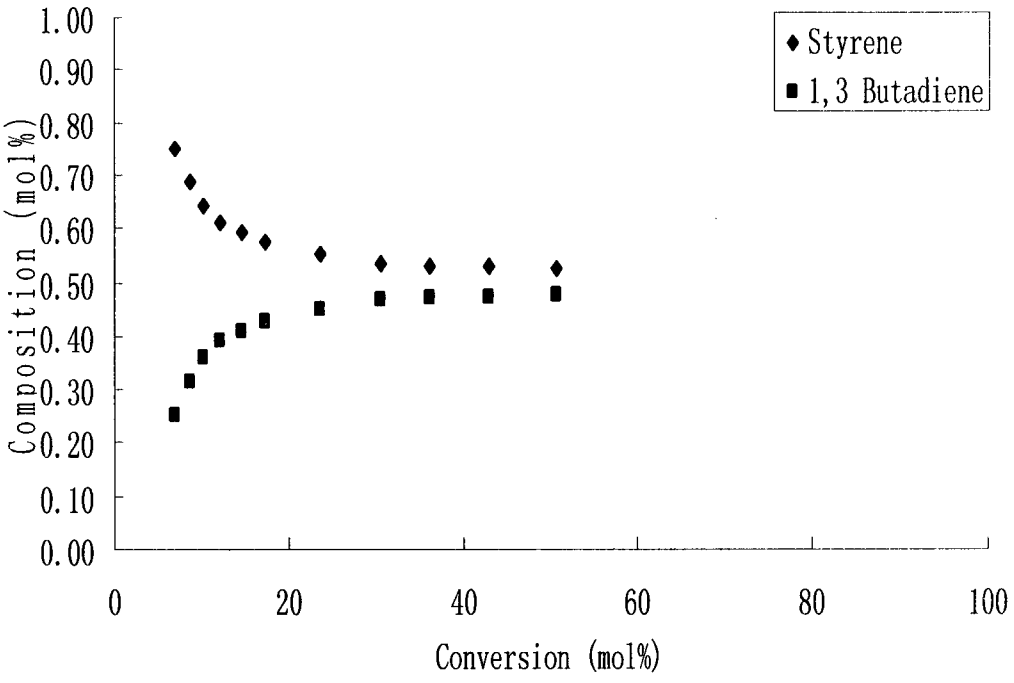

Figure C.21: Cumulative copolymer composition for Run 4

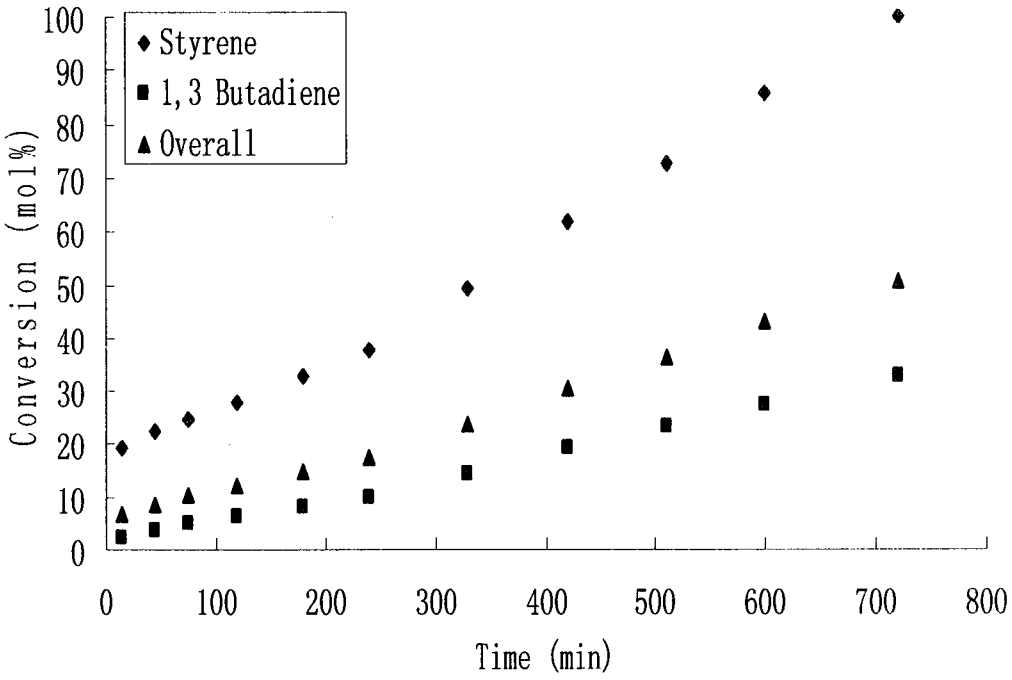

Figure C.22: Conversion versus time for Run 4

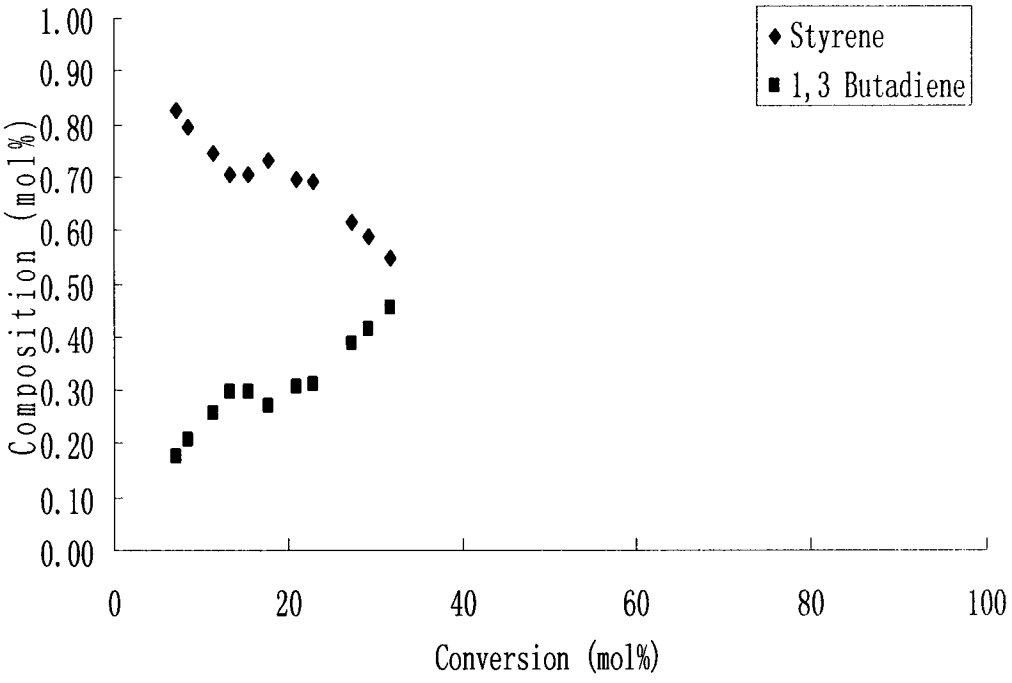

Figure C.23: Cumulative copolymer composition for Run 5

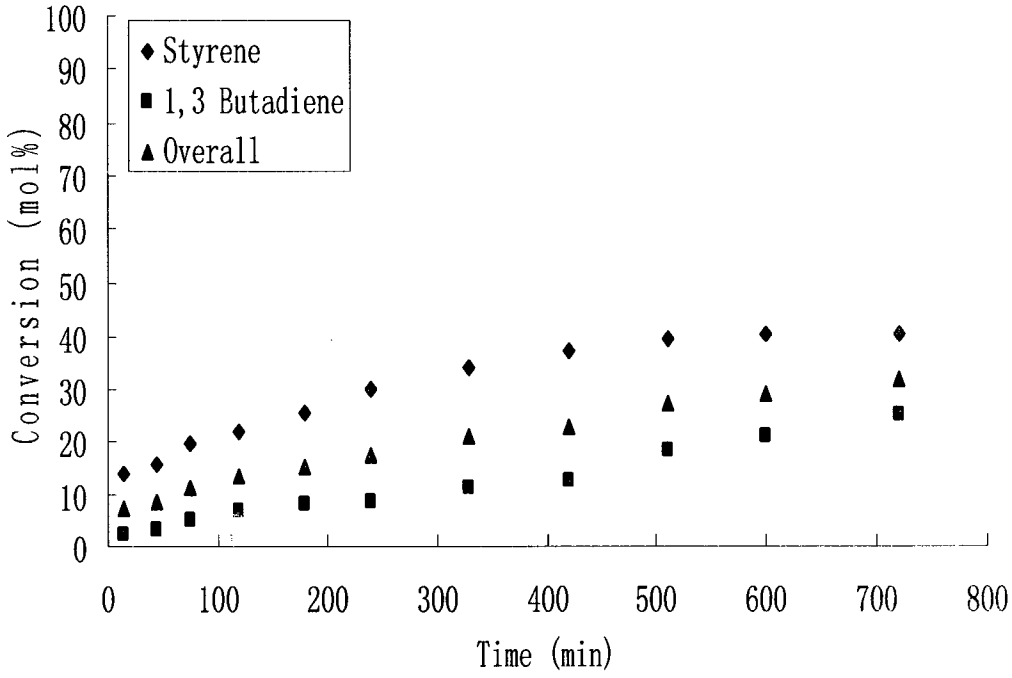

Figure C.24: Conversion versus time for Run 5

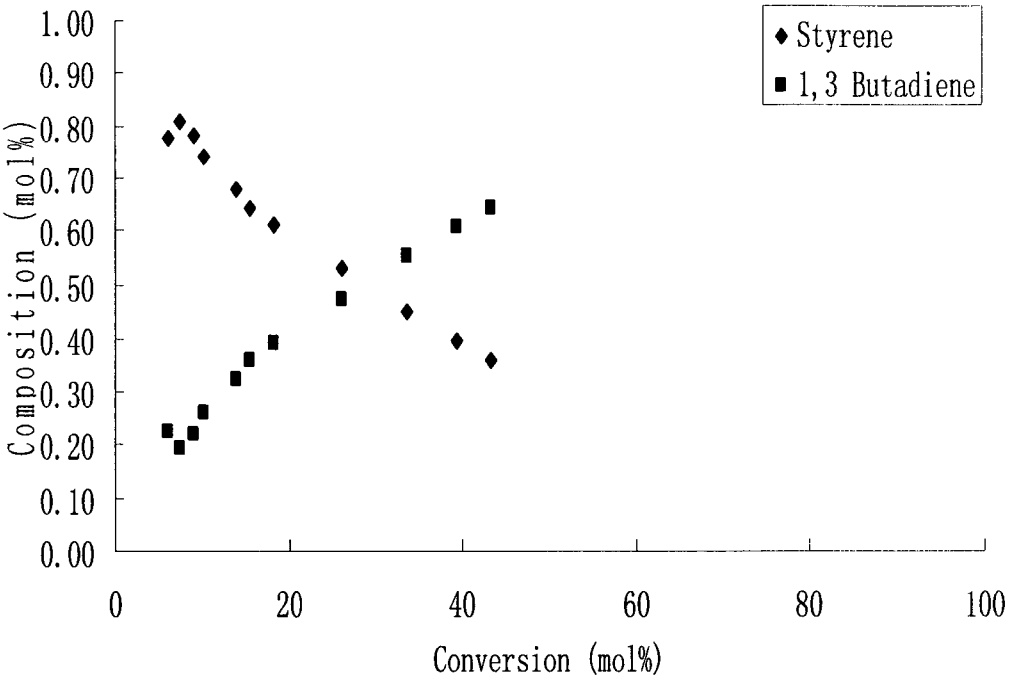

Figure C.25: Cumulative copolymer composition for Run 7

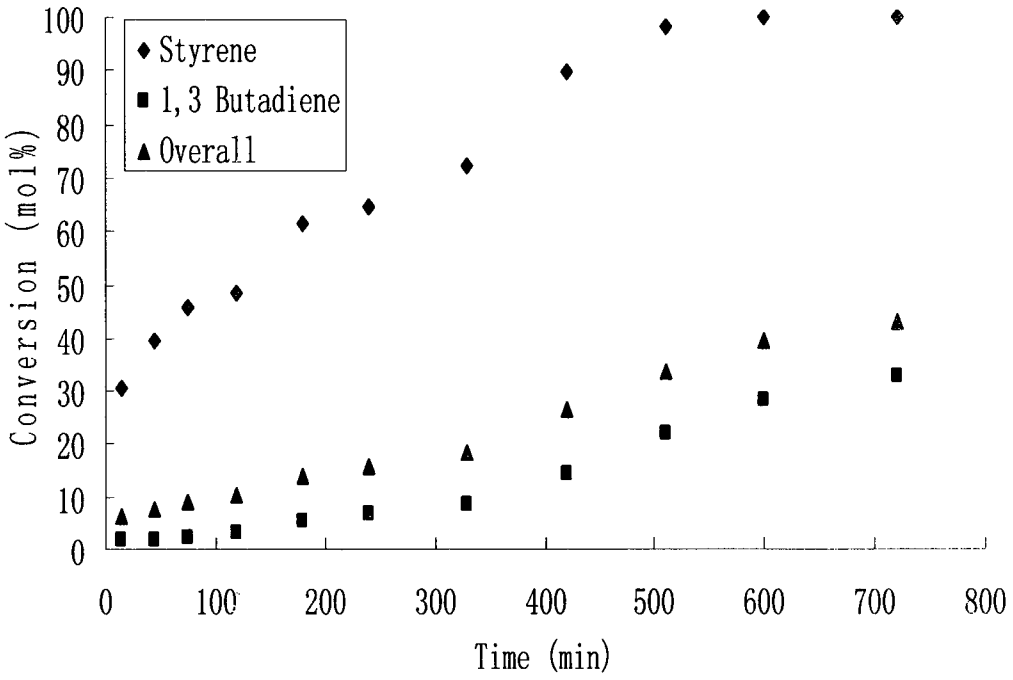

Figure C.26: Conversion versus time for Run 7

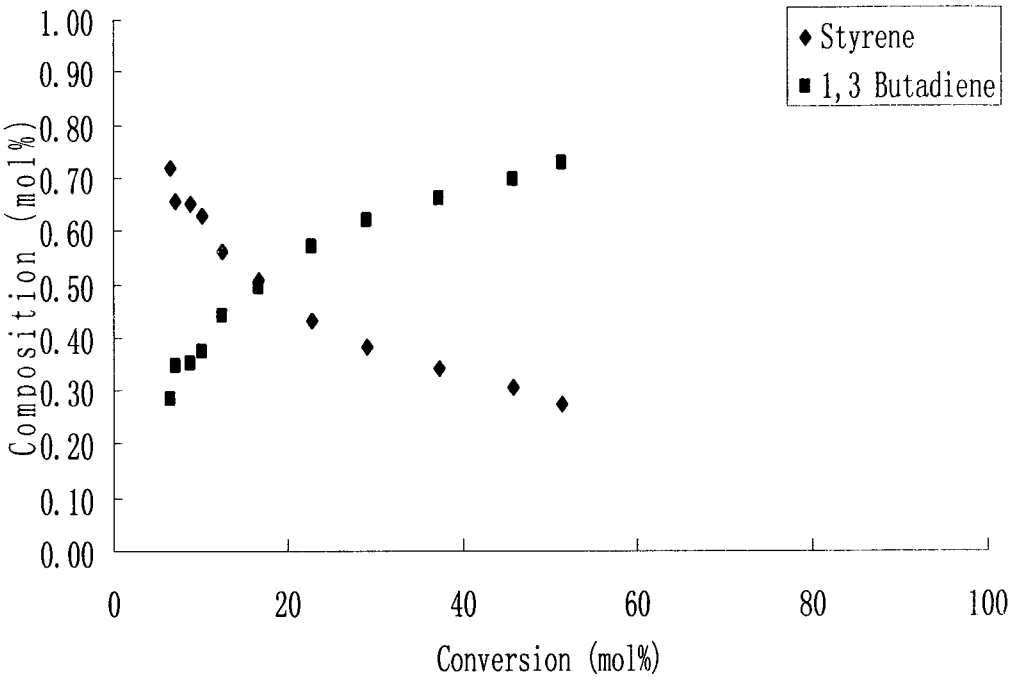

Figure C.27: Cumulative copolymer composition for Run 8

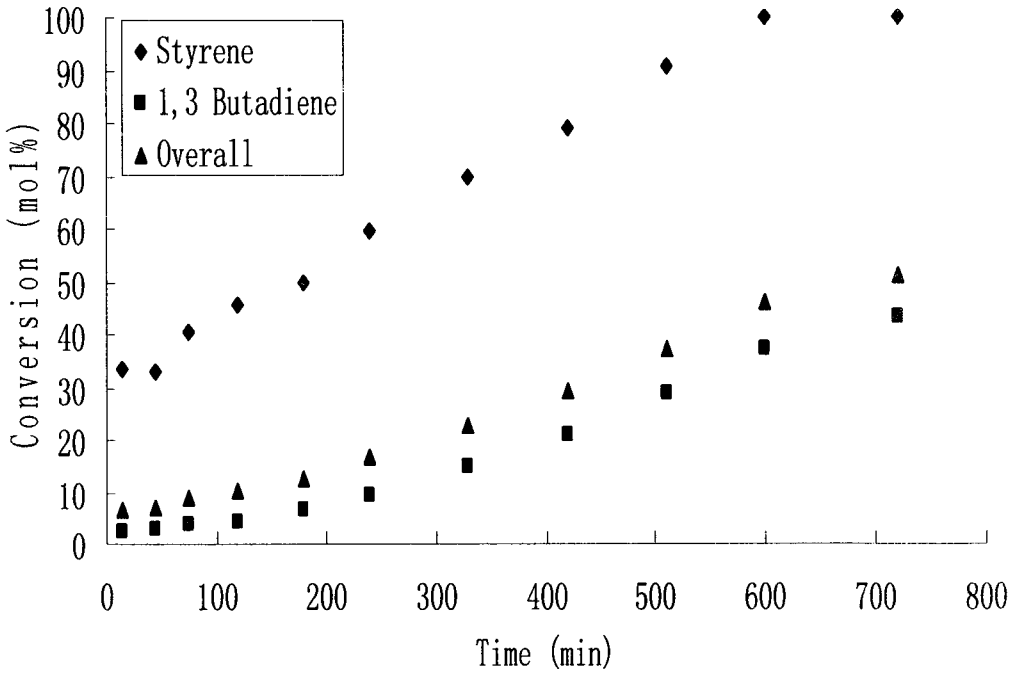

Figure C.28: Conversion versus time for Run 8